The Abdus Salam
International Centre for Theoretical Physics

United Nations
Educational, Scientific
and Cultural Organization

International Atomic
Energy Agency

H4.SMR/1645-1

"2nd Workshop on Earthquake Engineering for Nuclear Facilities: Uncertainties in Seismic Hazard"

14 - 25 February 2005

Seismological Database Methodological Approach

G.F. Panza[1, 2]

[1] Department of Earth Sciences
University of Trieste

[2] ICTP SAND Group, Trieste

ELSEVIER

Engineering Geology 66 (2002) 315–317

ENGINEERING GEOLOGY

www.elsevier.com/locate/enggeo

Opinion paper

PSHA: is it science?

Heriberta Castaños [a], Cinna Lomnitz [b,*]

[a] *Instituto de Investigaciones Económicas, National University of Mexico, Mexico*
[b] *Instituto de Geofísica, National University of Mexico (UNAM), 04510 D.F., Mexico*

Accepted 18 February 2002

Abstract

Probabilistic seismic hazard analysis (PSHA) is beginning to be seen as unreliable. The problem with PSHA is that its data are inadequate and its logic is defective. Much more reliable, and more scientific, are deterministic procedures, especially when coupled with engineering judgment. © 2002 Elsevier Science B.V. All rights reserved.

Keywords: Probabilistic seismic hazard analysis; Deterministic seismic hazard analysis; Earthquakes

1. Introduction

First it was the turn of earthquake prediction.

Not that it was all that unscientific. True, the science in earthquake prediction might have fitted into Peter Potter's cocked hat, and there were all the jokes about Chinese cookies and Parkfield capers making the rounds among seismologists (Lomnitz, 1994). But watching it sink so fast, without a bang or a whimper—that was a black eye for science. A lot of credible research went down with it.

Now it is the turn of probabilistic seismic hazard analysis (PSHA). Critical discussions of some aspects of PSHA are beginning to appear in the scientific literature (e.g., Atkinson et al., 2000; Krinitzsky, 2002; Newman et al., 2001). PSHA predicts, for part of the central United States at the 2% probability level in 50 years, a seismic hazard comparable with that of the San Andreas Fault, a notorious plate boundary. To what extent are these results based on sound science? Should earthquake hazard be assumed as high in Memphis as it is in San Francisco, and where does probability come in? The criterion of "2% in 50 years" has been sanctioned by the International Code Council (2000) as being realistic for the central United States. Why 50 years? Is it conservative or the opposite? People are beginning to wonder, "Is this science?"

2. Misunderstandings in probability and statistics

When the Senior Seismic Hazard Analysis Committee (1997) of the US Nuclear Regulatory Commission officially distinguished between "aleatory" and "epistemic" uncertainty their decision was a direct result of admitting expert opinion as evidence on the same level as hard earthquake data. An earthquake was regarded as a *nonrepeatable natural experiment*, which needed to be interpreted by a seismologist.

But it was Gauss (1823) who firmly established the foundations of probability in measure theory, not in epistemology. It is not intelligent to make an opposi-

* Corresponding author.
E-mail address: cinna@prodigy.net.mx (C. Lomnitz).

PII: S0013-7952(02)00039-X

tion between the two, but the difference is not difficult to see. Suppose that someone wished to buy life insurance and, being asked about her age, felt tempted to reply as follows: "Well, my mental age is 43 but of course my physical age is 29, and most of my friends claim that I don't look a day over 30…." The insurance man might interrupt: "Your date of birth, please?" In this context, it will hardly do to object that one is an individual, not a statistic, and thus a *non-repeatable natural experiment*.

Insurance firms use mortality tables, not the Bill of Rights. In fact, this is why Gauss refused to indulge in philosophical speculations. He proposed instead to estimate the length of a certain table that stood in his living room. With a yardstick, he measured the length of the table over and over again, jotting down the results every time. His patience was rewarded with the discovery of a bell-shaped distribution of measurements now known as the Gaussian. But his investigations did not stop there. He showed that the Gaussian could be derived mathematically from three simple assumptions: (a) errors are independent from one measurement to the next, (b) small errors are more likely than large errors, (c) positive and negative errors are equally likely.

What Gauss did not do is just as interesting. He refrained from claiming that he had found the *true* length of the table. Truth is the concern of epistemology, a branch of philosophy. Mathematics could go only as far as showing that the Gaussian estimate was consistent and unbiased, and letting scientists decide how to use it.

PSHA proposes to generate estimates of ground motion at sites and over time periods where no relevant seismic measurements are available. This is somewhat like estimating the length of a table no one has ever seen. We are not even sure of its existence. It is certainly possible to measure pieces of furniture in nearby homes and make inferences, but this is not really statistics.

Consider an example from social science. Statistical methods are often used to predict the outcome of US elections. A random sample of voters is selected according to certain criteria, and the preferences of the voters are obtained. For a sample the size of the electorate the result would be an actual election, and no statistics would be needed. However, the sample is always much smaller and the probable errors of estimation, as Gauss had shown, depend on the sample size. Also, the survey is conducted in advance of the election, which explains the prefatory disclaimer "If the election was held today…."

But would it not be much better to forget about surveying voters and ask the opinions of academics, European journalists and other knowledgeable people instead? After all, what do voters know? This is the aristocratic fallacy. If you do not have the facts, ask the experts. Newman et al. (2001) submit that the predicament of PSHA is common to all science and they cite the systematic error in the speed of light in support of their view. But the bias in the speed of light had nothing to do with a supposed limitation of scientific knowledge. It was due to a preventable violation of independence between measurements (Gauss' first assumption!).

3. The "P" in PSHA

In short, the problem of PSHA may be attributable to the first letter in its acronym. PSHA cannot claim the rigor and objectivity of a statistical method as long as it countenances the view that an earthquake—the source of all our data—is not a statistic but a "non-repeatable experiment". Nonrepeatability necessarily implies a dependence on the vagaries of expert testimony—which is presumably what the NRC means by "epistemological error".

Statistics was never intended to work that way. It cannot supplement a scarcity of data. Sir Harold Jeffreys, a statistician turned seismologist, once quipped that statistics is most useful when it is least needed: "No physical effect can be confirmed to exist when you need statistics to bring it out." This makes sense. Statistics works best with plenty of data. It is based on the Law of Large Numbers.

True, recent earthquake disasters, from Tangshan to Chi-Chi by way of Michoacan, Loma Prieta, Northridge and Kobe, have caught many seismologists and engineers by surprise: but it is hard to see how PSHA can help. It lends itself too easily to buttressing engineering decisions, good or bad, which have been reached by other means.

In the course of updating the Mexico City Building Code in 1987, the PSHA exercise produced (surprise!) a design event nearly identical to the 1985 earthquake. But this earthquake had generated peak spectral accel-

erations as high as 1 g in Mexico City. Following a suggestion by the Building Code Committee, the experts agreed to lower the design spectrum to a cutoff value of 0.4 g. Ductility, they argued, would take up the slack.

There are alternatives to PSHA. The physical upper bound to earthquake effects at the earth's surface is currently estimated at about 2 g. Thus it is feasible to build structures that are invulnerable to earthquakes. Expensive? The pre-Hispanic cultures of Mesoamerica built homes made of light materials and pyramids that last forever. Automobiles are basically invulnerable to earthquakes, and so are structures that incorporate modern techniques of structural damping to eliminate damaging resonant frequencies (e.g., Trombik and Fleischer, 2001).

Then there is deterministic seismic hazard analysis (Krinitzsky, 2002). DSHA is basically a method of engineering design that incorporates available data from geology leading to estimates of earthquake activity, plus everything else we know about a site and its environment: the tectonics, the past seismicity, the soil mechanics, the statistics and the sociology. It is not "deterministic" in the philosophical sense, as it emphasizes the role of judgment in engineering decisions. It might be called "scientific seismic hazard analysis" because every kind of relevant scientific information is utilized.

4. Conclusions

The shortcomings of PSHA appear to be due to a series of misunderstandings. Statistics has sometimes been presented as a collection of recipes for data processing, and such an approach may occasionally be valid when there is a large amount of data. But the assumptions made about the connections of statistics with probability, and of probability with measure theory, become increasingly critical as one attempts to squeeze the data or extrapolate a small data set over regions of sample space where no data exist (Lomnitz, 1994).

This is not to say that probability is totally useless in earthquake hazard estimation. But probability is primarily a branch of mathematics, not a technique. Applications can be extremely powerful as long as the logic of the field is fully understood. For example, assumptions such as "independence" or "stationarity" are never actually verified in natural systems. Strictly speaking, a Poisson process (or any process) is a theoretical construct, and the transition from theory to reality must be managed at the risk of the user.

Other options of evaluating earthquake hazard are available. In the social sciences such approaches are known as *strategies.* They use all the scientific information one can get, but the optimal way of combining such information to reach a decision cannot always be defined in advance. It involves judgment and experience. Clearly there is a considerable body of available research in decision theory to find optimal strategies in the presence of uncertainty; but PSHA has made use only of some rudimentary applications (decision trees), perhaps because the available information is rarely sufficient to guarantee an optimal decision.

References

Atkinson, G., et al., 2000. Reassessing the New Madrid seismic zone. Eos, Trans. Am. Geophys. Union 81 (97), 402–403.

Gauss, C.F., 1823. Theoria Combinationis Observationum Erroribus Minimis Obnoxiae. Henricus Dieterich, Göttingen.

International Code Council, 2000. International Building Code. Falls Church, Virginia.

Krinitzsky, E., 2002. How to obtain earthquake ground motions for engineering design. Eng. Geol., in press.

Lomnitz, C., 1994. Fundamentals of Earthquake Prediction. Wiley, New York, 326 pp.

Newman, A., Schneider, J., Stein, S., Mendez, A., 2001. Uncertainties in seismic hazard maps for the New Madrid Seismic Zone and implications for seismic hazard communication. Seism. Res. Lett. 72, 647–663.

Senior Seismic Hazard Analysis Committee, 1997. Recommendations for Probabilistic Seismic Hazard Analysis: Guidance on Uncertainty and Use of Experts, US Nuclear Regulatory Commission, NUREG/CR-6372.

Trombik, P., Fleischer, P., 2001. Erdbebenertüchtigung: Einbau viskoser Dämpfer. D-A-CH Mitteilungsblatt 20 (3), 14–18.

Unclassified **NEA/CSNI/R(2003)18**

Organisation de Coopération et de Développement Economiques
Organisation for Economic Co-operation and Development

22-Dec-2003

English - Or. English

NUCLEAR ENERGY AGENCY
COMMITTEE ON THE SAFETY OF NUCLEAR INSTALLATIONS

NEA/CSNI/R(2003)18
Unclassified

OECD/NEA WORKSHOP ON THE RELATIONS BETWEEN SEISMOLOGICAL DATA AND SEISMIC ENGINEERING

Istanbul, 16-18 October 2002

English - Or. English

JT00156210

OECD Workshop on the Relations Between Seismological DATA and Seismic Engineering Istanbul, 16-18 October 2002

SEISMIC GROUND MOTION MODELLING AND DAMAGE EARTHQUAKE SCENARIOS A BRIDGE BETWEEN SEISMOLOGISTS AND SEISMIC ENGINEERS

G.F. Panza[1,2], F. Romanelli[1]
[1]Dipartimento di Scienze della Terra - Universita' di Trieste
[2]The Abdus Salam International Center for Theoretical Physics – Miramar, Trieste
panza@dst.univ.trieste.it, romanel@dst.univ.trieste.it

F. Vaccari
INGV - Oss. Vesuviano, c/o Dipartimento di Scienze della Terra - Universita' di Trieste
vaccari@dst.univ.trieste.it

L. Decanini, F. Mollaioli
Dipartimento di Ingegneria Strutturale e Geotecnica - Universita' di Roma "La Sapienza"
Luis.Decanini@uniroma1.it, Fabrizio.Mollaioli@uniroma1.it

Abstract

The input for the seismic risk analysis can be expressed with a description of "groundshaking scenarios", or with probabilistic maps of perhaps relevant parameters.

The probabilistic approach, unavoidably based upon rough assumptions and models (e.g. recurrence and attenuation laws), can be misleading, as it cannot take into account, with satisfactory accuracy, some of the most important aspects like rupture process, directivity and site effects. This is evidenced by the comparison of recent recordings with the values predicted by the probabilistic methods.

We prefer a scenario-based, deterministic approach in view of the limited seismological data, of the local irregularity of the occurrence of strong earthquakes, and of the multiscale seismicity model, that is capable to reconcile two apparently conflicting ideas: the Characteristic Earthquake concept and the Self Organized Criticality paradigm.

Where the numerical modeling is successfully compared with records, the synthetic seismograms permit the microzoning, based upon a set of possible scenario earthquakes. Where no recordings are available the synthetic signals can be used to estimate the ground motion without having to wait for a strong earthquake to occur (pre-disaster microzonation). In both cases the use of modeling is necessary since the so-called local site effects can be strongly dependent upon the properties of the seismic source and can be properly defined only by means of envelopes.

The joint use of reliable synthetic signals and observations permits the computation of advanced hazard indicators (e.g. damaging potential) that take into account local soil properties. The envelope of synthetic elastic energy spectra reproduces the distribution of the energy demand in the most relevant frequency range for seismic engineering. The synthetic accelerograms can be fruitfully used for design and strengthening of structures, also when innovative techniques, like seismic isolation, are employed.

For these reasons the skill of seismology to estimate realistic ground motions at a particular site should be fully exploited by seismic engineers. In fact, even if recently strong motion records in near-fault, soft soil, or basin conditions have been obtained, their number is still very limited to be statistically significant for seismic engineering applications.

1. Introduction

Earthquakes, as many other natural disasters, have both immediate and long-term economic effects. Within a fraction of a minute, single earthquakes can inflict damage to houses, business, government buildings, and infrastructures. A single earthquake may trigger a global ecological catastrophe, cause up to thousands of casualties and global economic depression: the disruption of commerce will affect the rate of economic growth, inflation, productivity and trade balance.

Case studies of seismic hazard assessment techniques indicate the limits of the currently used methodologies, deeply rooted in engineering practice, based on a probabilistic approach. The probabilistic analysis supplies indications that can be useful but-not sufficiently reliable to characterize the seismic hazard.

The mathematical modelling, with different degrees of complexity, based on probabilistic concepts cannot fill in the gap due to the lack of knowledge about the physical process behind an earthquake, at the most it can supply some guidelines. Moreover, it may loose validity in dealing with uncertainties that are so large that may not be quantifiable in a meaningful sense (Chandler et al., 2001) as it happens in low to moderate seismicity regions, or regions lacking historical and instrumental earthquake data.

For a given zone, the mathematical modelling of the occurrence of seismic events and of the related values of probability are derived from empirical data that may fail to describe adequately the reality.

When constructing appropriate earthquake-resistant structures, design and construction should not be such that in extreme event no damage occurs but rather that an acceptable level of damage takes place as a function of the corresponding performance expectations (operational, safe-life, etc.).

Therefore the realistic definition of hazard in scenario-like format should be accompanied by the determination of advanced hazard indicators as, for instance, damaging potential. Such a determination, due to the limitation of the available strong ground motion records, requires resorting to broad band synthetic seismograms that allow us to perform realistic waveform modelling for different seismotectonic environments. The modelling takes into account source properties, like dimensions, directivity, duration, lateral heterogeneity's along the path and local site features. Such a procedure is a must since it has been proven both experimentally (e.g. Wang and Nisimura, 1999) and theoretically (Romanelli and Vaccari 1999; Field et al., 2000; Panza et al, 2001) that the so-called local site effects can be strongly dependent upon the characteristics of the seismic source generating the seismic input. At present, only from a careful performance of modelling experiments it is possible to realistically account for effects such as long duration pulses, shaking duration, temporal distribution of pulses, amplitude and, connected to them, the linear and nonlinear structural response in terms of strength, energy and displacement.

2. General problems in seismic hazard assessment

The typical seismic hazard problem lies in the determination of the ground motion characteristics associated to future earthquakes, both on regional and on local scale. The input for the subsequent seismic risk analysis can be expressed in various ways, e.g. with a description of the groundshaking severity due to an earthquake of a given distance and magnitude ("groundshaking scenario"), or with probabilistic maps of relevant parameters describing the ground motion. For example, the historically

most used parameter in the engineering analysis for the characterization of the seismic hazard is the PGA (Peak Ground Acceleration), which is a single-value indicator commonly used in seismic hazard assessment. Actually, it is recognized that the PGA alone can not describe adequately all the effects associated to the ground shaking, since the frequency content and the duration of a seismic wavetrain can play a decisive role. Although it has been understood that the characteristics of the ground motion such as its amplitude, frequency content and duration are relevant to estimate its damaging potential, some of these characteristics have been often ignored.

A more adequate definition of the seismic ground motion due to an earthquake with a given magnitude and source-to-site distance, can be done following two main approaches. The first one (denoted as engineering approach) is based on the analysis of the available strong motion databases, collected by existing seismic networks, and on the grouping of those accelerograms that contain similar source, path, and site effects (e.g. Decanini and Mollaioli, 1998). A fundamental step in this approach involves the estimation of realistic source-to-site transfer functions.

The second approach (seismological approach) is based on modeling techniques, developed from the knowledge of the seismic source process and of the propagation of seismic waves, that can realistically simulate the ground motion associated with the given earthquake scenario (Panza et al., 1996; Field et al., 2000). The ideal procedure is to follow the two complementary ways, in order to validate, for the different areas to be investigated, the numerical modeling with the available recordings (e.g. Decanini et al., 1999; Panza et al., 2000a,b). In the last decades the number of the recorded strong motions has considerably increased, especially for North America, Japan and Taiwan, but the installation and maintenance costs make the deployment of a dense seismic network in each earthquake prone area a too expensive operation. For most of the European seismic zones strong motion data are very scarce and most of the available data for destructive events are only the macroseismic intensities. In these cases synthetic signals, to be used as seismic input in a subsequent engineering analysis, must be produced (immediately and at a very low cost/benefit ratio) taking into account the source characteristics, the path and the local geological and geotechnical conditions and must be validated against observed intensities.

As a result, we suggests a scenario-based, deterministic approach in view of the limited seismological data and of the multiscale seismicity model formulated by Molchan et al. (1997). Accordingly to this model only the ensemble of events that are geometrically small, compared with the elements of the seismotectonic regionalization, can be described by a log-linear FM relation. This condition, largely fulfilled by the early global investigation by Gutenberg and Richter (e.g. see Fig. 49 of Båth, 1973), it has been subsequently violated in many investigations. This violation has given rise to the Characteristic Earthquake (CE) concept (Schwartz and Coppersmith, 1984) in opposition to the Self-Organized Criticality (SOC) paradigm (Bak and Tang, 1989). The multiscale model implies that, in order to apply the probabilistic approach the seismic zonation must be made at several scales, depending upon the self-similarity conditions of the seismic events and the linearity of the log FM relation, in the magnitude range of interest.

Moreover, the macroseismic observations made in correspondence of the destructive events of the last century have clearly evidenced the influence of other two fundamental aspects in the characterization of the damage distribution: the near-surface geological and topographical conditions. This observation highlights the large spatial variability of the destructive potential of earthquake ground motion. Since most of the anthropised areas are settled in correspondence of sedimentary basins (e.g. river valleys), a realistic definition of the seismic input that takes into account the site response has become one of the most relevant tasks in the seismic engineering analysis. The soft surface layering often controls local amplification of the ground motion. The impedance contrast between the soft surface soils and the underlying bedrock leads to the trapping of the seismic energy,

and the relatively simple onset of vertical resonance can be transformed into a complex resonance's pattern, strongly dependent on the characteristics of the sub-surface layers and the bedrock configuration.

The most traditional empirical techniques for the estimation of site effects are based on the computation of the spectral ratio between the signal (or a portion of it, e.g. a single phase) recorded at the sedimentary site and a reference one, preferably recorded at a nearby bedrock site (Borcherdt, 1970). Quite often a signal recorded on bedrock is not available close to the investigated sites, so that directional effects due to the source could become relevant. Even in the favorable condition that such a reference site exists, unless well isolated single phases are used, the spectral ratios are not completely free from source influences (e.g. Romanelli and Vaccari, 1999). Some techniques have been proposed that are non-reference-site dependent (e.g. Boatwright et al., 1991).

An alternative approach, originally applied by Langston (1979) for crustal and upper mantle studies, is based on the measurement of the spectral ratio between the horizontal and vertical components of motion. The method is based on the assumption, not always fulfilled, that the propagation of the vertical component of motion (in general only S-waves are considered) is not perturbed by the uppermost surface layers, and can therefore be used to remove source and path effects from the horizontal components. Anyway, this method produced unsatisfactory results, as verified in recent severe earthquakes.

As a matter of fact, local site effects can be strongly dependent upon the characteristics of the seismic source (e.g. Romanelli and Vaccari, 1999). Therefore, the use of synthetic seismograms is fundamental even when relevant observational data are available, in order to explore the local responses that may correspond to sources that are different from the known ones.

The wide use of synthetic signals allows us to easily construct scenarios based on ground motion descriptors, strictly linked with energy and displacement demands (Decanini and Mollaioli, 2001).

3. Shortcomings of the probabilistic approach

The probabilistic analysis of the seismic hazard determines the probability rate of exceeding, over a specified period of time, various levels of ground motion. It is basically conditioned by the definition of the seismogenic zones, which is affected by serious uncertainties. Within each of them the seismogenic process is frequently assumed to be rather uniform, however the uncritical assumption of homogeneity can introduce significant errors in the estimate of the seismic hazard in a given site. For a recent extreme example concerning the Italian territory reference can be made to the 17 July 2001 (M_b=4.9; M_s=4.0, NEIC), event occurred in NorthEast Italy outside the defined seismogenic zones (Meletti et al., 2000), thus in a region not considered for hazard analysis.

The multiscale seismicity model supplies a formal framework that describes the intrinsic difficulty of the probabilistic evaluation of the occurrence of earthquakes (Molchan et al., 1997). The problem is chiefly due to the difficulty to properly choose the size of the region to analyze, so that it is large enough to guarantee the applicability of the Gutenberg-Richter law and related concepts. In order to apply the probabilistic approach, the seismic zonation must be made at several scales, depending upon the self-similarity conditions of the seismic events and the linearity of the log frequency-magnitude (FM) relation, in the magnitude range of interest.

The difficulty to evaluate the occurrence of the earthquakes (log FM relations) and the propagation of their effects (attenuation laws), as well as the parameters characterizing the destructive

potential of the ground motion leads to a probabilistic estimate of the seismic hazard that could represent a gross approximation of the reality. When the multiscale seismicity model is applied to analyze the seismicity, the time dependence of seismicity becomes unimportant. In fact, the classical Poisson hypothesis (seismic events are time independent) can hardly be accepted if the considered seismic events are those associated to a specific source (where there are processes of storage and release of energy). The Poisson hypothesis can be physically acceptable when the considered area is large enough to contain a great number of sources.

To deal with the time dependence of seismicity, that is relevant only if we consider a very small number of seismic sources, the concept of renewal process has been introduced (Esteva, 1970; Araya and Der Kiureghian, 1988; Hagiwara, 1974; Savy et al., 1980). Accordingly with the renewal process models a memory is introduced so that each event, with some probability, depends from the previous one. In these models the intercurrence time between two events does not follow an exponential distribution, thus the probability of occurrence of an earthquake is not constant with time. Assuming that the seismic crisis is over or during a seismic sequence, the occurrence of the events is interpreted using mixed functions of the density of probability, obtained with the combination of two different functions. These functions depend upon the seismogenetic properties of the sources and upon the time evolution of the sequences; therefore they differ from place to place. Such models rely upon several assumptions that to be verified require the availability of observations that often are not available or insufficient, and this makes it difficult, if not impossible, the calibration of the distribution functions. The application of the renewal process model requires the evaluation of the time elapsed from the last event. Such an evaluation can be impossible if the length of the catalogue is smaller than the storage and release time interval and palaeoseismological data are not available, or when a linear source does not correspond to a single fault but to a system of several faults almost parallel. In the latter a case the occurrence of severe seismic events, within close epicentral zones and during short time intervals, could not be analyzed resorting to criteria based on the existence of seismic gaps.

Further shortcomings of the probabilistic approach are connected with (1) the choice of the parameters characterizing the destructiveness potential of earthquake ground motion, and (2) the attenuation relationships for the estimation of the ground motion at a site for a given earthquake.

3.1 Characterization of earthquake destructiveness potential

The characterization of seismic motion in earthquake prone areas requires the identification of adequate parameters that characterize accurately the earthquake destructiveness potential. The specification of these parameters in general requires the selection of significant signals for the design of new structures or the seismic safety assessment of existing ones. To define, in general, a design earthquake represents a fundamental step in a seismic hazard analysis. The adoption of inadequate parameters can lead to the definition of a non-realistic design earthquake and, consequently, to the unreliable evaluation of the seismic risk. Recent earthquakes (e.g. Imperial Valley 1979, Loma Prieta 1989, Landers 1992, Northridge 1994, Kobe 1995, Turkey 1999, Taiwan 1999, Greece 1999, Gujarat, 2001) have demonstrated that the seismic hazard evaluation, based prevalently on a probabilistic approach, has underestimated considerably these demands, particularly in near-fault regions.

The quite large number of near-fault records from recent earthquakes indicate that, for a given soil condition, the characteristics of strong ground motion and consequently of the damage potential can vary significantly as a function of the location of the site with respect to the propagation of the rupture. Particularly, in the case of *forward rupture directivity* most of the energy arrives in a single large pulse of motion which may give rise to an amplification of the ground motion at sites toward which fracture propagation progresses (e.g. Bolt, 1983; Panza and Suhadolc, 1987; Heaton et al.,

1995). The long-period parts of the signals in forward directivity locations can be energetic due to the development of one or more, unidirectional, long-period pulses. The dynamic response of a structure depends simultaneously on its mechanical properties and on the characteristics of the induced excitation. Therefore it is necessary to investigate if certain properties which are efficient to mitigate the structure response when subjected to certain inputs might have an undesirable effect during other seismic inputs. Moreover, the presence of long duration accelerometric pulses in the ground motion constitutes an important factor in causing damage, as it involves the transmission of large energy amounts to the structures in a very short time, with high energy dissipation and displacement demands.

The quantification of the ground motion expected at a particular site, that would drive the structure to its critical response, resulting in the highest damage potential, requires: (a) the identification of the ground motion parameters that characterize the severity and the damage potential of the earthquake ground motion (for a more complete discussion on this topic see Appendix), and (b) the seismological, geological, and topographic factors that affect them. In this context, energy-based and displacement demand parameters constitute an adequate approach to highlight the damaging potential of these kind of signals (Decanini and Mollaioli, 1998; Decanini et al., 2000). This necessity is confirmed by the analysis performed by Panza et al. (1999) when seeking for a correlation between maximum observed macroseismic intensity, I, (MCS) and computed peak values of ground motion, like Design Ground Acceleration (DGA), Peak Ground Velocities (PGV) and Peak Ground Displacements (PGD). They do not show any significant improvement in the regression scatter when going from DGA to PGV and PGD. The slope value is always close to 0.3, a value that corresponds to the relation DGA(I-1)/DGA(I)=PGV(I-1)/PGV(I)=PGD(I-1)/PGD(I)=2. Such a value is not contradicted by the numerous empirical relations (see Shteinberg et al., 1993 and references therein) found when considering peak values of ground acceleration.

The large energy demand in the near-field region ($D_f \leq 5$ km), with respect to larger distance ranges, is clearly evidenced in Tab. 1. In the table, a comparison between maximum input energy E_{Imax} and a Seismic Hazard Energy Factor AE_I (Decanini and Mollaioli, 1998) is given for sites located on a soil of intermediate mechanical properties, S2; for different values of interval of magnitude (M) and source-to-site distance (D_f) classes. D_f is defined as the closest distance from the intersection with the free surface of the fault plane, or of its extension to the surface for blind faults.

SOIL S2 $5.4 \leq M \leq 6.2$			
D_f (km)	**$AE_{I(design)}$ cm^2/s**	**$E_{I(max)}$ cm^2/s^2**	**$AE_{I(max)}$ cm^2/s**
$D_f \leq 5$	45000	39000	34568
$5 < D_f \leq 12$	18000	13000	8960
$12 < D_f \leq 30$	10000	7600	5828
$D_f > 30$	3000	480	420
SOIL S2 $6.5 \leq M \leq 7.1$			
D_f (km)	**$AE_{I(design)}$ cm^2/s**	**$E_{I(max)}$ cm^2/s^2**	**$AE_{I(max)}$ cm^2/s**
$D_f \leq 5$	110000	90000	98446
$5 < D_f \leq 12$	75000	41000	31320
$12 < D_f \leq 30$	50000	31000	42683
$D_f > 30$	15000	9400	9836

Table 1. Comparison between AE_I (design and maximum observed) and E_I (maximum observed). Soil S2 (intermediate).

The input energy per unit of mass, $\frac{E_I}{m} = \int \ddot{u}_t du_g = \int \ddot{u}_t u_g dt$, has been extensively used for the evaluation of the damage potential of earthquake ground motion (Akiyama, 1985; Uang and Bertero, 1988; Fajfar and Fishinger, 1990; Uang and Bertero, 1990; Bertero and Uang, 1992; Krawinkler 1997; Decanini and Mollaioli, 1998; Decanini and Mollaioli, 2001). The parameter $AE_I = \int_{0.05}^{4.0} E_I(x = 5\%, T)\, dT$, which represents the area enclosed by the elastic input energy spectrum in the interval of periods between 0.05 and 4.0 seconds, may be considered a global hazard index in energy terms (Decanini and Mollaioli, 1998). In fact it considers the influence of the energy demand in the whole period range. The proposed values of E_I and AE_I were determined from a database of 300 acceleration time histories taken from 37 different seismic events with magnitude ranging from 4 to 8.1 and distance, from the horizontal projection of the causative fault, from 0 to 390 km.

The large difference among the energy parameters in the near-fault ($D_f \leq 5$ km) and at other locations ($5 < D_f \leq 12$ km; $12 < D_f \leq 30$ km; $D_f > 30$ km) has been found for the displacement demand too, as shown in Fig. 1. The largest displacements can be observed on soft soil sites (S3), in the same distance and magnitude range (Fig. 2), as the amplification of ground motions may be significantly affected by the combined effect of the source and of the soil stiffness and thickness.

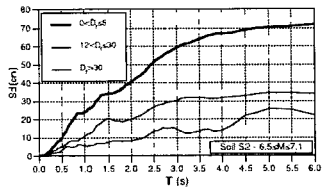

Fig. 1. Mean Displacement Spectra for different source-to-site distance ranges. Intermediate soil class (S2). $6.5 \leq M \leq 7.1$.

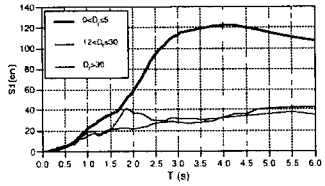

Fig. 2. Mean Displacement Spectra for different source-to-site distance ranges; soft soil (S3); $6.5 \leq M \leq 7.1$.

Each recorded strong ground motion history is a useful addition to the time record database, which increases our choices in selecting acceleration histories for various analyses. The growing database for near-field and soft soil strong motion records, gives the opportunity to enhance the state of knowledge in damage potential evaluation. Anyway, it has been noted that other seismological characteristics, such as the different styles of faulting, the radiation pattern, the orientation of the seismic source, etc., should inevitably be taken into account. These issues may be clearly understood resorting to seismological modeling techniques. For example, due to the lack of data, the nature of near-fault ground motions from larger magnitude earthquakes should be examined using seismologically based ground motion simulation methods.

3.2 Attenuation relationships

The other factor which influences a seismic-hazard estimate is represented by the assessment of the attenuation relationships of the ground motion parameters. These relationships can differ in the assumed functional form, the number and definition of independent variables, the data selection criteria, and the statistical treatment of the data. Anyway, in general, attenuation laws assume the same propagation model for all the size and type of events, but such a hypothesis is not very realistic. The

most frequently used attenuation models of ground motion parameters, like PGA, PGV, etc., have the form:

$$\log y = a + b\,M + c\,\log r_f + d\,D_f + e\,S \qquad (1)$$

where y is the ground motion parameter, a, b, c, d, and e are coefficients empirically determined, r_f is derived from D_f by considering a conventional depth h_0, with $r_f = \sqrt{D_f^2 + h_0^2}$, and S is a binary variable (0, 1) which depends on the soil type. Generally, the coefficients are determined empirically by means of regression analyses and they turn out to be quite sensitive to the data set utilized. Usually regional data sets are statistically not significant, while the national or global data sets, even if statistically significant, they can represent very different seismotectonic styles that therefore are not mixable. Quite often the coefficients are obtained in such a way that they turn out to be (almost) independent from magnitude, distance and soil type. A nice example of the strong dependence of attenuation laws on the procedure followed in the data processing is given by Parvez et al. (2001) for the Himalayas. Moreover, typically the standard deviation associated with the predictions of the attenuation relationships ranges between 50% and 100% of the mean value.

Introducing the relative decay

$$R_y = y_{rf}/y_{source} \qquad (2)$$

where the suffix "source" indicates the values at the closest instrument to the source (typically D_{source} may be about 2 km), we obtain

$$\log R_y = c(\log r_f - \log r_{source}) + d(D_f - D_{source}) \qquad (3)$$

Thus the relative decay does not depend upon the magnitude (size of the event) and the type of soils (local soil conditions). In general, r_f is different for PGA and PGV because a different conventional depth h_0 is assumed: usually $3 \leq h_0 \leq 10$ km for PGA and PGV The parameter h_0 has a strong influence on the relative decay, conditioning the reliability of the results.

In the particular case of Sabetta and Pugliese (1987) relations (SP87) c=-1, d=0 thus

$$\log R_y = \log r_{source} - \log r_f \qquad (4)$$

and h_0 is 5.8 km for PGA and 3.6 km for PGV

The attenuation relationships utilized by Ambraseys et al. (1996) for the evaluation of peak ground acceleration (PGA), with h_0 equal to 3.5 km, results (AMB96):

$$\log R_y = 0.922\,(\log r_{source} - \log r_f) \qquad (5)$$

Finally, the attenuation law for PGA suggested for the South East Sicily (ASI) by the Authors (Decanini et al., 2001), for h_0=10 km, is:

$$\log R_y = 0.92\,(\log r_{source} - \log r_f) + 0.0005\,(D_{source} - D_f) \qquad (6)$$

These results seem to be in contrast with the physical phenomenon, often observed. For example, it has been found that the PGV and PGD (and consequently energy) attenuate differently with distance than accelerations, depending on the magnitude range and soil type.

The analysis of selected events and of a set of strong motion records, classified accordingly to magnitude intervals and soil conditions, indicates that the trend of the relative decay of AE_I energy hazard parameter (Decanini and Mollaioli, 1998) is not constant. It depends on magnitude and soil type (see Tab. 2 to 6).

If we consider that the energetic parameter AE_I is a good and relatively stable indicator of the global damaging potential of ground motion, it is natural to assume that PGA and PGV cannot follow

	S1			S2		S3
D_f(km)	M (6.5-7.1)	M (5.4-6.2)	M (4.2-5.2)	M (6.5-7.1)	M (5.4-6.2)	M (6.5-7.1)
2.5	1.00	1.00	1.00	1.00	1.00	1.00
8.5	0.34	0.35	0.70	0.49	0.33	0.59
21	0.15	0.18	0.19	0.27	0.12	0.39
30	0.11	0.15	0.07	0.21	0.08	0.32
50	0.07	0.13	0.01	0.13	0.03	0.24

Table 2. Relative attenuation of AE_I as determined from the regression analysis of about 300 recordings worldwide, classified by magnitude (M) and soil type (S1, S2, S3)

	R(PGA)				R(PGV)		R(AE_I)	R(AE_I)$^{0.5}$
D_f(km)	Observ.	SP87	AMB96	ASI	Observ.	SP87	Observ.	Observ.
4.5	1.00	1.00	1.00	1.00	1.00	1.00	1.00	1.00
15	0.88	0.46	0.40	0.62	0.54	0.37	0.52	0.72
19	0.54	0.37	0.33	0.53	0.34	0.30	0.29	0.54
24	0.67	0.30	0.26	0.44	0.28	0.24	0.08	0.28
31.5	0.55	0.23	0.21	0.35	0.27	0.18	0.18	0.42

Table 3. Kobe (1995 event), soft soil (S3), relative attenuation, R, of PGA, PGV and AE_I. Comparison between observed and predicted values.

	R(PGA)				R(PGV)		R(AE_I)	R(AE_I)$^{0.5}$
D_f(km)	Observ.	SP87	AMB96	ASI	Observ.	SP87	Observ.	Observ.
1.0	1.00	1.00	1.00	1.00	1.00	1.00	1.00	1.00
27.5	0.18	0.21	0.15	0.36	0.18	0.14	0.13	0.36
34	0.35	0.17	0.13	0.30	0.25	0.11	0.12	0.35
106	0.17	0.06	0.05	0.10	0.17	0.04	0.05	0.23

Table 4. Kobe (1995 event), soil S2, relative attenuation, R, of PGA, PGV and AE_I. Comparison between observed and predicted values.

	R(PGA)				R(PGV)		R(AE_I)	R(AE_I)$^{0.5}$
D_f(km)	Observ.	SP87	AMB96	ASI	Observ.	SP87	Observ.	Observ.
19.0(*)	1.00	1.00	1.00	1.00	1.00	1.00	1.00	1.00
20.5	0.58	0.93	0.93	0.94	0.45	0.93	0.44	0.66
33	0.46	0.59	0.61	0.64	0.17	0.58	0.34	0.58
36	0.32	0.55	0.56	0.59	0.18	0.53	0.17	0.41

(*)The closest station is as far as 19 km, therefore these data are only indicative (far fault reference)
Table 5. Irpinia (1980 event), soil S2, relative attenuation, R, of PGA, PGV and AE_I. Comparison between observed and predicted values.

	R(PGA)				R(PGV)		$R(AE_I)$	$R(AE_I)^{0.5}$
D_f(km)	Observ.	SP87	AMB96	ASI	Observ.	SP87	Observ.	Observ.
0.2(*)	1.00	1.00	1.00	1.00	1.00	1.00	1.00	1.00
3.2	1.51	0.88	0.76	0.95	0.48	0.75	0.34	0.58
4.8	0.58	0.77	0.62	0.90	0.68	0.60	0.32	0.57
7.3	0.41	0.62	0.46	0.82	0.39	0.44	0.19	0.43
9.0	0.58	0.54	0.39	0.75	0.44	0.37	0.22	0.47
10.2	0.56	0.50	0.36	0.71	0.22	0.33	0.10	0.32

(*)The closest station is at 0.2 km from the surface projection of the source, therefore this is a good example of near fault reference.

Table 6. Imperial Valley (1979 event), soil S2, relative attenuation, R, of PGA, PGV and AE_I. Comparison between observed and predicted values.

the same law of relative attenuation. This is a clear example of the difficulty, which is intrinsic when using attenuation laws. The introduction of the parameter $(AE_I)^{0.5}$ allows a better comparison of therelative decay of destructive potential of earthquake ground motion than peak ground values (PGA and PGV).For the events herein illustrated, and considering the relative decay of PGA, the average values of the ratio Observed/Predicted are: 1.4 for SP87, 1.7 for AMB96, and about 1 for ASI. The ratio corresponding to PGV is about 1.3 for the SP87 relationship.

By considering the specific cases illustrated in Tables 3 to 6, it can be seen that the predictions of the relative attenuation of PGA and PGV are generally in disagreement with the observed values and between the predicted themselves. This aspect evidences the great uncertainties deriving from the existing attenuation functional forms relative to the adopted hazard parameter.

4. Deterministic seismic zoning, hazard assessment and damaging seismic energy

While waiting for the accumulation of new strong motion data, a very useful approach to perform immediate microzonation is the development and use of modeling tools. These tools are based, on one hand, on the theoretical knowledge of the physics of the seismic source and of wave propagation and, on the other hand, exploit the rich database, already available, that can be used for the definition of the source and structural properties. Actually, the realistic modeling of ground motion requires the simultaneous knowledge of the geotechnical, lithological, geophysical parameters and topography of the medium, on one side, and tectonic, historical, palaeoseismological, seismotectonic models, on the other, for the best possible definition of the probable seismic source. The initial stage for the realistic ground motion modeling is thus devoted to the collection of all available data concerning the shallow geology, and the construction of a three-dimensional structural model to be used in the numerical simulation of ground motion.

With these input data, we model the ground motion using two approaches based on the modal-summation technique (Panza, 1985; Panza and Suhadolc, 1987; Florsch et al., 1991; Panza et al., 2001). The hybrid technique (e.g. Fäh et al., 1993), which combines the modal-summation and the finite-difference scheme, and the mode-coupling analytical technique for laterally heterogeneous models (e.g. Vaccari et al., 1989; Romanelli et al., 1996; 1997; Panza et al., 2001).

To minimize the number of free parameters we account for source finiteness by properly weighting the double-couple point source spectrum using the scaling laws of Gusev (1983), as

reported in Aki (1987). Even if this is a rough approximation of the physical source process, when a large earthquake is considered in the calculation of synthetic seismograms at distances of the same order of the fault dimensions, the adoption of a spectral scaling law ensures to obtain reliable spectral scenarios. The adoption of a spectral scaling law corresponds to averaging on the directivity function and on the regional variations due to different tectonic regimes. This limitation is therefore much less severe if spectral or PGA amplification is the main topic of interest instead of actual time-histories, and small- to medium-magnitude events are considered.

However, also kinematics models for a spatially extended source (e.g. Panza and Suhadolc, 1987) can be tackled by our approach. In such a case the generation of seismic waves due to an extended source is obtained by approximating the source with a rectangular plane surface corresponding to the fault plane on which the main rupture process is assumed to occur. Effects of directivity and of the energy release on the fault can be easily modeled, simulating the wide-band radiation process from a finite earthquake source/fault. The source is represented as a grid of point subsources, and their seismic moment rate time functions are generated considering each of them as realizations (sample functions) of a non-stationary random process. Specifying in a realistic way the source length and width, as well as the rupture velocity, one can obtain realistic far-field source time functions. Furthermore, assuming a realistic kinematic description of the rupture process, the stochastic structure of the accelerograms can be reproduced, including the general envelope shape and peak factors.

The methods have been applied, for the purpose of seismic microzoning, to several urban areas like Augusta (e.g. Panza et al., 2000b), Beijing (Sun et al., 1998), Benevento (e.g. Marrara and Suhadolc, 1998a), Bucharest (e.g. Moldoveanu et al., 2000), Catania (e.g. Romanelli and Vaccari, 1999), Mexico City (e.g. Fäh et al., 1994), Naples (e.g. Nunziata et al., 2000a,b), Rome (e.g. Fäh et al., 1993) and Thessaloniki (e.g. Marrara and Suhadolc, 1998b) in the framework of the UNESCO/IUGS/IGCP project "Realistic Modelling of Seismic Input for Megacities and Large Urban Areas" (Panza et al., 1999a). For urban areas where the realistic numerical modeling has been compared with recorded data (like Beijng, Benevento, Bucharest, Mexico City, Naples, Thessaloniki), the results of such comparison is fully satisfactory for engineering purposes and no data fitting is required. For events with magnitude in the range 6.5-7.1 and distances in the range 10-30 km, these pilot studies show that, distances from the causative fault, D_f, being equal, the elastic energy spectra computed from synthetic signals are comparable with those computed from real records (e.g. see Fig. 3)

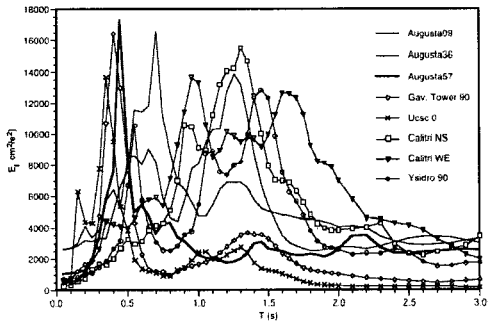

Fig. 3. Elastic energy E_I (cm^2/s^2) spectra. Comparison between Augusta synthetic signals and strong motion records of Irpinia 1980 (Calitri station) and Loma Prieta 1989 (Gav Tower, Ucsc and Ysidro stations) earthquakes (from Decanini et al., 2001).

Thus, where recordings are absent or very limited, the synthetic time series can be reasonably used to estimate the expected ground motion, including ground velocity and displacement time series, before the next strong earthquake will occur. These time series can be readily used for the estimation of the damaging potential in energetic terms (Fig. 3).

4.1 Umbria-Marche (Central Italy) sequence

The Umbria-Marche earthquake sequence started on September 26, 1997 and took place in a complex deforming zone, along a normal fault system in the Central Apennines. The seismic sequence left significant ground effects, which were mainly concentrated in the Colfiorito intermountain basin.

The crustal events generated extensive ground motion and caused great damage in several urban areas. The extent of macroseismic data and the abundance of recorded ground motions permits a good knowledge of the source and structural parameters to better understand the nature of the ground shaking and the resulting damage patterns.

Predicting the intensity of shaking due to an earthquake before it occurs can prevent damage. Doing this rapidly after an earthquake can be useful for emergency rescue.

These objectives all belong to the overall objective of understanding and predicting the ground motion, therefore reducing the seismic risk.

Before the seismic sequence, started on September 1997, probabilistic (Fig 4) and deterministic maps were available for the Italian territory. The probabilistic map (Fig 4) indicates, for the Umbria-Marche region, peak ground accelerations (PGA) not exceeding 0.4g, for 475 years return period, and 0.24g, for 100 years return period (Corsanego et al. 1997). A first-order deterministic seismic zoning of Italy (Fig. 5), obtained by the application of the method developed by Costa et al. (1993) and its extensions (Panza et al., 1996) lead to theoretical peak values (Panza et al., 1996; 1997; 1999b) well in agreement with the representative EPA (effective peak acceleration) values observed ~ 0.3g. The EPA is defined as the average spectral acceleration in the period interval from 0.1 s to 0.5 s divided by 2.5, therefore it is equivalent to the DGA calculated by Panza et al. (1996) using design response spectra.

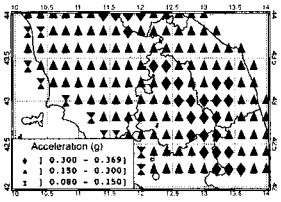

Fig. 4. Probabilistic estimation of maximum acceleration for 475 years return period (from Corsanego et al., 1997).

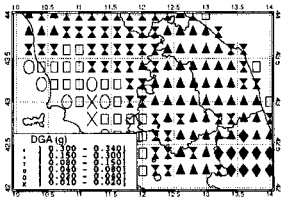

Fig. 5. Deterministic design ground acceleration focussed on the Umbria-Marche region (modified from Panza et al., 1996).

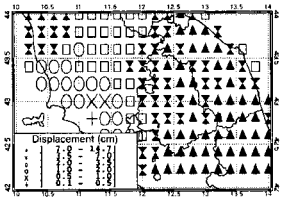

Fig. 6. Computed peak ground displacements, consistent with the acceleration values given in Fig. 5.

The information about ground displacement can be of great importance, but such information is difficult to be extracted from analog recordings, thus the available experimental database is very scarce. The realistic ground motion modelling we have developed represents an efficient way to

minimize the problem arising from the lack of statistically significant observations about ground displacement. In fact, the good agreement obtained between modeled and observed acceleration and velocities makes it reasonable to use the modeled displacements (Fig. 6), as boundary conditions in the design.

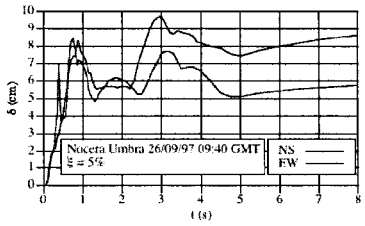

Fig.7 Displacement spectra of Nocera Umbra strong motion records (rock site). 5% damping. Event of September26, 1997, 09:40 GMT, $M_L = 5.8$, $M_W = 6.0$.

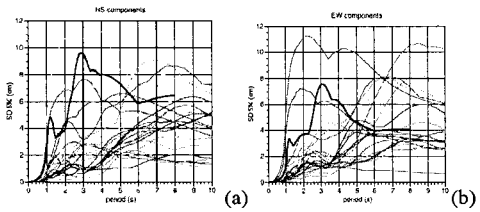

Fig. 8. a) Displacement response spectra (5% damping) computed at the grid point close to Nocera Umbra for 23 sources located in the surroundings at distances between 13 and 90 km. Thick black line corresponds to the spectrum of the signal, NS component of motion, recorded at Nocera Umbra (R1168), filtered at 1 Hz. b) Same as a) but for the EW component of motion.

The displacement response spectra (5% damping) of the observed signals are shown in Fig. 7 for the NS and EW components of motion recorded at Nocera Umbra during the main shock of the sequence. The same kind of response spectra, but obtained with the observed signals filtered with the cut off frequency used in our modeling (1 Hz), are compared (Fig. 8) with the displacement response spectra obtained from all the synthetic signals computed in the grid point (43.2°N, 12.8°E), i.e. the grid point closer to Nocera Umbra. The predictive capabilities of our modeling, made in 1996, are quite evident and indicate that future events may generate even larger seismic input.

4.2 Bovec event of Easter 1998

For Bovec, Slovenia, event (12 April 1998) the only available strong motion records belong to the Rete Accelerometrica of Friuli Venezia Giulia (RAF) (minimum epicentral distance >30 km), therefore the only relevant comparison is with the epicentral macroseismic intensity, which has been observed equal to IX (MCS).

From the deterministic maps shown in Fig. 9 and considering the conversion tables between peak values of ground motion and macroseismic intensity (MCS), proposed by Panza et al. (1999), the epicentral macroseismic values observed, IX (MSC), are in perfect agreement with the values predicted by our modelling.

5. Conclusions

Case studies of seismic hazard assessment techniques indicate the limits of the currently used methodologies, deeply rooted in engineering practice, based prevalently on a probabilistic approach,

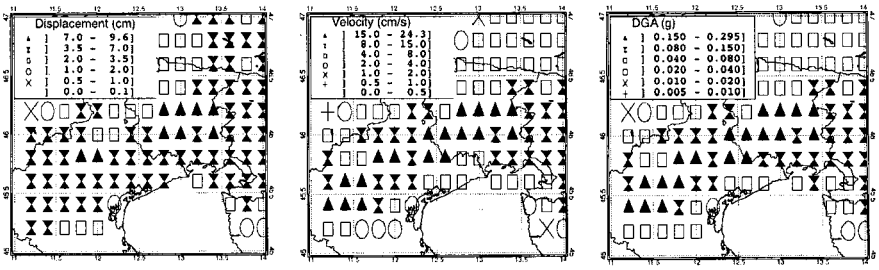

Fig. 9. Deterministic peak ground displacement, velocity and EPA=DGA, computed by Panza et al. (1996; 1997; 1999b).

and show that the related analyses are not sufficiently reliable to characterize seismic hazard. The probabilistic analysis of the seismic hazard is basically conditioned by the definition of the seismogenic zones. Within each of them the seismogenic process is assumed to be rather uniform, however the uncritical assumption of homogeneity can introduce severe errors in the estimate of the seismic hazard in a given site. Further shortcomings are connected with the choice of the other components needed for the calculation of the rate of probability of exceeding various levels of ground motion, over a specified period of time, i.e. the parameters characteristic of the damage potential of earthquake ground motion, and the attenuation relationships for the estimation of the ground motion at a site for a given earthquake.

The quantification of the critical ground motion expected at a particular site, requires the identification of the parameters that characterize the severity and the damage potential. Such critical ground motion can be identified in terms of energy and displacement demands which should be evaluated by considering the seismological, geological, and topographic factors that affect them.

In view of the limited seismological data, it seems more appropriate to resort to a scenario-based deterministic approach, as it allows us the realistic definition of hazard in scenario-like format to be accompanied by the determination of advanced hazard indicators as, for instance, damaging potential in terms of energy. Such a determination, due to the limitation of the number of strong motion records, requires to resort to broad band synthetic seismograms, that allow us to perform realistic waveform modeling for different seismotectonic environments, taking into account source properties (e.g. dimensions, directivity, duration, etc.), lateral heterogeneities, and path effects.

Each synthetic strong ground motion history, characterized as a function of its damage potential, constitutes a useful addition to the records database which increases our choices in selecting acceleration histories for various analyses. The growing database for near-field and soft soil strong motion signals (recorded and modeled), which can be considered as limit conditions, gives the opportunity to enhance the state of knowledge in damage potential evaluation.

The results we have reported are the outcome of a rather unusual but very fruitful close collaboration between seismologists and seismic engineers, that we consider a prerequisite for the achievement of significant step forward in the future.

Appendix: Parameters used to describe the severity of an earthquake

A fundamental need for the definition of the seismic hazard of a given site or, in general, a region, is to select a parameter descriptive of the earthquake severity. A large number of parameters has been proposed for measuring the capacity of earthquakes to damage structures. However, recently observed damage distribution and strong motion acceleration records indicate the need for a more comprehensive definition of the existing parameters and for the introduction of new ones to account for the complex characteristics of earthquake induced strong ground motions in the engineering analysis and design. The adoption of inadequate parameters can lead to the definition of unrealistic design earthquakes and consequently to the unreliable evaluation of the seismic risk for the existing built environment, or to the insufficient protection of new one.

The parameters fundamentally involved in the evaluation of the level of severity associated with strong motion are, for engineering purposes, the frequency content, the amplitude and the effective duration. Because of the complexity of the earthquake ground motions, generally more than one parameter is required to describe the most important ground motion characteristics.

In general, these parameters can be obtained either directly or with some simple calculation from the digitized and corrected records, from the parametric integration of the equation of motion of elastic and inelastic single-degree-of-freedom (SDOF) systems, and considering the energy balance equation for elastic and inelastic systems. Application of the Duhamel (convolution) integral to a linear elastic SDOF system gives the expressions for the displacement response time history u(t) and allows to define a pseudo-velocity, $v(t)= \omega\, u(t)$, and a pseudo-acceleration, $a(t)= \omega^2\, u(t)$ (Clough & Penzien 1993, Chopra, 1995). They get their names from the fact that they have units of velocity and acceleration, respectively, but they are not equal to instantaneous velocity, and acceleration, respectively, of the system, since earthquake time histories are far from being purely harmonic motions. In terms of peak values, one can define the displacement, pseudo-velocity and pseudo-acceleration response spectra:

$$S_d(x,\omega) = |u|_{max}, \qquad S_d(x,\omega) = \frac{1}{\omega} S_{pv}(x,\omega); \qquad S_{pa}(x,\omega) = \omega S_{pv}(x,\omega)$$

where ω is the natural frequency (spectral variable) of the SDOF, u is the displacement, $S_d(\xi,\omega)$ is the spectral displacement $S_{pv}(\xi,\omega)$ is the pseudo-spectral velocity, and $S_{pa}(\xi,\omega)$ is the pseudo-spectral acceleration. Accordingly with the following equation, the pseudo-velocity $S_{pv}(\xi,\omega)$ can be related to the maximum energy stored in the SDOF during the earthquake ground motions:

$$E = \frac{k S_d^2(x,\omega)}{2} = \frac{k S_{pv}^2(x,\omega)/\omega^2}{2} = \frac{m S_{pv}^2(x,\omega)}{2}$$

where k and m are the stiffness and the mass of the SDOF systems. Note that a SDOF system of zero natural period (infinite natural frequency) would be rigid, and its spectral acceleration would be equal to the peak ground acceleration.

PGA, PGV, PGD, EPA and EPV

The most commonly used measure of amplitude of a particular ground motion is the peak ground acceleration, PGA, which corresponds to the largest value of acceleration obtained from the recorded accelerogram. As the inertia forces depend directly on acceleration, PGA is one of the parameters widely used to describe the intensity and damage potential of an earthquake at a given site. However, PGA is a poor indicator of damage, since it has been observed that time histories with the same PGA

could be very different in frequency content, strong motion duration, and energy level, thus causing varying amounts of damage. In fact, PGA may be associated with high frequency pulses which do not produce significant damage to the buildings as most of the impulse is absorbed by the inertia of the structure with little deformation. On the other hand, a more moderate acceleration may be associated with a long-duration pulse of low-frequency (acceleration pulse) which gives rise to a significant deformation of the structure.

For example, after the 1971 Ancona earthquake (M_L = 4.7) a large PGA value (716 cm/s^2) was recorded at the Rocca station, located at a distance of about 7 km from the surface projection of the fault rupture. This high PGA value is associated with a short duration pulse of high frequency, as indicated in Fig. A1 where the acceleration time histories is shown, and generated a limited damage. A peak ground acceleration quite close (827 cm/s^2) to the above mentioned one, was recorded at the Sylmar station (Fig. A2), sited at about 2 km from the surface projection of the fault rupture, after the destructive 1994 Northridge earthquake (M_w=6.7). In this case, the peak ground acceleration is associated with a long duration pulse of low frequency. The moderate difference between these two PGA values seems to disagree with the large difference between the magnitude of the two seismic events. In other words, analyses of strong motion data have shown clearly that even small earthquakes can produce high accelerations and that these accelerations are not necessarily damaging.

The peak ground velocity PGV (shown in Fig. A3) is another useful parameter for the characterization of ground motion amplitude. Since the velocity is less sensitive to the higher-frequency components of the ground motion, the PGV, more likely than the PGA, should characterize the damaging potential of ground motion.

Peak ground displacement PGD is generally associated with the lower-frequency components of an earthquake ground motion. It is, however, difficult to determine accurately PGD, due to signal processing errors in the filtering and integration of accelerograms and due to long-period noise. The situation will certainly improve with the dissemination of good quality digital instruments.

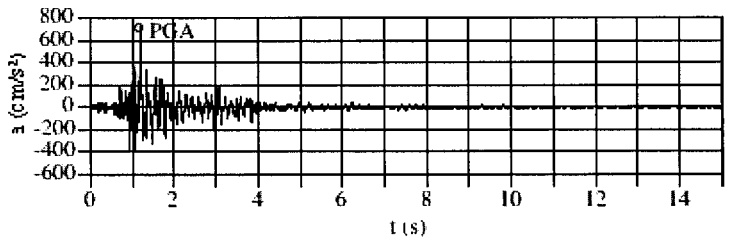

Fig. A1. 1971 Ancona earthquake (M_L=4.7); acceleration time history: Rocca NS record.

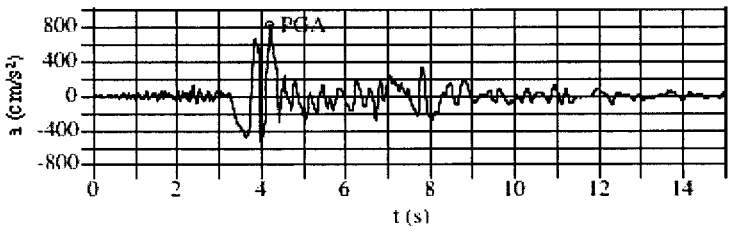

Fig. A2. 1994 Northridge earthquake (M_w=6.7); acceleration time history: Sylmar N360 record.

From the point of view of damage potential, the area under the largest acceleration pulse, which represents the incremental velocity (IV), makes many earthquake strong motion records particularly damaging. As indicated in Fig.A3, the maximum incremental velocity represents the distance between two consecutive peaks. The larger is the change in velocity, the larger is the acceleration pulse. In the case of the Takatori record obtained after the 1995 Kobe earthquake (Fig.3), the PGV is equal to 127 cm/s, while the IV is equal to 227 cm/s).

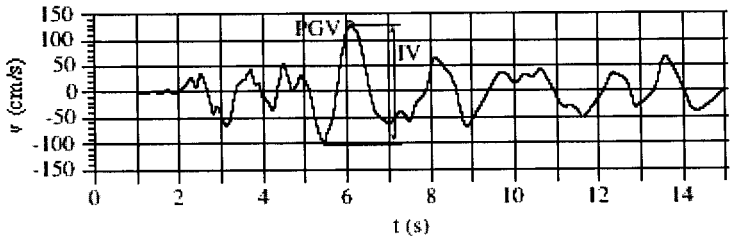

Fig. A3 – Velocity time history. Takatori 000 record. 1995 Kobe earthquake (M_w=6.9)

Realizing the limitation of using peak instrumental values, since damage can not be related only to the peak values, but it may require the occurrence of several repeated cycles, Applied Technology Council (1978) ATC introduced the concept of effective peak acceleration, EPA. The effective peak acceleration EPA is defined as the average spectral acceleration over the period range 0.1 to 0.5 s divided by 2.5 (the standard amplification factor for a 5% damping spectrum), as follows:

$$EPA = \frac{\overline{S}_{pa}}{2.5}$$

where $\overline{S}_{pa}$ is the mean pseudo-acceleration value. The empirical constant 2.5 is essentially an amplification factor of the response spectrum obtained from real peak value records. Thus EPA is correlated with the real peak value, but not equal to nor even proportional to it. If the ground motion consists of high frequency components, EPA will be obviously smaller than the real peak value. It represents the acceleration which is most closely related to the structural response and to the damage potential of an earthquake. The EPA values for the two records of Ancona and Sylmar stations are 205 cm/s^2 and 774 cm/s^2 respectively, and describe in a more appropriate way, than PGA values, the damage caused by the two earthquakes.

The effective peak velocity EPV is defined as the average spectral velocity at a period of 1 s divided by 2.5. The process of averaging the spectral accelerations and velocities over a range of periods minimizes the influence on the EPA and EPV of local spikes in the response spectrum. EPA and EPV can be thought of as normalizing factors for the development of smooth response spectra. Although effective peak acceleration is a conceptually sound parameter for the damage potential characterization of earthquake ground motion, at present there is no clear and standardized definition of this parameter.

Other ground motion parameters

Several observations derived from analyses of strong motion records of recent earthquakes indicate the considerable influence of the duration on the cumulative damage of the structures. For example, time histories with high amplitudes but short duration can be associated to moderate damages compared to ground motion with lowest amplitude but with longest duration. Moreover, it is

well known that the major drawback in the use of elastic response spectra, S_{pa}, is the neglecting of the duration. Different approaches have been taken to the problem of evaluating the duration of strong motion in an accelerogram. The bracketed duration (Bolt, 1973) is defined as the time between the first and the last exceedances of a threshold acceleration (usually 0.05g). Among the different duration definitions that can be found in the literature, one commonly used is that proposed by Trifunac and Brady (1975), $t_D = t_{0.95} - t_{0.05}$, where $t_{0.05}$ and $t_{0.95}$ are the time at which respectively the 5% and 95%, of the time integral of the history of squared accelerations are reached, which corresponds to the time interval between the points at which 5% and 95% of the total energy has been recorded.
The Arias Intensity (Arias, 1969), I_A, is defined as:

$$I_A = \frac{p}{2g}\int_0^{t_t} a_g^2(t)dt,$$

where t_t and a_g are the total duration and ground acceleration of a ground motion record, respectively. The Arias intensity has units of velocity. I_A represents the sum of the total energies, per unit mass, stored, at the end of the earthquake ground motion, in a population of undamped linear oscillators. Arias Intensity, which is a measure of the global energy transmitted to an elastic system, tends to overestimate the intensity of an earthquake with long duration, high acceleration and broad band frequency content. Since it is obtained by integration over the entire duration rather than over the duration of strong motion, its value is independent of the method used to define the duration of strong motion.

Housner (1952) defined a measure expressing the relative severity of earthquakes in terms of the area under the pseudo-velocity spectrum between 0.1 and 2.5 seconds. Housner's spectral intensity I_H is defined as:

$$I_H = \int_{0.1}^{2.5} S_{pv}(T,\xi)\,dT = \frac{1}{2\pi}\int_{0.1}^{2.5} S_{pa}(T,\xi)\,TdT,$$

where S_{pv} is the pseudo-velocity at the undamped natural period T and damping ratio ξ, and S_{pa} is the pseudo-acceleration at the undamped natural period T and damping ratio ξ. Thus, Housner's spectral intensity is the first moment of the area of S_{pa} ($0.1<T<2.5$) about the S_{pa} axis, implying that the Housner spectral intensity is larger for ground motions with a significant amount of low frequency content. The I_H parameter captures important aspects of the amplitude and frequency content in a single parameter, however, it does not provide information on the strong motion duration which is important for a structural system experiencing inelastic behaviour and yielding reversals. Housner (1956) gave also a definition of the maximum input energy of an elastic SDOF system on the basis of the pseudo-velocity spectrum S_{pv}. In fact, the pseudo-velocity spectrum S_{pv} reflects the energy demand of an elastic SDOF system as follows:

$$E_v = \frac{1}{2}m\left(S_{pv}\right)^2$$

This parameter can be utilized for the estimation of earthquake damage potential from an energy perspective. The pseudo-velocity spectrum constitutes approximately the lower bound of the hysteretic energy spectrum adjusted in terms of equivalent velocity (Decanini & Mollaioli 1998, Uang & Bertero, 1988).

Araya & Saragoni (1984) proposed the destructiveness potential factor, P_D, that considers both the Arias Intensity and the rate of zero crossings, ν_0 and agrees with the observed damage better than other parameters. The destructiveness potential factor, which simultaneously considers the effect of the ground motion amplitude, strong motion duration, and frequency content on the relative destructiveness of different ground motion records, is defined as:

$$P_D = \frac{\pi}{2g}\frac{\int_0^{t_0} a_g^2(t)dt}{\nu_0^2} = \frac{I_A}{\nu_0^2} \qquad \nu_0 = \frac{N_0}{t_0}$$

where t is the time, a_g is the ground acceleration, $\nu_0 = N_0/t_0$ is the number of zero crossings of the acceleration time history per unit of time (Fig. A4), N_0 is the number of the crossings with the time axis, t_0 is the total duration of the examined record (sometimes it could be a particular time-window), and I_A is the Arias intensity.

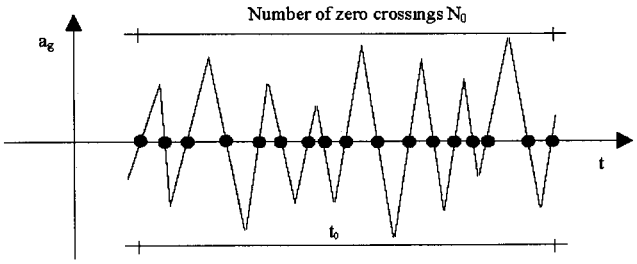

Fig. A4. Evaluation of the parameter ν_0.

The amplitudes of ground motion acceleration and strong motion duration are incorporated in the Arias intensity, while ν_0 [sec-1] results an average index of the frequency content of the time history. Araya and Saragoni (1984) and Saragoni et al. (1989) have shown that the horizontal earthquake destructiveness potential factor PDH (sum of the PD values corresponding to the two horizontal components, PDH=PDx+PDy) correlates well with the Modified Mercalli macroseismic Intensity I_{MM} values. However, it is possible that two different time histories have similar destructiveness potential factors but very different values of the zero crossings rate and Arias intensity. A time history with a small zero-crossing rate would cause less damage to short period structures than a time history with a larger zero-crossing rate close to the fundamental period of the structures, although both time histories have the same destructiveness potential factor.

In designing structures to perform satisfactorily under earthquake excitations the concept of response spectrum was introduced as a practical mean of characterizing ground motions and their effects on structures. The response spectrum, a concept that has been recognized for many years in the literature (e.g., Newmark & Hall 1982), describes the maximum response of a SDOF system to a particular input motion as a function of its natural frequency (or period) and damping ratio. The response may be expressed in terms of acceleration, velocity, or displacement. The importance of the response spectra in earthquake engineering has led to the development of methods for predicting them directly as a function of soil conditions, magnitude and source-to-site conditions. Response spectra are often used to represent seismic loading in terms of design spectra, which are the result of the smoothing, averaging or enveloping of the response spectra of multiple motions.

Although the response spectrum provides the basis for the specification of design ground motions in all current design guidelines and code provisions, there is a growing recognition that the response spectrum alone does not provide an adequate characterization of the earthquake ground motion. In order to give a major conceptual improvement, methods using ground motion spectra based on EPA and EPV have been suggested.

Energy based parameters

Linear elastic response spectra or linear elastic design response spectra recommended by seismic codes have been proved to be inadequate by recent seismic events, as they are not directly related to structural damage. Extremely important factors such as the duration of the strong ground motion and the sequence of acceleration pulses are not taken into account adequately. Therefore response parameters based on the inelastic behaviour of a structure should be considered with the ground motion characteristics.

In current seismic regulations, the displacement ductility ratio μ is generally used to reduce the elastic design forces to a level which implicitly considers the possibility that a certain degree of inelastic deformations could occur. To this purpose, employing numerical methods, constant ductility response spectra were derived through non-linear dynamic analyses of viscously damped SDOF systems by defining the following two parameters:

$$C_y = \frac{R_y}{mg}$$

$$\eta = \frac{R_y}{m\ddot{u}_{g(max)}} = \frac{C_y}{\ddot{u}_{g(max)}/g}$$

where R_y is the yielding resistance, m is the mass of the system, and $\ddot{u}_{g(max)}$ is the maximum ground acceleration. The parameter C_y represents the structure's yielding seismic resistance coefficient and η expresses a system's yield strength relative to the maximum inertia force of an infinitely rigid system and reveals the strength of the system as a fraction of its weight relative to the peak ground acceleration expressed as a fraction of gravity. Traditionally, displacement ductility was used as the main parameter to measure the degree of damage sustained by a structure.

One significant disadvantage of seismic resistance (C_y) spectra is that the effect of strong motion duration is not considered. An example of constant ductility C_y spectra, corresponding to the 1986 San Salvador earthquake (CIG record) and 1985 Chile earthquake (Llolleo record) is reported in Fig. A5 a,b, respectively By comparing these spectra it seems that the damage potential of these ground motions is quite similar, even though the CIG and Llolleo are records of two earthquakes with very different magnitude, 5.4 and 7.8, respectively.

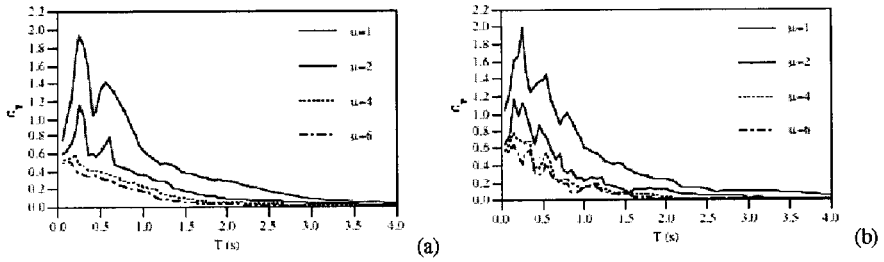

Fig. A5. Comparison between constant ductility C_y spectra. (a) 1986 San Salvador earthquake (CIG record); 1985 Chile earthquake (Llolleo record)

In other words, the elastic and inelastic (in terms of displacement ductility) response spectra are not sufficient for the estimation of the damage potential of the earthquake ground motion because they do not give a precise description of the quantity of the energy that will be dissipated through hysteretic behaviour; in the inelastic case they give only the value of the maximum ductility requirement. To overcome this problem other ductility definitions, e.g. hysteretic or cyclic ductility, were introduced.

However, in this context, the introduction of appropriate parameters defined in terms of energy can lead to more reliable estimates, since, more than others, the concept of energy provides tools which allow to account rationally for the mechanisms of generation, transmission and destructiveness of seismic actions. Moreover, energy-based parameters could provide more insight into the ultimate cyclic seismic performance than traditional design methods do, and could be considered as effective tools for a comprehensive interpretation of the behaviour observed during recent destructive events. In fact, energy-based parameters, allowing us to characterize properly the different types of time histories (impulsive, periodic with long durations pulses, etc.) which may correspond to an earthquake, could provide more insight into the seismic performance.

Among all the different parameters proposed for defining the damage potential, perhaps the most promising is the Earthquake Input Energy (E_I) and associate parameters (the damping energy E_ξ and the plastic hysteretic energy E_H) introduced by Uang & Bertero (1990). This parameter considers the inelastic behavior of a structural system and depends on the dynamic features of both the strong motion and the structure. The formulation of the energy parameters derives from the following balance energy equation (Uang & Bertero, 1990), $E_I = E_k + E_\xi + E_s + E_H$, where ($E_I$) is the input energy, ($E_k$) is the kinetic energy, (E_ξ) is the damping energy, (E_s) is the elastic strain energy, and (E_H) is the hysteretic energy.

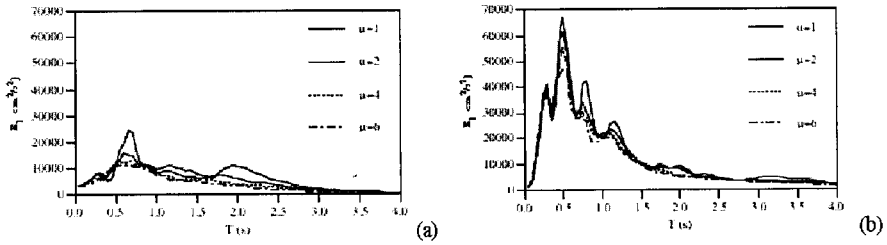

Fig. A6 – Comparison between constant ductility input energy E_I spectra. (a) 1986 San Salvador earthquake (CIG record); 1985 Chile earthquake (Llolleo record)

The absolute input energy, according to the definition of Uang & Bertero (1990), which seems suitable for the estimation of the energy terms in the range of periods of interest for the majority of structures, has the advantage to point to the physical input energy. In fact, E_I represents the work done by the total base shear at the foundation displacement. The input energy can be expressed by:

$$\frac{E_I}{m} = \int \ddot{u}_t du_g = \int \ddot{u}_t u_g dt$$

where m is the mass, $u_t = u + u_g$ is the absolute displacement of the mass, and u_g is the earthquake ground displacement. Usually the input energy per unit mass, i.e. E_I/m, is simply denoted as E_I.

Re-examining the comparison of the damage potential of the CIG and Llolleo records in terms of input energy (Fig. A6), a completely different picture is obtained. In fact, the E_I of the Llolleo record is considerably higher than that of the CIG record, both in the elastic and inelastic cases.

A similar picture is obtained using another energy-based parameter, recently introduced (Decanini et al. 1994, Decanini & Mollaioli 1998) and denoted as *seismic hazard energy factor*, AE_I, which represents the area enclosed by the elastic input energy spectrum according to different intervals of periods:

$$AE_I = \int_{T_1}^{T_2} E_I(\xi = 5\%, T)\, dT$$

In their procedure for the evaluation of the design earthquake Decanini and Mollaioli (1998) consider the interval of periods between T_1=0.05 and T_2=4.0 seconds.

The advantage of using AE_I derives from the fact that, unlike the peak energy spectral value, which generally corresponds to a narrow band of frequencies, it takes into account the global energy structural response amount, and therefore it is the most stable parameter in energetic analysis. AE_I can be seen as the energy version of the Housner Intensity I_H, with the difference that the pseudo-velocity spectrum constitutes the lower bound of the input energy spectrum (Uang & Bertero, 1988), as illustrated in Fig. A7

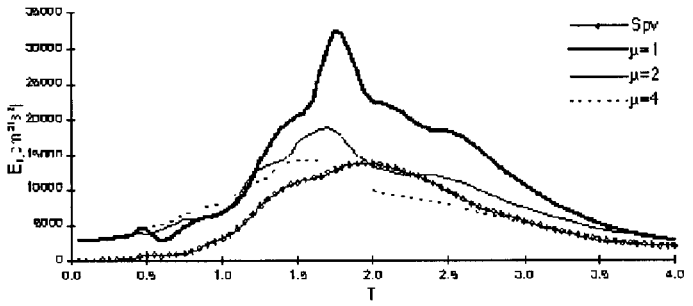

Fig. A7 – Comparison between input energy E_I and pseudo-velocity S_{pv} spectra. 1977 Bucarest earthquake

In conclusion, for a reliable estimation of the destructiveness potential of earthquake ground motions it seems appropriate to perform a comparison of their input and hysteretic energy spectra and associated seismic hazard energy factors, taking also into account the influence of the factors that may be considered external to the structural systems (magnitude, local soil conditions, source-to-site distance, etc.).

References

Aki, K, 1987, *"Strong motion seismology"* In: Strong ground motion seismology. M. Erdik and M. Toksöz (Editors), NATO ASI Series, Series C: Mathematical and Physical Sciences, D. Reidel Publishing Company, Dordrecht, 204, 3-39

Akiyama, H., 1985, *"Earthquake-Resistant Limit-State Design for Buildings"* University of Tokyo Press.

Ambraseys N.N., Simpson K.A., Bommer J.J. (1996), *"Prediction of horizontal response spectra in Europe"* Earthquake Engineering and Structural Dynamics, 25, 371-400.

Applied Technology Council,1978, *"Tentative Provisions for the Development of Seismic Regulations for Buildings"* U.S. National Bureau of Standards, Special Publication 510, 1978.

Araya, R., Der Kiureghian, A., 1988, *"Seismic Hazard Analysis: Improved Models, Uncertainties and Sensitivities"* Report No. UCB/EERC-90/11, Earthquake Engineering Research Center, University of California at Berkeley, March 1988.

Araya, R. and Saragoni, R., 1984, *"Earthquake accelerogram destructiveness potential factor"* Proc. 8th WCEE, San Francisco, USA, 1984, vol.2, 835-841.

Arias A., 1969, *"A Measure of Earthquake Intensity"* Massachusetts Institute of Technology, Cambridge, Massachusetts.

Bak, P., Tang, C., 1989, *"Earthquakes as a self-organized critical phenomenon"* J. Geophys. Res., 94, 15635-15637

Båth, M., 1973, *"Introduction to Seismology"* Birkhauser, Basel.

Bertero, V. V., 1989, *"Lesson learned from recent catastrophic earthquake and associated research"* First Torroja International Lecture, 1989 ICCET.

Bertero, V V., Uang, C. M., 1992, *"Issues and future directions in the use of energy approach for seismic-resistant design of structures"* In: Nonlinear Seismic Analysis of RC Buildings, 3-22, Elsevier.

Boatwright, J., Fletcher, J.B., Fumal, T., 1991, *"A general inversion scheme for source, site and propagation characteristics using multiply recorded sets of moderate size earthquakes"* Bull. Seism. Soc. Am., 81, 1754-1782.

Bolt, B.A., 1973, *"Duration of strong ground motion"*, Proceedings 5th World Conference on Earthquake Engineering, Rome, Italy, Vol.1, 1304-1313.

Bolt, B.A., 1983, *"The contribution of directivity focusing to earthquake intensities"*, Report 20, U.S. Army Corps of Engineers, Waterways Experiment Station, Vicksburg.

Borcherdt, R.D., 1970, *"Effects of local geology on ground motion near San Francisco Bay"* Bull. Seism. Soc. Am., 60, 29-61.

Chandler, A.M., Lam, N.T.K., Wilson, J.L., Hutchinson, G.L., 2001, *"Response spectrum for regions lacking earthquake records"* Electronic Journal of Structural Engineering, 1, 60-73.

Chopra A.K., 1995, *"Dynamics of Structure. Theory and Applications to Earthquake Engineering"*, Prentice Hall, Upper Saddle River, New Jersey.

Clough R.W., Penzien J. 1993, *"Dynamics of Structures"*, McGraw-Hill Inc., Second edition, Singapore.

Corsanego, A., Faccioli, E., Gavarini, C., Scandone, P., Slejko, D., Stucchi, M., 1997, *"L'attivita' nel triennio 1993-1995"* CNR – Gruppo Nazionale per la Difesa dai Terremoti, Rome.

Costa, G., Panza, G.F., Suhadolc, P., Vaccari, F., 1993, *"Zoning of the Italian territory in terms of expected peak ground acceleration derived from complete synthetic seismograms"* J. Appl. Geophys., 30, 149-160.

Decanini, L., Mollaioli, F., 1998, *"Formulation of Elastic Earthquake Input Energy Spectra"* Earthquake Engineering and Structural Dynamics, 27, 1503-1522.

Decanini, L., Mollaioli, F., 2001, *"An energy-based methodology for the assessment of the seismic demand"* Soil Dynamics and Earthquake Engineering, 21, 113-137

Decanini, L., Mollaioli, F., Panza, G. F., Romanelli, F., 1999, *"The realistic definition of the seismic input: an application to the Catania area"* Earthquake Resistant Engineering Structures II (G. Oliveto and C.A. Brebbia eds.), WIT press, Boston, 425-434.

Decanini, L., Mollaioli, F., Panza, G. F., Romanelli, F., Vaccari, F., 2001, *"Pericolosità sismica della Sicilia sud orientale. Terremoti di scenario per Augusta, Siracusa e Noto"*. In Scenari di pericolosità sismica ad Augusta, Siracusa e Noto (A cura di L. Decanini e G.F Panza), CNR-Gruppo Nazionale per la Difesa dai Terremoti, Roma, 80-151.

Decanini, L., Mollaioli, F., Saragoni, R., 2000, *"Energy and Displacement Demands Imposed by Near-Source Ground Motions"* 12th World Conference on Earthquake Engineering, Auckland, New Zealand, 30 January-4 February 2000.

Decanini, L., Mollaioli, F., Oliveto, G., 1994, "Observations and lessons learned from the earthquake of 13th December 1990 in South-East Sicily Proc. of the 10th European Conference on Earthquake Engineering, Duma ed. 1995 Balkema, Wien, 1935-1943.

Esteva, L., 1970, *"Seismicity Risk and Seismic Design Decisions"* Seismic Design for Nuclear Power Plants, ed. R.J. Hansen, M.I.T. Press, Cambridge, Mass.

Fäh, D., Iodice, C., Suhadolc, P., Panza, G.F, 1993, *"A new method for the realistic estimation of seismic ground motion in megacities: the case of Rome"*. Earthquake Spectra, 9, 643-668.

Fäh, D., Suhadolc, P., Mueller, St., Panza, G.F., 1994, *"A hybrid method for the estimation of ground motion in sedimentary basins: quantitative modelling for Mexico City"* Bull. Seism. Soc. Am., 84, 383--399.

Fajfar, P., Fishinger, M., 1990, *"A seismic design procedure including energy concept"* Proc. 9th ECEE, Moscow, 2, 312-321.

Field, E.H., the SCEC Phase III Working Group, 2000, *"Accounting for site effects in probabilistic seismic hazard analyses of Southern California: overview of the SCEC Phase III report"* Bull. Seism. Soc. Am., 90, 6B, S1-S31.

Florsch, N., Fäh, D., Suhadolc, P., Panza, G.F., 1991, *"Complete Synthetic Seismograms for High-Frequency Multimode SH-Waves"* PAGEOPH , 136, 529-560.

Gusev, A. A., 1983, *"Descriptive statistical model of earthquake source radiation and its application to an estimation of short period strong motion"* Geophys. J. R. Astron. Soc. 74, 787-800.

Hagiwara, Y., 1974, *"Probability of Earthquake Occurrence as obtained from a Weibull Distribution Analysis of Crustal Strain"* Tectonophysics, 23, 313-318.

Heaton, T. H., Hall, J. F., Wald, D. J., Halling, M. W., 1995, *"Response of High Rise and Base Isolated Buildings to Hypothetical M_W 7.0 Blind Thrust Earthquake"* Science Magazine, 267, 206-211.

Housner, G.W., 1952, *"Spectrum Intensities of Strong Motion Earthquakes*. Proc. Symposium of Earthquake and Blast Effects on Structures, EERI, Los Angeles, California, 1952, 21-36.

Housner, G. W., 1956,"Limit design of structures to resist earthquakes. *Proc. of the 1st World Conference on Earthquake Engineering, Berkeley, California*, 5.1-5.13.

Krawinkler, H., 1997, *"Impact of Duration/Energy in Design"* Proceedings of the FHWA/NCEER Workshop on the National Representation of Seismic Ground Motion for New and Existing Highway Facilities (Friedland, Power, Mayes Eds.), Technical Report NCEER-97-0010.

Langston, C.A., 1979, *"Structure under Mount Rainier, Washington, inferred from teleseismic body waves"* J. Geophys. Res., 84, 4749-4762.

Marrara, F., Suhadolc, P., 1998a, *"Site amplifications in the city of Benevento (Italy): comparison of observed and estimated ground motion from explosive sources"* J. Seism., 2, 125-143.

Marrara, F., Suhadolc, P., 1998b, *"Observation and modelling of site effects in the Volvi basin, Greece"* In: The effects of surface geology on Seismic Motion. K. Irikura, K. Kudo, H. Okada and T. Sasatani (Editors), Balkema, Rotterdam, The Netherlands, 973-980.

Meletti, C., Patacca, E., Scandone, P., 2000, *"Construction of a seismotectonic model"* PAGEOPH., 157, 11-35.

Molchan, G., Kronrod, T., Panza, G. F., 1997, *"Multi-scale seismicity model for seismic risk"* Bull. Seism. Soc. Am., 87, 1220-1229

Moldoveanu, C.L., Marmureanu G., Panza, G.F., Vaccari, F., 2000, *"Estimation of site effects in Bucharest caused by the May 30-31 1990, Vrancea seismic events"*. PAGEOPH., 157, 249-267

Newmark N.M., Hall W.J., 1982, *"Earthquake spectra and design"*, Monograph Series, Earthquake Engineering Research Institute.

Nunziata, C., Costa G., Marrara F., Panza, G. F., 2000a, *"Calibrated estimation of the response spectra for the 1980 Irpinia earthquake in the eastern area of Naples"* Earthquake Spectra, 16, 643-660.

Nunziata, C., Luongo, G., Panza, G.F., 2000b, *"Mitigation of seismic hazard in Naples and the protection of cultural heritage"* Proceedings of the Second EuroConference on Global Change and Catastrophe Risk Management: Earthquake Risks in Europe, IIASA, Laxenburg, Austria, 6–9 July 2000.

Panza, G.F., 1985, *"Synthetic Seismograms: the Rayleigh Waves Modal Summation"* J. Geophys., 58, 125-145.

Panza, G.F., Cazzaro, R., Vaccari, F., 1997, *"Correlation between macroseismic intensities and seismic ground motion parameters"* Annali di Geofisica, 40, 1371-1382.

Panza, G.F., Romanelli, F., Vaccari, F., 2000a, *"Realistic modelling of waveforms in laterally heterogeneous anelastic media by modal summation"* Geophys. J. Int., 143, 1-20.

Panza, G.F., Romanelli, F., Vaccari, F., 2001, *"Seismic wave propagation in laterally heterogeneous anelastic media: theory and applications to the seismic zonation"* Advances in Geophysics, Academic press, 43, p. 1-95.

Panza, G.F., Romanelli, F., Vaccari, F., Decanini, L., Mollaioli, F., 2000b, *"Contribution of the deterministic approach to the characterization of seismic input"* OECD-NEA Workshop on Engineering characterization of Seismic Input, BNL, Upton, New York, 15-17 November, 1999, NEA/CSNI/R(2000)2.

Panza, G.F., Suhadolc, P., 1987, *"Complete strong motion synthetics"* In: Computational techniques, Vol. 4, Seismic strong motion synthetics, B.A. Bolt (Editor), Academic Press, 153-204.

Panza, G.F., Vaccari, F., Cazzaro, R., 1999b, *"Deterministic seismic hazard assessment"* Vrancea Earthquakes: Tectonics, Hazard and Risk Mitigation. F.Wenzel et al (eds.), Kluwer Academy Publishers, 269-286.

Panza, G.F., Vaccari, F., Costa, G., Suhadolc, P., Fäh, D., 1996, *"Seismic input modelling for Zoning and microzoning"*. Earthquake Spectra, 12, 529-566.

Panza, G.F., Vaccari, F., Romanelli, F., 1999a, *"The IUGS-UNESCO IGCP Project 414: Realistic modelling of Seismic Input for Megacities and Large Urban Areas"* Episodes, 22, 26-32.

Parvez, A. I. , Gusev, A.A., Panza, G.F., Petukhin, A.G., 2001, *"Preliminary determination of interdependence among strong motion amplitude, earthquake magnitude and hypocentral distance for the Hymalayan region"* Geophys. J. Int., 144, 577-596.

Romanelli F., Bekkevold J., Panza, G.F., 1997, *"Analytical computation of coupling coefficients in non-poissonian media"* Geophys. J. Int., 129, 205-208.

Romanelli, F Bing, Z., Vaccari, F., Panza, G.F., 1996, *"Analytical computation of reflection and transmission coupling coefficients for Love waves"* Geophys. J. Int., 125, 132-138.

Romanelli, F., Saraò, A., Suhadolc, P., Vaccari, F., 2001, *"Seismic input estimate at Fabriano from scaled and extended sources"* Italian Geotechnical Journal, in press.##Fabio:aggiornare##

Romanelli, F., Vaccari, F., 1999, *"Site response estimation and ground motion spectral scenario in the Catania Area"* J. of Seism., 3, 311-326.

Sabetta, F Pugliese, A., 1987, *"Attenuation of Peak Horizontal Acceleration and Velocity from Italian Strong-Motion Records"*. Bull. Seism. Soc. Am., 77, 1491-1511.

Saragoni, R. Holmberg, A. Saez, A., 1989, *"Potencial Destructivo y Destructividad del Terremoto de Chile de 1985"* Proceed. Sas. Jorn. Chilenas de Sismologia e Ing Antisismica, August 1989,Vol.1, 369-378.

Savy, J.B., Shah, H.C., Boore, D.M., 1980, *"Nonstationary Risk Model with Geophysical Input"* J. Struct. Div., ASCE, 106, n. ST1, 145-164.

Schwartz, D.P., Coppersmith, K.J., 1984, *"Fault behaviour and characteristic earthquakes: examples from the Wasatch and San Andres fault zones"* J. Geophys. Res., 89, 5681-5698.

Shteinberg, V., Saks, M., Aptikaev, F., Alkaz, V., Gusev, A., Erokhin, L., Zagradnik, I., Kendzera, A., Kogan, L., Lutikov, A., Popova, E., Rautian, T., Chernov, Yu., 1993, *"Methods of seismic ground*

motions estimation (Handbook)" Seismic ground motions prediction (Engineering seismology problems; Issue 34), Moscow, Nauka, 5-94. (in Russian)

Sun, R., Vaccari, F., Marrara, F., Panza, G.F., 1998, *"The main features of the local geological conditions can explain the macroseismic intensity caused in Xiji-Langfu (Beijing) by the Ms=7.7 Tangshan 1976 earthquake"* PAGEOPH, 152, 507-521.

Trifunac, M.D., Brady A.G., 1975, *"A Study on the Duration of Strong Earthquake Ground Motion.* Bulletin of Seismological Society of America, 65, 581-626.

Uang, C.M., Bertero, V.V., 1990, *"Evaluation of seismic energy in structures"* Earthquake Engineering and Structural Dynamics, 19, 77-90.

Uang, C. M., Bertero, V V., 1988, *"Implications of Recorded Earthquake Ground Motions on Seismic Design of Buildings Structures" Report No. UCB/EERC-88/13,* Earthquake Engineering Research Center, University of California at Berkeley.

Vaccari, F., Gregersen, S., Furlan, M., Panza G.F., 1989, *"Synthetic seismograms in laterally heterogeneous, anelastic media by modal summation of P-SV waves"* Geophys. J. Int., 99, 285-295.

Wang, H., Nisimura, A., 1999, *"On the behaviour of near-source strong ground motion from the seismic records in down-hole array at Hyogoken-Nanbu earthquake"* Earthquake Resistant Engineering Structures II, G.Oliveto and C.A. Brebbia (Editors), WIT Press, Southampton, 363-372.

Wells, D.L., Coppersmith, K.J., 1994, *"New empirical relationships among magnitude, rupture length, rupture width, rupture area, and surface displacement"* Bull. Seism. Soc. Am., 84, 974-1002.

Pure appl. geophys. 159 (2002) 1229–1251
0033–4553/02/061229–23 $ 1.50 + 0.20/0

Pure and Applied Geophysics

Shape Analysis of Isoseismals Based on Empirical and Synthetic Data

G. MOLCHAN,[1,3] T. KRONROD,[1,3] and G. F. PANZA[2,3]

Abstract—We present an attempt to compare modeled ground-motion acceleration fields with macroseismic observations. Two techniques for the representation of the observed intensities by isoseismals, a smoothing technique and one which visualizes the local uncertainty of an isoseismal, are tested with synthetic and observed data. We show how noise in the data and irregularities in the distribution of observation sites affect the resolution of the isoseismal's shape. In addition to "standard" elongated shapes, we identify cross-like patterns in the macroseismic observations for two Italian earthquakes of strike-slip type; similar patterns are displayed by the theoretical peak acceleration fields calculated assuming the point source models given in the literature.

Key words: Seismic intensity, macroseismic data, isoseismals, focal mechanism.

1. Introduction

Macroseismic intensity, I, is a descriptive quantity characterizing the impact of seismic ground motion on people, built environments and landscapes. The scales for I bear the imprint of historical time and reflect the national construction practices prevailing in a country (TRIFUNAC and BRADY, 1975), nevertheless, there is an unflagging interest in macroseismic data, because these are indispensable to seismic risk assessment (see e.g., KEILIS-BOROK *et al.*, 1984, 1984a).

The macroseismic data (hereafter MCS data) for an earthquake consists of a set of "site-intensity" pairs termed Intensity Data Point (IDP) map. The data have two features, which impede their effective use:

– measurement sites form an irregular set of points that depends on the distribution of the population in the area;

[1] International Institute of Earthquake Prediction Theory and Mathematical Geophysics, Russian Academy of Sciences, Warshavskoe sh., 79, k.2, Moscow 113556, Russia.
[2] Department of Earth Sciences, University of Trieste, Trieste, Italy.
[3] Abdus Salam International Centre for Theoretical Physics, SAND Group, Trieste, Italy.
George Molchan: E-mail: molchan@mitp.ru

– observed I values involve a "noise" component, which is due, for instance, to measurement errors and local inhomogeneities in the structure of the earth's crust. The observed spatial variations of I over distances ranging from 20 to 40 km may be as large as 3 to 4 intensity units (see below). This is usually true for the recent data due to the higher site density and to the poorer preprocessing with respect to historical data.

Recent electronic publications (BOSCHI *et al.*, 1995, 1997; MONACHESI and STUCCHI, 1997) have made available IDP maps for Italian earthquakes, and have renewed interest for certain old problems connected with MCS data:

– the automatic intensity data reduction or the objective generalization of IDP maps which help to lower the "noise" component and to represent the MCS observations with continuous isolines (DE RUBEIS *et al.*, 1992; TOSI *et al.*, 1995);
– the use of MCS data for refining and/or estimating the parameters of an earthquake source (KARNIK, 1969; SHEBALIN, 1972; ZAHRADNIK, 1989; PANZA *et al.*, 1991; JOHNSTON, 1996; GASPERINI *et al.*, 1999; SIROVICH and PETTENATI, 1999).

These two problems are interrelated. For instance, the macroseismic estimates of magnitude, M, and depth, h, are based on the areas of the isoseismal zones $G_I = \{\text{intensity} \geq I\}$ and on the so-called mean MCS field equation, i.e., a linear regression relation involving intensity, magnitude and logarithm of the hypocentral distance (BLAKE, 1941; SHEBALIN, 1959). This methodology is logically consistent with the generalization of an MCS field obtained by smoothing the associated IDP map.

The situation becomes more complicated when one is concerned about the geometry of the seismic source or about the comparison between the MCS data and theoretically predicted peak values of ground motion (PANZA *et al.*, 1991). In such cases reliable inferences regarding the isoseismal shape are needed. These cannot always be drawn from a smoothed IDP map and one needs a visualization of the local isoseismal resolution. For such a purpose one can replace each isoline with a boundary zone of variable width that reflects the uncertainty of the relevant isoseismal.

We consider two approaches for the generalization of IDP maps. One involves a smoothing procedure, which generalizes the local polynomial filtering used by DE RUBEIS *et al.* (1992) and TOSI *et al.* (1995). In our approach, the Modified Polynomial Filtering (MPF), the radius of the local filtering is variable and it is adapted to the local structure of the MCS data, incorporating the discreteness of the intensity scale I.

The other approach, which we call the Diffused Boundary (DB) method, visualizes the uncertainty of isoseismals. This method essentially relies on the fact that I is a discrete quantity. This property of the MCS data has rarely been integrated in automated smoothing techniques applied to IDP maps.

Tests applied to real data demonstrate that the two methods are complementary when one has to determine the shape of isoseismals.

2. Smoothing Techniques for IDP Maps

2.1. Informal Techniques

Hand techniques for smoothing IDP maps are not reproducible, however one can discuss the principles on which they are based. SHEBALIN (2000) summarized the requirements on isoseismals as follows:

(a) isoseismal zones G_I must be simply-connected and embedded, expanding with increasing isoseismal rank $I_0 - I$ (*the monotonicity condition*);
(b) any isoseismal of level I is an external contour enclosing areas of reliably determined intensities I (the generally accepted *convention* to define an isoseismal);
(c) adjacent isoseismals are approximately similar (*similarity*);
(d) the curvature of an isoseismal must be as small as possible, and nonnegative (the *simplicity condition*, which provides an additional guarantee of smoothness for the isoseismals);
(e) the number of sites with $I \geq J$ outside a zone G_J is approximately equal to that of sites with $I < J$ in the G_J zone itself (*equality of the errors of the two kinds*);
(f) consecutive isoseismals along an azimuth must be neither too close nor too far from each other (*a mild control of the mean field model*).

Contemporary data show that the boundary between two adjacent intensities may be rather diffused. For this reason requirement (e) relating the equality of the errors of the two kinds may contradict the definition of isoseismals (convention (b)). In fact, let the MCS field be isotropic and the observations with $I - 1$ and I be well mixed in the annulus $r_1 < r < r_2$. If we assume that there are no points with $I - 1$ inside the circle $r \leq r_1$ and no points with I outside the circle $r = r_2$, then, according to (b), the circular line $r = r_2$ must separate the intensities $I - 1$ and I. As a result all the observations of level I but not all of level $I - 1$ will be correctly identified.

The monotonicity, similarity and smoothness properties unfortunately can be tested using only some instrumental analogues of MCS intensity: peak values of the wavefield in terms of acceleration, velocity or displacement. PANZA *et al.* (1991) use the modal summation technique to model the wavefield produced by an instantaneous seismic point source in a plane-stratified earth. These computations point to complexities in the structure of the modeled ground-motion fields in the zone near the epicenter (within 200 km). In particular, one may have 2 to 4-lobe isoseismals, violations of the similarity condition and of the other requirements listed above. The reasons given in BURGER *et al.* (1987) support the local violations of monotonicity of the peak acceleration field at distances of 60–120 km from the

source, due to the competitive effect of direct and postcritically reflected S waves from the Moho.

Taken as a whole, SHEBALIN (2000) conditions are based on the experience gained when working with small data sets and they aim at the simplest problems in MCS data interpretation, such as the determination of the earthquake scalar seismic moment, source location and azimuth. That is why they reduce the isoseismal shape to a simple oval, unless the data definitely states to the contrary.

2.2. Filtering Techniques

To smooth IDP maps DE RUBEIS *et al.* (1992) and TOSI *et al.* (1995) applied a local polynomial filtering. The method is based on the assumption that the macroseismic field can be well fitted locally with a polynomial of degree two, $P_2(g)$. The fit to the field at a given point g_0 is found by considering a circle $B(g_0, R)$ centered at g_0 and having radius R. Let $P_2(g)$ approximate the I data in $B(g_0, R)$ with minimal squared error. Then the polynomial at the center of the circle is taken to be the desired estimate of the field $\hat{I}(g_0)$ at g_0. Following requirement (b) in Section 2.1, the isoline $\hat{I}(g) = I - \Delta I/2$ can be regarded as the isoline of the macroseismic field relevant to level I, ΔI being the discretization interval of the intensity scale. It should be borne in mind, when choosing the smoothing parameter R, that the real density of the observations is generally nonuniform.

Constant value of R. DE RUBEIS *et al.* (1992) used a constant value of R. In this case the residual noise component in a smoothed MCS field may be subject to great lateral variability; the associated variance being obviously greater in areas of lower observation site density, because of fewer data in the averaging circle. The deterministic component of the MCS field varies rapidly in the epicentral zone and more slowly at the periphery. According to SHEBALIN (1959), the mean distance between isolines of levels I and $I-1$ increases with I decreasing in a geometric progression with the coefficient $k \approx 2$, if the epicentral distances are within 300 km. For this reason the choice of large R is generally neutral to the smoothing of the deterministic part of the MCS field at the periphery, but can significantly affect the isoseismal shapes in the near zone.

In many IDP maps of Italian earthquakes we have noticed that the density of the I points appreciably decreases from the epicenter to the periphery (*effect A*). We see it on the three of four Italian earthquakes, considered in this paper (Fig. 1). One possible explanation of the effect A may be the nonuniform inspection, which is more detailed at the epicenter, where the MCS effect is high, and much less at the periphery, owing to both economic reasons and the *a priori* slow variability of the MCS field. When R is constant, the effect A favors an increase of the residual noise component at the periphery of the MCS field.

The shortcoming of a constant R has been overcome in a later work by TOSI *et al.* (1995), where the smoothing cell remains standard, but it is defined in polar

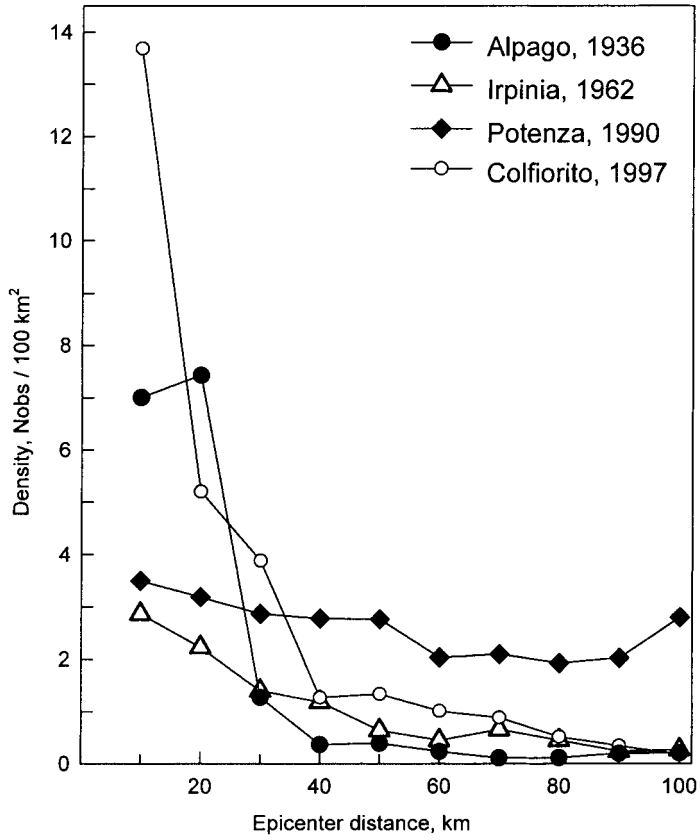

Figure 1
Number of intensity points per 100 km^2 as a function of the epicentral distance for four Italian earthquakes.

coordinates, centered at the epicenter of the event. For this reason the actual linear size of the smoothing area is decreasing toward the center. Nevertheless, the density of observations may be rather irregular, so that the smoothing cells remain, generally speaking, nonuniform with respect to the number of measurement sites. One natural way out of this difficulty is to use areas $B(g_0, R)$ of variable radius by adapting them to the geometry of the measurement sites around g_0.

Non-constant R value (Modified Polynomial Filtering, MPF). For every point g_0 the radius R is chosen within a specified set $\{R_i\}$ with the condition $R < L/3$, where $2L$ is the diameter of the circle enclosing the entire set of all measurement sites. Taking values of R_i in increasing order, we can find the first area $B(g_0, R)$ that contains at least n_p observation sites and in which the number of different integer intensity values is not below a threshold $n_1 > 1$.

When the threshold n_p has been overcome, small values of n_I are practically negligible in the epicentral zone because of the large variations in the deterministic component of the MCS field. For this reason the radius R will be small near the epicenter. On the other hand it is natural to use a larger averaging radius at the periphery. Assume we have slight noise in the MCS data. Then using $n_I = 2$ we will expand the averaging area until it reaches the boundary of the adjacent intensity. Since the intensity scale is discrete and the noise is slight, the expansion will not distort our estimate near g_0 of the trend of MCS field, which is almost constant in the considered case.

The set $\{R_i\}$ has been used as $\{id, i = 1, 2, \ldots\}$, where d is the typical radius of the highest (lowest rank) isoseismal, $d \cong 5$–10 km. The threshold n_p is taken equal to 6 m. The two-dimensional polynomial P_2 has six parameters; therefore "m" is the average number of measurements per parameter. Usually we set $m = 2$–3, because larger values of "m" increase the averaging area, leading to poorer isoseismal resolution. The poor resolution controls the choice of the degree, k, of the smoothing polynomial, P_k, as well. In fact, in general P_k has $(k+1)(k+2)/2$ parameters. Therefore, if $k > 2$ and the number of I points in $B(g_0, R)$ is small, the estimates of the polynomial parameters will be not stable. On the other hand, however, the degree k should be greater than 1 because the boundary between adjacent intensities is curved. For data involving moderate (large) noise we use for the threshold n_I the values 2–3 (3–4).

The procedure gains in stability when the averaging areas strongly overlap, as in the case of small spacing $|\Delta g_0|$ of the grid $\{g_0\}$, whose knots are the centers of the regions $B(g_0, R)$. In actual practice one has $|\Delta g_0| = 3$–5 km. The obvious bias in the estimates of the local trend of P_2 occurs at the periphery of an IDP map when the observation sites, falling into the averaging area $B(g_0, R)$, are seen from g_0 at an angle $\varphi < 180°$. Then g_0 is a point where the field $I(g)$ has to be extrapolated, i.e., it is a location where the fit $P_2(g)$ is not constrained by observations. An additional threshold for the angle φ, $\varphi \geq \varphi_0$, is then used to exclude such effects. This either increases the averaging radius or excludes the point from consideration. In our examples $\varphi_0 = 200°$.

Figure 2a gives an example of the spatial distribution of $R(g)$ for the 1997 Colfiorito earthquake (Central Italy). It shows that R automatically increases from the epicenter toward the periphery. In addition, Figure 2b shows the number, $v(g)$, of the intensity measurements in each area $B(g, R)$. This quantity has weak fluctuations along the isolines and at the periphery, e.g., $v \cong 20$, $R \cong 20$ km along the isoline of the third rank, $I =$ VI. Some perturbations of $v(g)$ at the periphery are explained by the boundary effect in the filtering, which is controlled by the parameter φ_0.

Overall, the merit of formalized filtering techniques is that they are reproducible and do not involve *a priori* restrictions on the shape and connectedness of the isoseismals. The polynomial filtering partly suppresses the noise and the local components in the observations does not distort the polynomial trend of degree two

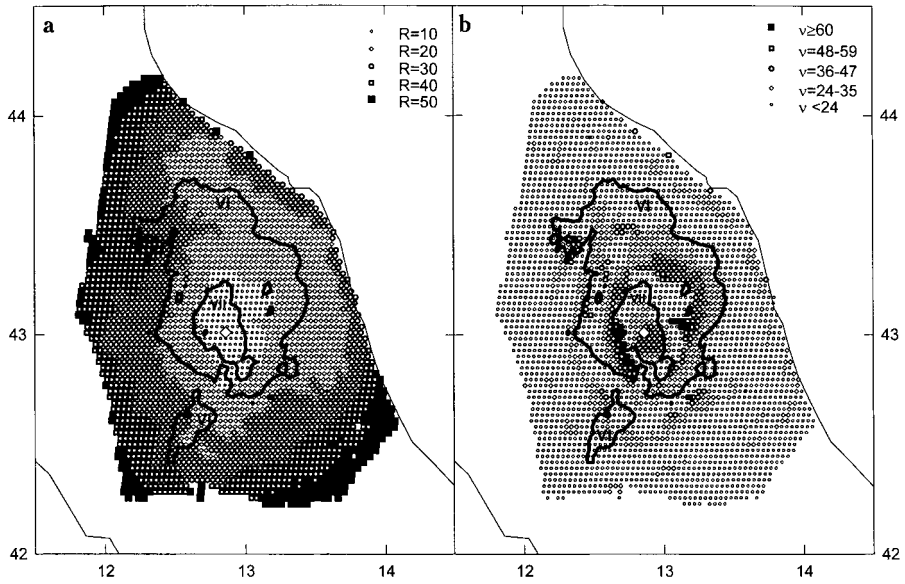

Figure 2
Parameters of the MPF method for the 26.09.1997 Colfiorito earthquake: (a) radius of smoothing, R; (b) number of sites, v, contained in the smoothing circle with radius R. *Bold lines*: MPF isolines of $I =$ VI and VII.

when there is no noise. However the interpretation of the shape of the isoseismals remains problematical, owing to possible smoothing-out of details. The use of filtering techniques is natural with respect to continuous fields, however the intensity takes integer values, in our case ranging from III to IX, and there may be only two or three different values in the vicinity of the boundary between two intensities. The effect of the discreteness of the I scale on the isoseismal's shapes of a smoothed IDP map has not yet been investigated.

3. Visualization of the Uncertainty in the Isoseismals

3.1. The Diffused Boundary (DB) Method

The analysis of the shape of an isoseismal requires the visualization of its local uncertainty. Speaking in terms of mathematical statistics, the problem can be interpreted as the passage from the point estimation of an isoline to the interval estimation. The local thickness or uncertainty of an isoline must depend on the local geometry of the measurement sites and on the noise component present in the data. The solution we propose in this section essentially relies on the fact that the intensity scale is discrete. We assume that the isoseismal zones G_I are simply connected and monotonic. The connectedness assumption is not absolutely indispensable, as we shall see.

1-D case. To explain the principles of the DB concept we start from the case of 1-D MCS data. Isoseismals on a line make a set of embedded intervals with intensity $\geq I$ that are increasing with decreasing I. For a given intensity level, we must separate points of two types on the line: "+" with intensity $\geq I$ and "0" with intensity $< I$ (Fig. 3a). When the observations are error-free, a cluster of pluses lies between two

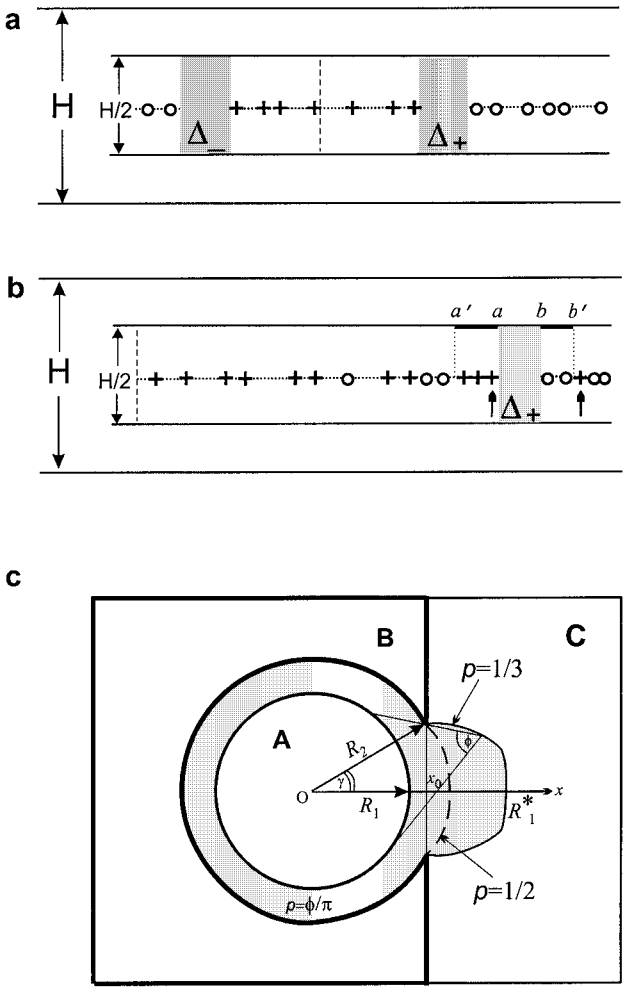

Figure 3
Illustration of the DB method (for more details see text). (a) Local Diffused Boundary (LDB) (*shadow* zone) for the data without noise. *Dashed* and *dotted* lines are the axes of the strip; (b) the same as in (a) for noisy data; (c) example of Diffused Boundary (DB) of level $p = 1/3$ (*shadow* zone) under the conditions: $H = 0$; the areas A delimited by *bold line*, and B, delimited by *fat line*, contain the noise-free and everywhere dense observations of intensity $\geq I$ and $\leq (I - 1)$ respectively; the complementary area to A and B (C plus the shaded area) does not contain intensity data. The local variation of the DB for the case $p = 1/2$ is indicated by the *dashed* curve.

clusters of zeroes. (As cluster on a line we mean a nonempty sequence of identical characters that cannot be expanded without adding a different character.) The true boundary of level I is covered by two intervals, Δ_- and Δ_+, that separate the clusters and supply all available information on the boundary uncertainty, no smoothing techniques are able to improve the boundary between "+" and "0".

When MCS observations contain noise, the pattern is more complex: some pluses percolate into the zeroes zone and conversely (see Fig. 3b). For simplicity Figure 3b presents only the right semi-axis which starts from the barycenter of the pluses. In view of possible errors in the observations we allow some pluses, up to the amount $\varepsilon\%$ of the total number of pluses on the semi-axis, to be considered as erroneous. Because of the convention (b) relative to isoseismals we are primarily interested in the outer boundary of pluses. For this reason the first candidates to be classified as erroneous will be those pluses farthest from the center. Under these new conditions the interval, say Δ_+, is specified uniquely by the following requirements. It is the interval (a, b) which separates the pluses cluster contained in the interval $[a', a]$ and the zeroes cluster contained in the interval $[b, b']$ (see Fig. 3b). We assume that $I(\infty) = 0$, so that the point "∞" always belongs to the set of measurements, and requires that in the interval (a, ∞) the number of pluses is $\leq\varepsilon\%$ of all pluses on the semi-axis, and $>\varepsilon\%$ in the interval $[a', \infty)$.

Let us consider the following example (Fig. 3b). Two pluses, marked with arrows in Figure 3b, of the twelve could be removed at the level $\varepsilon = 20\%$. We remove only one plus (the rightmost one) because the other belongs to the cluster of 3 pluses and can be removed only together with the cluster. The removal of the cluster (3 pluses) violates our rule on the ε-threshold since $(1+3)/12 > 20\%$. The resulting boundary Δ_+ is shown in Figure 3b. Thus a distant cluster of pluses cannot be classified as erroneous, unless it is comparatively small, and as a rule it is preserved as a whole, when its size is evident that the observed intensity is a genuine effect.

2-D case. The local uncertainty of an isoseismal in the 2-D case can be obtained by inspection of the I points in the vicinity of each straight line traced on the MCS field. The traces of G_I on any cross section of the MCS field will inherit the connectedness and monotonicity of the MCS field, therefore to find an intensity boundary we may use the criteria defined in the 1-D case.

Let us consider a strip across an IDP map. The strip is specified by the distance, r, of its axis from the epicenter, by the direction, φ of that axis, and by the width, H, playing the role of a smoothing parameter. Projecting all points lying in this strip onto its major axis, we derive a 1-D variant of the problem. Figures 3a and b now illustrate the decisions regarding the boundary between the observations that fall into the strip. Since the strip is two-dimensional, we consider rectangles of size $H/2 \times \Delta_\pm$ (see Figs. 3a,b) as the local boundary of level I along the straight line (r, φ). This rectangle is called the *Local Diffused Boundary* (LDB), and its indicator function, having the values 1 for points of the rectangle and 0 otherwise, will be termed *LDB-function*.

Evidently, a single LDB can be unstable due to the strong dependence on the choice of ε. But sorting out all possible sections (r, φ) of the IDP map, we obtain a 2-D family of local boundaries, the *Diffused Boundary* (DB), for a given intensity. The new object, DB, is more stable and supplies information on the uncertainty of G_I at any point of the space, in any direction, while a number of overlapping LDB elements in each point can be interpreted as a local measure of the reliability for the diffused boundary.

The visualization of DB can be made with two different methods. With one method only LDB axes are plotted in the MCS field with some discretization of (r, φ). The emerging picture looks like a thorny "hedgehog." This visualization will therefore be called a "*thorny*" *diffused boundary*. With the other method we take into account the fraction of overlapping LDB elements in each point. To do this we sum all LDB-functions and obtain a *DB-function* with a maximum M. The area where the DB-function exceeds the level pM, $0 < p < 1$ is considered to be the *p-diffused boundary* of G_I.

When an isoseismal G_I is not convex or not simply connected, the DB-function can be underestimated for the boundary points of G_I which are internal to the convex hull of G_I. This results because we take into consideration only two (the left- and right-most) boundary points of G_I in any cross section of the MCS observations.

Threshold p. It is advisable to consider idealized situations in order to choose the threshold p. Let us assume that we have noise-free observations, the observation sites with intensity $\geq I$ filling the entire circle of radius R_1, $B(O, R_1)$, and those with intensity $<I$ filling a circle of radius $R_2 > R_1$ at the same center, O. We also assume that there are no observations in the annulus $R_1 < r < R_2$. If the strip width is $H = 0$ then the DB-function is equal to the angle $\varphi(g)$ at which the area $B(O, R_1)$ is seen from g; $\varphi(g) \equiv 0$ for g out of the annulus. Hence the threshold p is connected with the distance $r \geq R_1$ by the relation

$$p(r) = \begin{cases} 2\pi^{-1}\arcsin(R_1/r), & R_1 \leq r \leq R_2 \\ 0, & r > R_2 \end{cases}$$

i.e., $p = 1$, $1/2$, and $1/3$ for $r = R_1$, $\sqrt{2}R_1$, and $2R_1$, respectively if $r < R_2$.

Frequently MCS data are interrupted by a coastline. The theoretical analysis of the DB in this case is important for the correct interpretation of DB peculiarities of lobe-like type. As a model let us consider the previous example and eliminate all observations with intensity $<I$ from the half-plane $x > x_0$ where $R_1 < x_0 < R_2$ (see Fig. 3c). If $H = 0$ the DB-function has the same geometric meaning as above. Therefore when $R_2 > R_1/\sin(\pi p/2) = R_1^*$ the p-diffused boundary of G_I is identical to the annulus $R_1 \leq r \leq R_1^*$. Otherwise (see Fig. 3c) the p-diffused boundary consists of the annulus $\{R_1 < r < R_2\}$ and of a local outgrowth on it directed toward the axis x within $R_2 < x < \min(R_1^*, R_2^*)$, where

$$R_2^* = R_2 \sin(\pi p/2 + \gamma)/\sin(\pi p/2), \quad \gamma = \arccos(x_0/R_2) \ .$$

In the real cases $R_2 < (1.5\text{–}2)R_1$ and therefore the DB zone contains the entire annulus if $p = 1/3\text{–}1/2$; for $R_2 \leq \sqrt{2}R_1$ and $p = 1/2$ the R_2^* value is $\sqrt{2}R_1$.

The main parameters of the DB method. To analyze MCS data for Italy we use the following values of the main parameters: $\varepsilon = 5\text{–}15\%$, strip width $H = 20\text{–}40$ km, threshold $p = 1/3\text{–}1/2$. The other parameters are connected with the discretization of the family of strips: (r, φ) are discretized with steps $\Delta r = 0.1H$ and $\Delta\varphi = 5^\circ$, respectively.

Many recommendations pertaining to hand treatment of IDP maps contain advice to map the local reliability of the isoseismals (see e.g., SHEBALIN, 2000). The diffused boundary of G_I is derived by inspection and by incorporation of the uncertainty in the isoseismals at each point and in each direction. For this reason the proposed version of the boundary of G_I, as a stripe of varying thickness, can be regarded as one of the possibilities for the visualization of the uncertainty in the isoseismals.

Colfiorito earthquake, 26.IX.1997, $M_w = 6.0$, $I_0 = \text{IX}$, IDP map by GNDT (1997), number of I points $n_{\text{obs}} = 362$.

We have illustrated the filtering technique MPF (see Fig. 2) using this event, which is the largest earthquake in Italy in the recent past with a good set of MCS data. In fact, the Italian catalog NT4.1 by CAMASSI and STUCCHI (1997) contains only 10 events, for the period 1900–1980, with $n_{\text{obs}} \geq 300$. The main event has been preceded by a foreshock ($M_w = 5.7$ about 8 hours before) with a similar focal mechanism (normal faulting) but different location, nevertheless the intensity data of the Colfiorito event, for $I \geq \text{V}$, are low-noise and relatively dense in space. As a result the residuals between the observed and the smoothed values of I are, in general, within 0.5 over the entire area considered. Figure 4 shows that the isoseismals derived by MPF and DB methods are reasonably consistent. Both methods indicate a possible lack of connectedness in the $I = \text{VI}$ isoseismal. On the whole, Figure 4 can be regarded as an illustration of the isoseismal resolution based on intensity data of good quality. Concurrently, Figure 4 is not suitable for an interpretation in terms of source and site effects owing to the superposition of the effects of two large shocks (TOSI *et al.*, 1999).

4. Empirical and Synthetic Isoseismals: Examples of Comparison

The developed technique can be applied to the comparison between the empirical and the synthetic isoseismals. To this end we choose three Italian earthquakes of strike-slip type because their synthetic isoseismals show non-trivial cross-like shapes instead of the "standard" elongated shapes.

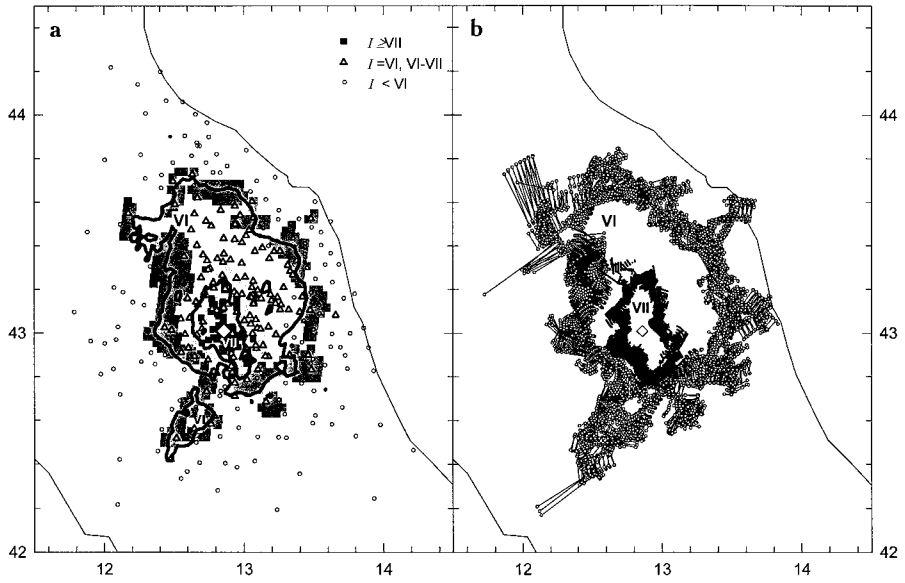

Figure 4
26.09.1997, $M_w = 6.0$ Colfiorito earthquake: (a) 40% DB for $I = \text{VI}$ and $I = \text{VII}$ (*shaded zones*) and the MPF isolines (*bold*); background: IDP map (*point symbols*); (b) thorny DB for $I = \text{VI}$ and $I = \text{VII}$.

The synthetic isoseismals are defined as follows. We generate the synthetic seismograms by mode summation (PANZA, 1985; PANZA and SUHADOLC, 1987; FLORSCH *et al.*, 1991) at frequencies below 1 Hz. These calculations are based on a plane-stratified schematic crustal model for Italy (COSTA *et al.*, 1993) and on the instantaneous point source approximation taken from the literature, scaled accordingly with GUSEV (1983) source spectra, as reported by AKI (1987). The synthetic isoseismals are defined in terms of peak values of acceleration a_p, velocity V_p or displacement d_p. For example, the a_p-isoseismal of the intensity level I_a is the area $\{a_p > a_p(I_a)\}$ where

$$\log a_p(I_a)\,[\text{cm/s}^2] = b_0 + b_1(I_a - 6) \quad . \tag{1}$$

The value $b_1 = 0.3$ that corresponds to the relation $a_p(I_a)/a_p(I_a - 1) = 2$ is usually used for the classification of MCS effect and not contradicted by the numerous empirical relations (see SHTEINBERG *et al.*, 1993 and references therein); the gauge coefficient $b_0 = \log a_p(I_1 = 6) = 0.47$ was derived for Italian earthquakes by PANZA *et al.* (1997, Table 1, $I = \text{VI}$).

The main difficulty, which arises in such as approach to the isoseismal comparison problem is that the intensity data sometimes are the result of the cumulative effects of a sequence of events that includes the mainshock and its fore- and aftershocks. Additional factors affecting the isoseismal size and shape are:

– the local soil effect or more generally the local inhomogeneites in the earth structure which *a priori* are unknown;
– the discretization given by (1); PANZA *et al.* (1997) found that the average coefficient b_0 depends on the choice of the version of the Italian catalogs and this leads to the shift in the intensity I_a by one unit; in addition, the parameter, b_0, depends on the quality factor, Q, which varies with the crust;
– the earthquake depth; it is usually a poorly defined parameter, if the wavefield, near the fault zone of the large shallow earthquake, is modeled with a point source; therefore the isoseismals of the first and/or second rank cannot be suitable for the comparison, due to the point approximation of the source.

To control the depth effect we use the condition $D(I) > 3\ell$, where D is the average hypocentral distance of the intensity I and ℓ is the linear size of the source; following GASPERINI *et al.* (1999) we assume:

$$\log l\,[\mathrm{km}] \cong 0.6M_w - 2.3 \ . \tag{2}$$

The isoseismals of high rank for Italy are often unsuitable as well since their boundaries are not closed. Thus the choice of the isoseismals for the shape analysis, in general, is limited to one or two intensity degree for each earthquake.

Potenza earthquake (Southern Italy), 5.V.1990, $M_w = 5.8$, $I_0 = 7$, $I_{\max} =$ VII–VIII, IDP map by BMS (1990).

The MCS data for the Potenza earthquake are unusual due to the high density of IDP (Figs. 1, 5a), $n_{\mathrm{obs}} = 1372$, and the exceptionally high "noise" in the data. For example, the spatial variation in intensity is occasionally as high as four units over distances of about 40 km. This can be seen in Figure 6 which gives a subdivision of the relevant space into rectangular cells in polar coordinates and the histograms of the observed I in three representative cells. This is also shown by the residuals δI between the observed and the filtered values of I. They are very large $\delta I \in (-3, 3)$ and vary over space (see Fig. 5a). The "noise" is not the result of the cumulative effects of the aftershocks sequence because they are concentrated near the mainshock (see Fig. 5b) and the strongest aftershock has a local magnitude $M_L = 4.7$.

Of the two sources of noise, namely, the spatial distribution of the observation points and the noise in I, the latter becomes the most important, when the measurement sites are dense. Therefore from *a priori* considerations the polynomial filtering is preferable in the present example. The MPF method focuses on local smoothing of the noise, while the DB method incorporates observations contained in complete cross sections of an IDP map. Figure 5 shows that the two methods yield very different results for the rank 1 isoseismal ($I =$ VI), although they are moderately consistent for the rank 2 isoseismal, the other isoseismals being non-closed.

We calculate ground-motion fields for a scaled point source with the parameters:

$$\text{strike } 184^\circ, \text{dip } 73^\circ, \text{rake } 13^\circ, \text{focal depth } 10 \text{ km (CMT)}.$$

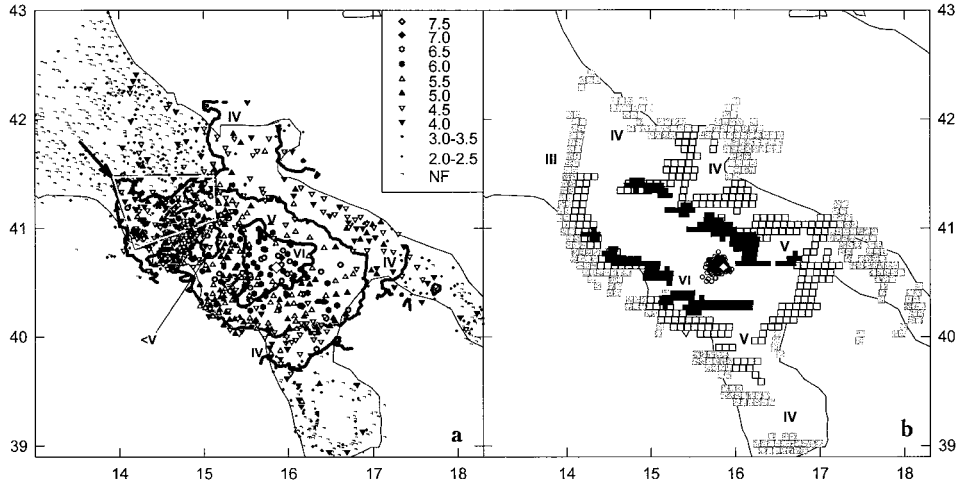

Figure 5
5.05.1990, $M_w = 5.8$ Potenza earthquake: (a) the MPF isolines (*bold line*); the *dashed quadrangle* indicated by an arrow delimits a zone of anomalous residuals in I: $|\delta I| \geq 2.5$; background: IDP map (*point symbols*), NF = "not felt". (b) 35% DB (*small squares*) for I in the range from III to VI and aftershocks (*open circles*).

The theoretical a_p-isoseismals, shown in Figure 7a as thin continuous lines, have a cross-like shape and are not consistent with the isolines of the IDP map shown in Figure 5. Since the noise is large, to see what part it played in producing the inconsistency, we add noise to the theoretical a_p values computed in the real observation sites.

The noise varies over the area. For this reason we use the analysis of the spatial variation of I as shown in Figure 6. A frequency histogram of the observed I is calculated for each elementary area. Each histogram is centered at the median and it is assumed to represent the error distribution in the elementary area concerned.

Figure 7 shows the results of the reconstruction of the a_p field when dealing with noisy synthetic data. The DB method (Fig. 7b) gives a good reconstruction of the cross-like structure of the $I_a = \text{VII}$ isoseismal, while the MPF method reconstructs the $I_a = \text{VI}$ and $I_a = \text{V}$ isoseismals. The DB method does not work for the $I_a = \text{VI}$ isoseismals because of the presence of the quadrangular large noise anomaly, indicated in Figure 5a by a bold arrow.

It thus appears that even if the noise level is high, the availability of a dense set of observation sites allowed us to reconstruct the theoretical a_p field (thin line in Fig. 7a). The discrepancy between the thick lines in Figures 5a and 7a suggests that the assumption made about the source or/and the crust model is not adequate to describe the MCS data for the case under consideration.

Alpago earthquake (Northern Italy), 18.X.1936, $M_L = 5.8$, $I_0 = \text{IX}$, IDP map by BOSCHI *et al.* (1995, 1997), and by MONACHESI and STUCCHI (1997), $n_{\text{obs}} = 292$.

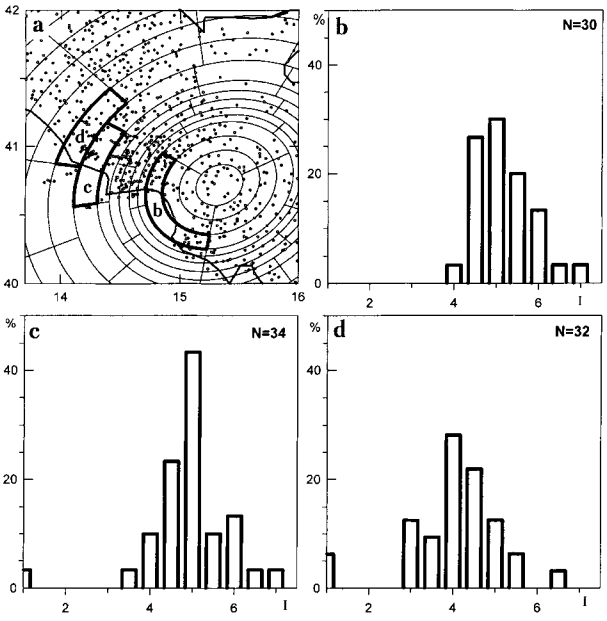

Figure 6
Local spatial variations in the MCS data for the 1990 Potenza earthquake: (a) subdivision of the MCS space into elementary areas (cells); (b–d) histograms for the observed intensity in the cells *b*, *c*, *d* of the subdivision in Figure 6a. *N* is the number of observation sites in each cell.

This earthquake has the following source parameters:

strike 193 ± 3°, dip 61 ± 1°, rake 7.5 ± 5.5°, focal depth $h = 18$ km (COSTA *et al.*, 1993).

From (2) the linear size of the source can be estimated as $l \cong 11$ km. (We assume that $M_L \approx M_w$ in the range $M_L \in (4, 6.3)$, according to the (M_L, M_w) regression by GIARDINI *et al.* (1997) for the Mediterranean region.) Therefore the critical epicenter distance for the shape analysis is $\Delta = ((3\ell)^2 - h^2)^{1/2} \cong 30$ km. Judging from Figure 8, where the isoseismals obtained by the MPF method are presented, the suitable isoseismal for the analysis is the area of third rank ($I = \text{VI}$). This isoseismal is triple-connected and the dominant part of this area has a cross-like shape (see Fig. 8a).

The synthetic isoseismals have a well delineated cross-like shape, independent of the focal depth h in the range 7–20 km, which was used in our calculations (see, for example, Fig. 8b for $h = 18$ km), and the area A of the a_p-isoseismal of level $I_a = \text{VI}$ is a weak function of h:

h	9	15	21
$\log A$ [km^2]	3.8	3.6	3.7

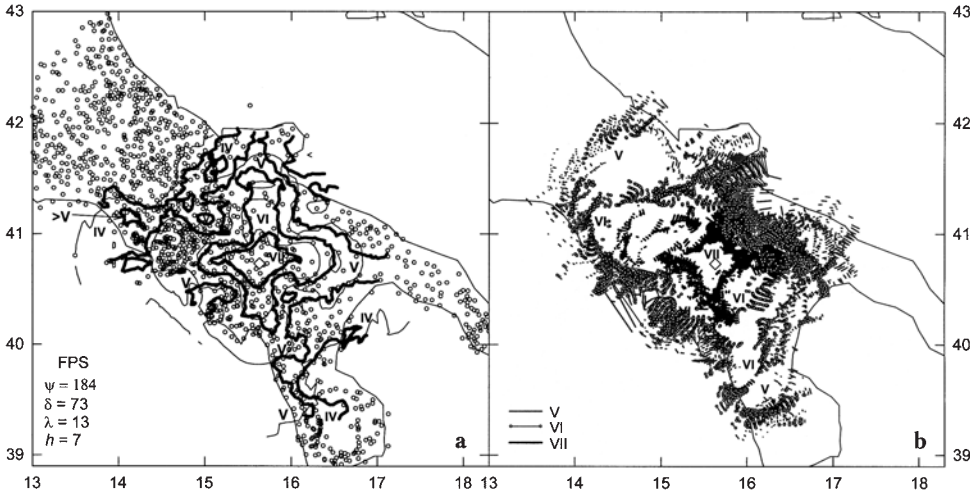

Figure 7
Reconstruction of noise contaminated synthetic a_p-field (see text for more details), for the 1990 Potenza earthquake, computed in the observation sites: (a) noise-free isolines of the synthetic a_p-field (*thin lines*) and their reconstruction by the MPF technique (*bold lines*); background: observation sites (*dots*); (b) thorny DB for $I = \text{VI}$, V, and IV.

These values are close to the empirical estimate $\hat{A}$: $\log \hat{A} = 3.9$, obtained by the MPF method.

Also Figure 8b shows the reconstruction of the isoseismal of $I_a = \text{VI}$, obtained for the synthetic a_p field calculated at the actual sites where the MCS data have been observed. In converting a_p to I using (1) we preserve the same accuracy (1/2 or 1 unit of I) as in each real intensity-point observation. Judging from Figures 8a and b the dominant parts of the synthetic and empirical isoseismals of level $I = \text{VI}$ are very similar in shape. The dominant part of the isoseismal area $I \geq \text{VI}$, G', is clearly divided into two parts by a straight line (AA′ in Fig. 8a). If Figure 8a is compared to the relief, the northeastern part of G' lies within a mountain landscape, while the southwestern one is on a plain covered by Quaternary deposits. Each part contains two lobes of G' that give a total cross-like shape to G'. This circumstance demonstrates that there is no relevant influence of the relief on the dominant part of the isoseismal $I = \text{VI}$.

Let us now consider the two secondary parts of the empirical isoseismal for $I = \text{VI}$ (VI-A and VI-B in Fig. 8a). Each of them is characterized by the value $\Delta I = I - I'$, where I' is the intensity level for the surrounding area; in our case $\Delta I = +1$. The largest secondary part (VI-A, Fig. 8a) occupies a portion of the NE Po Valley and it is natural to assume that the value $\Delta I = +1$ is caused by local soil conditions.

To test this hypothesis we consider the relevant Italian earthquakes which occurred after 1456 with well-defined ($n_{\text{obs}} \geq 100$ for the historical events) and

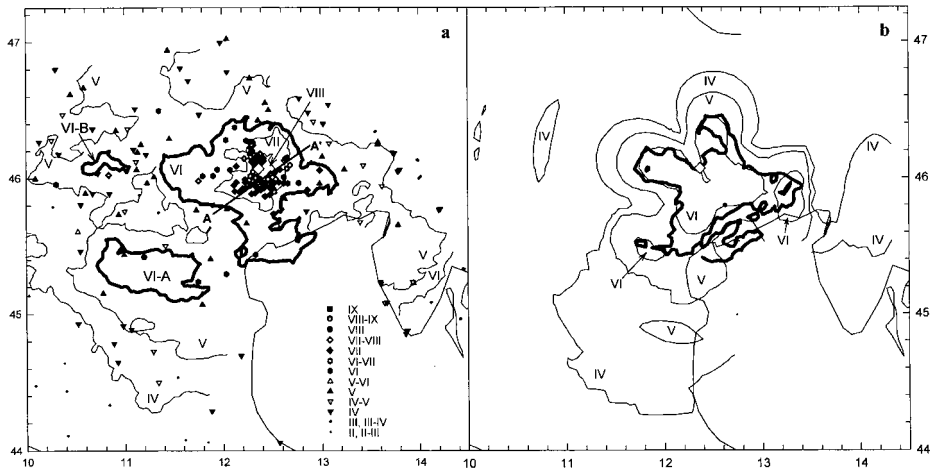

Figure 8
18.10.1936, $M_L = 5.8$, Alpago earthquake: (a) MPF isolines for the MCS observations and IDP map (*point symbols*); (A, A') separates the zone of $I \geq$ VI on mountain from that on the plain; (b) isolines of the synthetic a_p-field (*thin line*) and reconstruction of the theoretical $I_a =$ VI isoline (*bold line*) using the original observation points and the MPF technique.

multi-connected isoseismals. The number of such events, including the Alpago event, is 11 and their space distribution is given in the insert of Figure 9. This figure gives a synoptic picture of the secondary parts ("islands") of the multi-connected isoseismals for all these earthquakes. For all isoseismal parts $\Delta I \geq +1$, with the exception of isoseismal 4a, where $\Delta I = -1$.

As can be seen, half of the VI-A area (Fig. 9), roughly coinciding with the Euganei hills and Berici mountain, is covered by secondary parts of isoseismals of other earthquakes with the same intensity effect: $\Delta I = +1$. The other part of the VI-A area is extremely unstable and depends on a single measurement site with the anomalous value $I =$ VIII (see in Fig. 9 the bold point in the VI-A area). In the vicinity of the anomalous site, which is not reported in the MONACHESI and STUCCHI (1997) data base, $I \leq$ VI. If the anomalous point is eliminated, the VI-A area reduces to the small area VI-C (in Fig. 9), adjacent to the Euganei hills. Thus we can conclude that the synthetic model of the isoseismal $I =$ VI is in good agreement with the IDP-map. The two secondary parts of the observed isoseismal (VI-A, VI-B, Fig. 8a) result from local inhomogeneities in the earth's structure, from the geometry of the measurement points, and from gross errors in the observations.

Irpinia earthquake (Southern Italy), 21.09.1962, $M_L = 6.1$, $I_0 =$ IX, IDP map by BOSCHI *et al.* (1995, 1997) and by MONACHESI and STUCCHI (1997), $n_{\text{obs}} = 221$.
The results of the generalization of the third rank isoseismal ($I =$ VI) using the two methods are displayed in Figures 10a and b. The DB method delineates well the cross-like isoseismal shape and when the semi-infinite LDB zones related to the

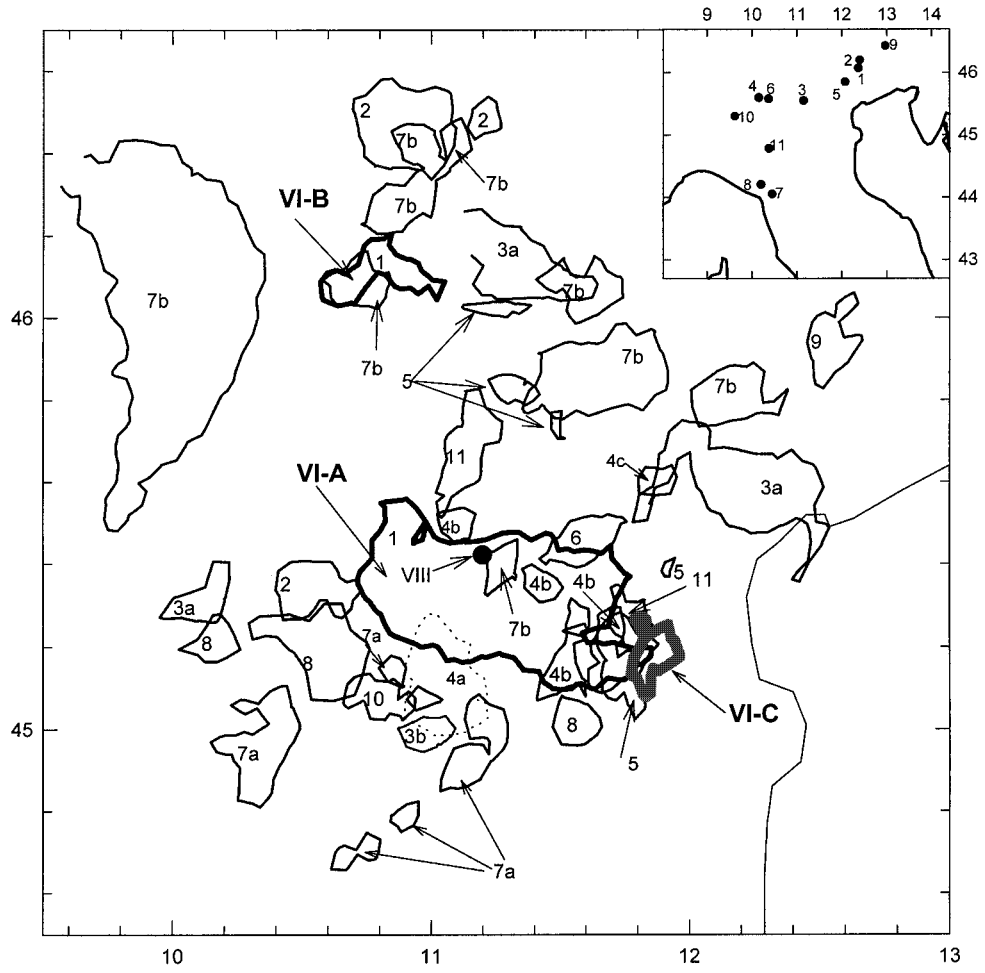

Figure 9

Secondary parts (*thin line*) of the multi-connected isoseismals for the 11 earthquakes in the zone of Alpago earthquake. List of the earthquakes (epicenters are shown in the insert): date; area; intensity level, $I + \Delta I$, of each secondary part and its identification in brackets (for ΔI see text: (1) 18.10.1936, Alpago, V + 1 (*thick line*; VI-A, VI-B), the area VI-C is an alternative to the area VI-A due to instability of the polynomial filtering (see text). (2) 29.06.1873, Bellunese, V + 1 (2). (3) 7.06.1891, Veronese, IV + 1 (3a), V + 1 (3b). (4) 27.11.1894, Fransiacorta, IV – 1 (4a, *dotted line*), III + 1 (4b), II + 1 (4c). (5) 4.03.1900, Valdobbiadene, IV + 1 (5). (6) 30.10.1901, Salo, IV + 1 (6). (7) 27.10.1914, Garfagnana, V + 1 (7a), IV + 1 (7b). (8) 7.09.1920, Garfagnana, IV + 1 (8). (9) 12.12.1924, Carnia, IV + 1 (9). (10) 15.05.1951, Lodigiano, V + 1 (10). (11) 15.07.1971, Parmense, IV + 1 (11).

coastline are removed, the cross-like structure becomes even more pronounced. At the same time, this structure is not resolved in the set of isolines derived by the MPF method, with the possible exception of isoline $I = \text{VI}$. The last isoline is compatible with the diffused boundary but we acquire more information about the shape

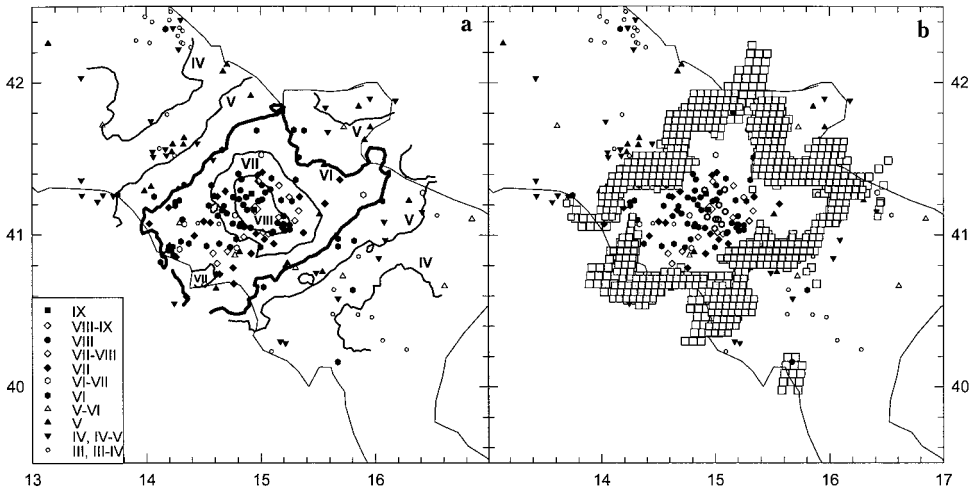

Figure 10
21.08.1962, $M_L = 6.2$ Irpinia earthquake: (a) MPF isolines for the MCS field (*bold*); (b) 35%-DB for $I = \text{VI}$ (*small squares*). The *light small squares* are generated by semi-infinite LDB (the coastline effect); background: epicenter (*diamond*), IDP map (*point symbols*).

considering in Figure 10b not one but the entire ensemble of reasonable versions of isoseismal $I = \text{VI}$, consistent with the MCS data. As regards the relief effect on the shape of the $I = \text{VI}$ isoseismal, our conclusion is practically identical with that reached in the previous example. The two well-expressed lobes north of G_{VI} (see Figs. 10a and b) belong to two different morphostructural zones; the left lobe lying within a mountain country, while the right lobe belongs to the Apulian peneplain, covered by Quaternary deposits. In the southern part of the G_{VI} zone the relief effect on the isoseismal shape cannot be assessed due to sparse observations and to the presence of the coastline.

The 1962 Irpinia earthquake is a multiple event consisting of a strong foreshock, $M_L = 5.9$, of a mainshock, $M_L = 6.1$, and of a moderate aftershock, $M_L = 4.5$ (DI FILIPPO and PERONACI, 1963). The first two events are separated by a 10-minute interval and have a very similar epicenter, therefore can be equally responsible for the MCS effect. According to GASPARINI *et al.* (1985) only the foreshock is a strike-slip event:

$$\text{foreshock FPS:} \quad \text{strike} = 32^\circ,\ \text{dip} = 65^\circ,\ \text{rake} = 11^\circ$$
$$\text{mainshock FPS:} \quad \text{strike} = 314^\circ,\ \text{dip} = 70^\circ,\ \text{rake} = 241^\circ$$

We take for the depth the values $h_{\text{for}} = h_{\text{main}} = 8$ km given by WESTAWAY (1987). Again, the a_p-isoseismal area for $I = \text{VI}$ is a weak function of the focal depth. For example, in the case of the mainshock we have the following relation:

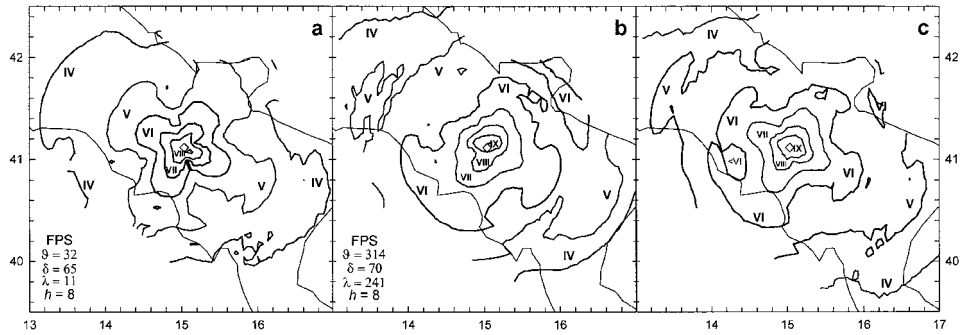

Figure 11
Isolines of the synthetic a_p-field for the 1962 Irpinia earthquake: (a) foreshock; (b) main shock; (c) cumulative a_p-effect for the foreshock and mainshock, assumed both with $M = 6.0$. The source parameters θ, δ, λ, h specify strike, dip, rake, and depth of the source respectively; the *diamond* is the epicenter.

h	8	16	24	32
$\log A\,[\mathrm{km}^2]$	4.1	4.1	3.7	3.9

For focal depths ranging from 8 to 20 km the shape of the a_p-isoseismal $I = \mathrm{VI}$ is elongated for the mainshock and it is cross-like for the foreshock. The case with $h = 8$ km is shown in Figure 11. Comparing Figures 10 and 11 we may conclude that the shape of the empirical isoseismal $I = \mathrm{VI}$ (Fig. 10b) is in good agreement with that of the theoretical one for the foreshock (Fig. 11a) but not for the mainshock (Fig. 11b). The foreshock and mainshock have magnitudes 6.0 ± 0.1, therefore we repeat our calculations assuming $M = 6.0$ for both events and we compute their cumulative effect, defined as the maximum of the a_p-values caused by the two events. In such a way we obtain the new picture shown in Figure 11c, compatible with Figure 10b.

5. Conclusion

This paper deals with the problem of the reconstruction of the isoseismal shape, and an original technique has been developed for this purpose. Since the problem is difficult, we attacked the issue (probably for the first time) from two sides at once: generalization of MCS data (discrete) to isoseismals (continuous), and modeling. The database of MCS data such as the one available now for Italy, the synthetic isoseismal modeling and the technique developed here provide a good basis for a systematic analysis of the relation between MCS observations and source geometry.

In the assumption that the observed MCS intensities always involve noise, we reduce the noise component with a modified polynomial filtering technique which controls the local maximum error. Following the principle "the IDP map is unique, while the number of isoseismals that is compatible with the map is infinite," in order

to visualize the uncertainty of the isoseismals we have developed the DB method. The method is suitable for the analysis of isoseismals of rank >1 and it is used to visualize the whole ensemble of reasonable versions of isoseismal consistent with the MCS data. We are unaware of approaches like the one proposed here, although the problem of visualizing the isoseismal's uncertainty has long been debated.

We show how the shape analysis of isoseismals may significantly benefit from synthetic modeling of ground motion. The theoretical modeling of ground motion and the simulation of the noise in IDP synthetic maps are independent sources for the delineation of the isoseismal shape and for the analysis of the effects of noise and of site geometry. Unfortunately, the model used and its parameters are inexact and the interconnection between intensity and acceleration remains open to discussion. Taking into account that the MCS data are affected by noise, site effect and space irregularity of observations, it is hardly justifiable to expect an exact coincidence between the shape of empirical and synthetic isoseismals. Therefore the results reported here for some Italian earthquakes should be regarded as the successes achieved by the joint use of the MCS data processing procedure, developed in this paper, and the ground-motion modeling with synthetic seismograms. For two strike-slip events we have found a cross-like pattern both in the MCS and in the synthetic data, and this contradicts the conventional recommendations for the generalization of MCS data, that usually advise the use of oval shapes. Finally, particularly important for engineering purposes, we show examples of the perspectives offered by the analysis of the multi-connected isoseismals to reveal site effects.

Acknowledgements

We are grateful to V. Ez, A. Lander, A. Nikonov and V. De Rubeis for useful comments. This work is supported by grants: ISTC (project 1293-99), NATO SfP 972266, USNSF: EAR 9804859, the Russian Foundation for Basic Research (00-05-64097) and by Italian MURST and CNR.

References

Aki, K. Strong motion Seismology. In *Strong Ground Motion in Seismology* (eds. M. O. Erdik and M. N. Toksöz) (D. Reidel Publ., 1987) pp. 3–39.

Blake, A. (1941), *On The Estimation of Focal Depth from Macroseismic Data*, Bull. Seismol. Soc. Am. *31*(3), 225–231.

BMS: Bolletino Macrosismico (1990), Instituto Nazionale di Geofisica, Unita Operativa Geodinamica, Roma.

Boschi, E., Ferrari, G., Gasperini, P., Guidoboni, E., Smriglio, G., and Valensise, G. *Catalogo dei Forti Terremoti in Italia dal 461 a.C. al 1980* (ING-SGA, Bologna 1995).

BOSCHI, E., GUIDOBONI, E., FERRARI, G., VALENSISE, G., and GASPERINI, P. *Catalogo dei Forti Terremoti in Italia dal 461 a.C. al 1990* (ING-SGA, Bologna 1997).

BURGER, R. W., SOMERVILLE, P. G., BARKER, J. S., HERRMANN, R. B., and HELMBERGER, D. V. (1987), *The Effect of Crustal Structure on Strong Ground Motion Attenuation Relations in Eastern North America*, Bull. Seismol. Soc. Am. *77*, 420–439.

CAMASSI, R. and STUCCHI, M. (1997), *NT4.1, un Catalogo Parametrico di Terremoti di Area Italiana al di Sopra della Soglia del Danno: A Parametric Catalogue of Damaging Earthquakes in the Italian Area*. Web site: http://emidius.itim.mi.cnr.it/NT/home.html

CMT: *Harvard Centroid Moment Tensor Database*, Harvard Seismology: CMT Search Results. Web site: http://www.seismology.harvard.edu

COSTA, G., PANZA, G. F., SUHADOLC, P., and VACCARI, F. (1993), *Zoning of the Italian Territory in Terms of Expected Peak Ground Acceleration Derived from Complete Synthetic Seismograms*, J. Appl. Geophys. *30*, 149–160.

DE RUBEIS, V., GASPARINI, C., and TOSI, P. (1992), *Determination of the Macroseismic Field by Means of Trend and Multivariate Analysis of Questionnaire Data*, Bull. Seismol. Soc. Am. *82*, 1206–1222.

DI FILIPPO, D. and PERONACI, F. (1963), *Indagine Preliminare della Natura Fisica del Fenomeno che ha Originato il Periodo Sismici Irpinio dell'Agosto 1962*, Ann. Geofis. *16*(4), 625–643 (in Italian).

FLORSCH, N., FÄH, D., SUHADOLC, P., and PANZA, G. (1991), *Complete Synthetic Seismograms for High-frequency Multimode Love Waves*, Pure appl. geophys. *136*, 529–560.

GNDT (1997), *Earthquakes of September and October 1997 in Umbria-Marche (Central Italy)*, *1997*. Web site: emidius.itim.mi.cnr.it/GNDT/T19970926-eng/home.html

GASPARINI, C., IANNACCONE, G., and SCARPA, R. (1985), *Fault-plane Solutions and Seismicity of the Italian Peninsula*, Tectonophysics *117*, 59–78.

GASPERINI, P., BERNARDINI, F., VALENSISE, G., and BOSCHI, E. (1999), *Defining Seismogenic Sources from Historical Earthquake Felt Reports*, Bull. Seismol. Soc. Am. *89*(1), 94–110.

GIARDINI, D., DONATO, M., and BOSCHI, E. (1997), *Calibration of Magnitude Scales for Earthquakes of the Mediterranean*, J. Seismol. *1*, 161–180.

GUSEV, A. A. (1983), *Descriptive Statistical Model of Earthquake Source Radiation and its Application to an Estimation of Short-period Strong Motion*, Geophys. J.R. Astr. Soc. *74*, 787–808.

JOHNSTON, A. C. (1996), *Seismic Moment Assessment of Earthquakes in Stable Continental Regions – II. Historical Seismicity*, Geophys. J. Int. *129*, 639–678.

KARNIK, V., *Seismicity of the European Area*, *Part 1* (Reid Publishing Company, Holland 1969).

KEILIS-BOROK, V. I., MOLCHAN, G. M., and KRONROD, T. L. (1984), *Seismic Risk for the Largest Cities of the World*, The Geneva Papers on Risk and Insurance *9*(32), 255–270. Full version: *Comput. Seismology*, Iss. 16, Moscow (in Russian).

KEILIS-BOROK, V. I., MOLCHAN, G. M., GOTSADZE, O. D., KORIDZE, A. Ch., and KRONROD, T. L. (1984a), *An Attempt of Seismic Risk Estimation for Rural Dwellings in Georgia*, Computational Seismology *17*, 58–67, Nauka, Moscow (in Russian). Translated in: The Geneva Papers on Risk and Insurance, 1984, Etudes et Dossiers, 77; Natural Disasters and Insurance (IV).

MONACHESI, G. and STUCCHI, M. (1997), *DOM 4.1, an Intensity Data Base of Damaging Earthquakes in the Italian Area*.Web site http://emidius.itim.mi.cnr.it/DOM/home.html (GNDT).

PANZA, G. F. (1985), *Synthetic Seismograms: The Rayleigh Waves Modal Summation*, J. Geophys. *58*, 125–145.

PANZA, G. F. and SUHADOLC, P. Complete strong motion synthetics. In *Seismic Strong Motion Synthetics* (ed., B. A. Bolt) (Academic Press, Orlando 1987), pp. 153–204.

PANZA, G., CRAGLIETTO, A., and SUHADOLC, P. (1991), *Source Geometry of Historical Events Retrieved by Syntethic Isoseismals*, Tectonophysics *193* 173–184.

PANZA, G., CAZZARO, R., and VACCARI, F. (1997), *Correlation between Macroseismic Intensities and Seismic Ground Motion Parameters*, Annali di Geofisica *40*(5), 1371–1382.

SHEBALIN, N. V. (1959), *Determination of Focal Depth from Macroseismic Data with Consideration of the Low Velocity Layer*, *Problems of Engineering Seismology*, Acad. Nauk SSSR, Inst. Fiz. Zemli Trudy *5*(172), 100–113.

SHEBALIN, N. V. (1972), *Macroseismic Data as Information on Source Parameters of Large Earthquakes*, Phys. Earth. Planet. Inter. *6*, 316–323.

SHEBALIN, N. V. (2000), *Selected Works*, vol. 2. (Academy of Mining Sciences, Moscow, *in press*) (in Russian).

SHTEINBERG, V., SAKS, M., APTIKAEV, F., ALKAZ, V., GUSEV, A., EROKHIN, L., ZAGRADNIK, I., KENDZERA, A., KOGAN, L., LUTIKOV, A., POPOVA, E., RAUTIAN, T., and CHERNOV, Yu. (1993), *Methods of Seismic Ground Motions Estimation* (Handbook). *Seismic ground motions prediction* (Engineering Seismology Problems; Issue 34), Moscow, Nauka, 5–94 (in Russian).

SIROVICH, L. and PETTENATI, F. (1999), *Seismotectonic Outline of South-Eastern Sicily: an Evaluation of Available Options for the Earthquake Fault Rupture Scenario*, J. Seismology *3*, 213–233.

TOSI, P., DE RUBEIS, V., and GASPARINI, C. (1995), *An Analytic Method for Separating Local from Regional Effects on Macroseismic Intensity*, Annali di Geofisica *38*(1), 55–65.

TOSI, P., TERTULLIANI, A., DE RUBEIS, V., and GASPARINI, C. (1999), *Preliminary Results of a Macroseismic Survey of the Colfiorito Sequence (Central Italy)*, Phys. Chem. Earth (A) *24*(6), 477–481.

TRIFUNAC, M. D. and BRADY, A. G. (1975), *On the Correlation of Seismic Intensity Scales with the Peaks of Recorded Strong Ground Motion*, Bull. Seismol. Soc. Am. *65*(1), 139–162.

WESTAWAY, R. (1987), *The Campania, Southern Italy, Earthquakes of 21 August 1962*, Geophys. J. R. Ast. Soc. *88*, 1–24.

ZAHRADNIK, J. (1989), *Simple Method for Combined Studies of Macroseismic Intensities and Focal Mechanisms*, Pure appl. geophys. *130*, 83–97.

(Received November 3, 2000, accepted February 12, 2001)

Pure appl. geophys. 161 (2004) 1725–1747
0033–4553/04/081725–23
DOI 10.1007/s00024-004-2532-3

Pure and Applied Geophysics

Shape of Empirical and Synthetic Isoseismals: Comparison for Italian $M \leq 6$ Earthquakes

G.M. MOLCHAN,[1,2] T.L. KRONROD,[1,2] and G.F. PANZA[2,3]

Abstract—We present results from a comparative analysis of empirical and synthetic shapes for isoseismals of low intensity (I = IV–VI on the MCS scale) for six Italian earthquakes of ML = 4.5–6. Our modeling of isoseismals is based on a plane-stratified earth model and on the double–couple point source approximation to calculate seismograms in the frequency range $f \leq 1$ Hz. With a minimum of parameter variation we demonstrate that the low intensity isoseismals provide information on source geometry. We strive to avoid subjectivity in isoseismal constructions by using the new Diffuse Boundary method, which visualizes isoseismals with their uncertainty. Similar results in this direction are known for large earthquakes ($M_L \approx 6$ or greater) with extended sources and for the higher isoseismals ($I \geq$ VI on the MM scale). The latter studies disregard the earth structure, use a greater number of parameters, and therefore have greater possibilities for fitting the data than our approach.

Key words: Intensity, macroseismic data, synthetic isoseismals, focal mechanism.

1. Introduction

Seismic hazard analyses deal with macroseismic intensity I and/or peak ground acceleration a_p. Acceleration is usually preferred, although the two quantities are essentially different. Macroseismic intensity is a measure of the *effect* that seismic motion produces on man and structures. This is influenced by resonance and residual displacements, the latter being only indirectly related to acceleration amplitude. The estimates of I are based on expert evaluations and questionnaire surveys, and, in this respect, intensity is less preferred when compared with accurate instrumental measurements of a_p. However, while a_p is measured at a site, I is relevant for an area, i.e., a group of type structures or the perceptions of people in a town or village as a whole. It follows that I has a statistical nature, so it is more stable than single–site a_p measurements. I–data are usually more dense in space. Furthermore, in spite of the

[1] International Institute of Earthquake Prediction Theory and Mathematical Geophysics, Russian Academy of Sciences, Warshavskoye sh., 79, k.2, Moscow 117 556, Russia.
E-mail: molchan@mitp.ru, Tel.: +007 (095) 110-7795, Fax: +007 (095) 310-7032
[2] The Abdus Salam International Center for Theoretical Physics, Sand Group, Trieste, Italy.
[3] Dipartamento di Scienze della Terra, Trieste University, Trieste, Italy.

Gutenberg–Richter law, the number of strong motion records with $I \leq 5$ (the MM scale) does not increase with decreasing I, because the engineers are not interested in low intensity excitations (see, e.g., APTIKAEV, 2001).

Theoretical modeling is only feasible for a_p, since it is extremely difficult to reproduce the detailed effects of an earthquake. The reason lies in the fact that the types of structures are rather diverse and are subject to aging, and the soil water content is always changing. Consequently, every observed I–data set is the result of a unique natural experiment, so it is not without reason that in recent years increasing attention is being paid to the development of macroseismic data bases (see BOSCHI *et al.*, 1997, 2000; MONACHESI and STUCCHI, 1997).

Instrumental observations of a_p are primarily needed to set up building codes for seismic regions. With this goal in view, probability maps of expected ground-motion acceleration are developed. However, when the insurance of type structures is at issue, one would prefer to use analogous maps of intensity, since intensity is directly related to damage statistics. It thus appears that none of the two quantities, I and a_p, is the one to be preferred. They are different and complementary quantities to be used jointly in seismic risk analysis.

I–data are successfully used to parameterize historical earthquakes, to be more specific, to determine magnitude and hypocenter position, as well as source azimuth and length for large events. The recent publications on this topic include BAKUN and WENTWORTH (1997); CECIĆ *et al.* (1996) GASPERINI *et al.* (1999) GASPERINI (2001) JOHNSTON (1999) MUSSON (1996) PERUZZA (2000). The remaining geometric source parameters (dip and rake) may be reflected in the shape of isoseismals as suggested in the paper by PANZA *et al.* (1991) (the history of relevant research can also be found in this reference), which seems to have been the first study to compare empirical isoseismals with theoretical ones, derived from complete synthetic seismograms for realistic earth models. The comparison was purely qualitative, since the theoretical isoseismals had not been calibrated in terms of intensity, while the empirical isoseismals provided no indication of their accuracy.

A characteristic frequency range (f = 0.5–10 Hz) is associated with macroseismic intensity I = IV–X (MSK scale) (SOKOLOV and CHERNOV, 1998). Consequently, the high frequency approximation of seismograms developed by BERNARD and MADARIAGA (1984) and SPUDICH and FRASER (1984) is of interest for the comparison between a_p and I. This approximation has been used recently as a theoretical background for a simple model of Intensity Attenuation Law for large earthquakes (BERARDI *et al.*, 1995; SIROVICH, 1996; PETTENATI *et al.*, 1999). In particular, the Attenuation Law developed by SIROVICH (1996) incorporates the direction of rupture propagation and the radiation pattern due to fault plane geometry. Since crustal inhomogeneity is disregarded, these generalizations of the I–attenuation are meant to deal with the geometry of the higher isoseismals for large ($M_w > 5.7$) events (SIROVICH, 1996). It was shown that the new I–attenuation models are good in some cases for fitting the higher isoseismals, especially when this fitting includes an

individual calibration of a_p (in terms of I) for each event. Thanks to the simplicity of the calculation involved, these approaches can possibly be used to invert I–data into source parameters. The question that arises however is, when the inversion is feasible and what are the bias and scatter due to unaccounted–for earth inhomogeneity; furthermore the interpretation of ''low–level experimental isoseismal shapes'' remains a ''highly questionable'' problem (SIROVICH, 1996).

The present study proceeds on the lines of PANZA *et al*. (1991). The complete synthetic seismograms are computed in the frequency range ≤ 1 Hz assuming lateral homogeneity of the crust and the point source model. For this reason we analyze the lower isoseismals of moderate ($5 \leq M_L \leq 6$) earthquakes, i.e., consider a situation that is adjacent to that described above as to M and I. The point source model involves the least possible number of source parameters, while the synthetic fields are calibrated in the same manner for all events. These limitations seriously constrain the degrees of freedom available for fitting the I–data.

The new part of our approach consists in mapping the isoseismal uncertainty. In recent years several formalized algorithms for isoseismal tracing have been put forward (TOSI *et al*., 1995; MOLCHAN *et al*., 2002; SIROVICH *et al*., 2002), and a persistent skepticism simultaneously arose regarding the use of isoseismals in the I–data analysis (see, e.g., GASPERINI *et al*., 1999; PETTENATI *et al*., 1999). The skepticism stems from the fact that the formalization of isoseismals taken by itself cannot overcome the subjectivity in isoseismal tracing, because the procedure invariably involves adjustable parameters. Speaking the language of mathematical statistics, one could restate the argument as follows: a point estimate of a parameter has little meaning without an associated confidence interval. For this reason we need a substitute interval estimation for the case of isoseismals as well, resulting in diffuse isoseismal boundaries. The problem has been treated by MOLCHAN *et al*. (2002), while KRONROD *et al* . (2002) have presented ordinary- and diffuse-boundary isoseismals of good quality for 55 earthquakes from Italian I–data bases (BOSCHI *et al*., 1997, 2000; and MONACHESI and STUCCHI, 1997). The present study aims to demonstrate, with examples of moderate events taken from the atlas of KRONROD *et al*. (2002), that diffuse boundaries provide some information on the source geometry.

2. Synthetic Intensity

We use the modal summation technique for Rayleigh and Love waves (PANZA, 1985; FLORSCH *et al*., 1991) to compute seismograms to be recorded within 200 km of the epicenter in the frequency range $f \leq 1$ Hz. The technique assumes the double–couple source model and a horizontally stratified earth, thus severely limits the degrees of freedom in the problem of comparing theoretical and empirical intensities.

Theoretical Intensity. There are many characteristics of strong motion that correlate with I: peak displacement, peak velocity, and peak acceleration; the Arias

intensity (ARIAS, 1970); Significant Acceleration (BOLT and ABRAHAMSON, 1982) and others. It is not, however, entirely clear which of these correlates with I best, and the problem seems to admit no unique solution. According to SOKOLOV and CHERNOV (1998) and CHERNOV and SOKOLOV (1999), each level of intensity I has its own optimal frequency band, which explains the diversity of instrumental counterparts of I. It is also known that, having to select between peak velocity and peak acceleration for the seismic design range $I > 6$ (MM scale), one should prefer the former (AMBRASEYS, 1974; APTIKAEV, 2001). However, since we use the point source model, we shall be interested in the interval $I =$ V–VII (MCS scale), which is, as a matter of fact, adjacent to $I > 6$ (MM scale).

The choice of the theoretical counterpart of I and the calibration of it are interrelated problems. Dealing with synthetic seismograms for the range $f \leq 1$ Hz we have suitable data for calibrating the above peak quantities only (see below). Our final option is the peak acceleration at frequencies $f \leq 1$ Hz, $\hat{a}_p$, as the theoretical counterpart of I. Since the vertical peak acceleration is usually smaller than the horizontal and since building are mainly damaged by horizontal motion, $\hat{a}_p$ was taken to be $\max_t \left\|a^H(t)\right\|$, where a^H is the horizontal acceleration vector and $||\cdot||$ is its norm.

Source Parameters. The point source model involves the following parameters: epicenter, depth (h), moment magnitude M_w , and the angles that specify the focal mechanism: (ψ, δ, λ) = (azimuth, dip, rake) or FPS (Fault Plane Solution) for brevity. This is the minimal possible set of source parameters. According to GUSEV and SHUMILINA (2000), the point source model is valid at distances greater than 1.5 the source length, nevertheless to be conservative, we will consider, in what follows, comparatively small events ($M_w \leq 6$) and examine lower empirical isoseismals.

Modeling of an event where the source is actually extended by using the point source model generates an uncertainty in h that is of the order of the source length. The typical magnitude uncertainty is 0.3, while an uncertainty of $\leq 20°$ is commonly assumed for the focal angles in cases where the fault plane solution is based on P–wave first motion data and is classified to belong to the highest category, class A (FREPOLI and AMATO, 1997).

A horizontally stratified earth is specified by velocity functions of depth for P and S waves, V_P (h) and V_S (h), the respective quality factors Q_P (h) and Q_S (h), and a density function $D(h)$. The earth model used for Italy (COSTA *et al.*, 1993) is based on data found in the literature. The velocity parameters are not uniform throughout the

►

Figure 1

Structural zones of Italy (**A** through **N**) and events discussed in the text. *Notations*: 1 — successfully modelled events (see Figs. 2–7); 2 — other events involved in the comparison of empirical and synthetic data: (24/06/1958, Aquiliano, $M_L = 5.0$; 15/07/1971, Parmense, $M_L = 5.3$; 13/12/1976, Riva del Garda, $M_L = 4.4$; 09/19/1979, Valnerina, $M_L = 5.5$; 09/11/1983, Parmense, $M_L = 4.9$; 29/04/1984, Gubbio, $M_L = 5.0$; 07/05/1984, Appenino Abruzzese, $m_b = 5.4$; 05/06/1993, Umbria, $M_L = 4.1$; 24/08/1995, Garfagnana, $M_d = 4.2$; 26/09/1997, Colfiorito, $M_w = 6.0$).

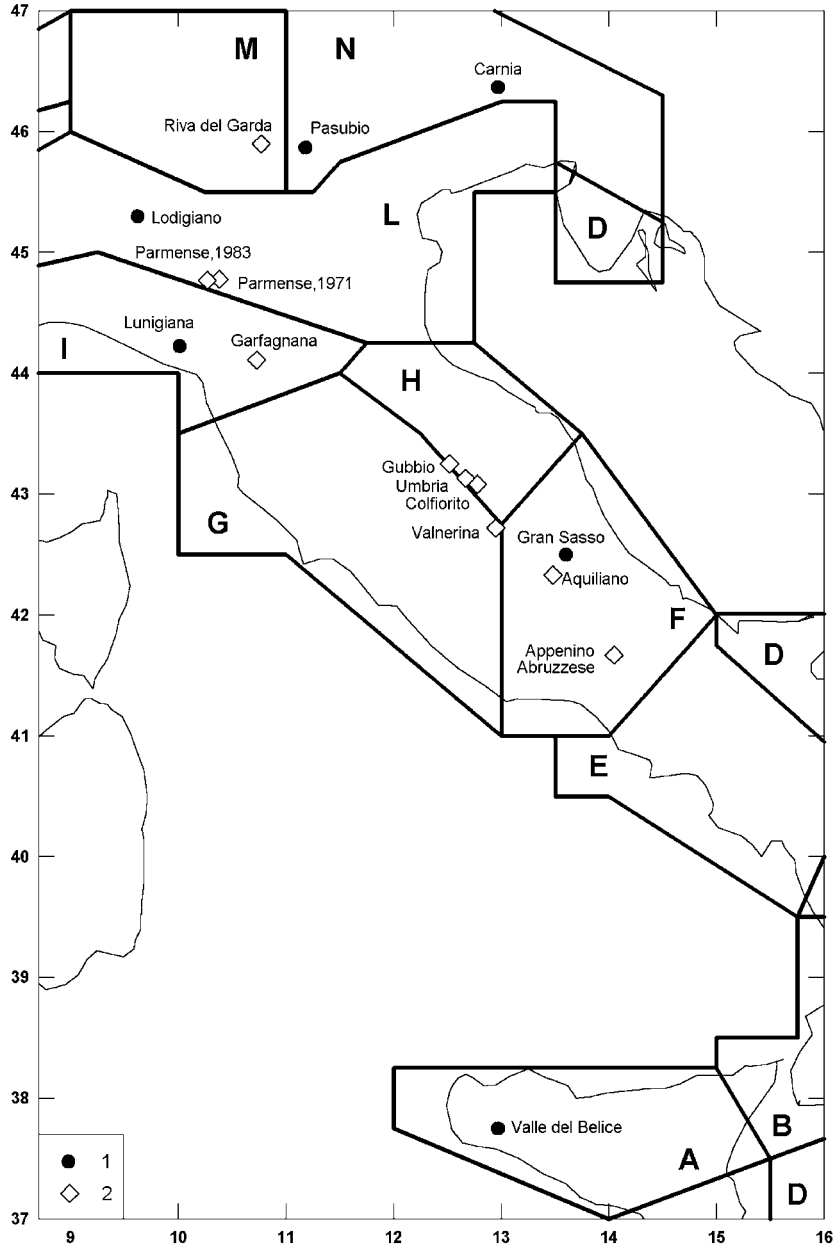

lithosphere in Italy, so COSTA *et al.* (1993) proposed a crude division of the lithosphere into several structural zones (Fig. 1), each having its own D, V and Q. The scale of lateral averaging for these functions must exceed the size of the isoseismals of interest. We recall that the $\hat{a}_p$ field is calculated for a horizontally

stratified earth. For this reason $\hat{a}_p$ may involve appreciable discontinuities across zone boundaries, when the parameters in the adjacent zones differ by significant amounts. Therefore, the presence of different structural zones means that any comparison of I and $\hat{a}_p$ fields must largely be based on those isoseismals which nearly fit into a single structural zone. We say "nearly ", because zone boundaries can well be transition zones in their own right.

The modal summation technique used here to compute seismograms is applied to events with a fixed moment, $M_0 = 1 \cdot 10^{-7}$ Nm. For an arbitrary moment the seismic signal spectrum is rescaled (differently at different frequencies) using the Gusev source spectrum (GUSEV, 1983; cf. an updated version in (AKI, 1987)). The spectrum was derived by averaging worldwide data and is, according to GUSEV (1983), a compromise to smooth both intra– and interregional variations. In practice this may produce a bias in the a_p amplitude, i.e., a mismatch between a_p and I, in cases where the $a_p - I$ relation is specified beforehand for the region of study.

The Calibration of $\hat{a}_p$. There are numerous empirical relations between peak acceleration and intensity. However, no I / $\hat{a}_p$ relation is available with the single exception of PANZA *et al.* (1999). These authors were comparing two types of field. The one, $I_{\max}(g)$, is the highest intensity ever observed at a point g. The other, $\hat{a}_p^{\max}(g)$, is a hypothetical maximum peak acceleration at point g in the frequency range $f \leq 1$ Hz. The map of $\hat{a}_p^{\max}$ is obtained by computing a family of accelerograms using earth models and focal mechanisms typical of Italian areas (COSTA *et al.*, 1993). The epicenters of the hypothetical events fill a regular grid, the depth of each event being assumed to be equal to 10 km for $M_w < 7$ and 15 km for $M_w \geq 7$. The magnitude of an event is set equal to the hypothetical maximum magnitude, $M_w^{\max}$, for the site of interest. The next step is to find, for each point on the map, the maximum value of the peak acceleration, $\hat{a}_p^{\max}$, that has been produced by some event of the family. PANZA *et al.* (1999) compared $I_{\max}$ and $\hat{a}_p^{\max}$ and obtained the regression equation

$$\log \hat{a}_p[\mathrm{cm/sec^2}] = b_0 + b_1 I + \varepsilon, \tag{1}$$

where ε is the regression residual, $b_0 = -1.61$ and $b_1 = 0.35$.

Since the models and the methodology we are using to compute seismograms are the same as in PANZA *et al.* (1999), we quantize the $\hat{a}_p$ scale according to the relation

$$\hat{a}_p = 3 \cdot 2^{I_a - 6}[\mathrm{cm/sec^2}], \tag{2}$$

where the integer quantity I_a will be called the theoretical (synthetic) intensity. Relation (2) means that we have adopted the rule of doubling $\hat{a}_p$ for a change of one in I_a , and we have $\hat{a}_p = 3$ for $I_a =$ VII according to (1).

Relation (2) is a very crude one. For instance, PANZA *et al.* (1999) note that $\hat{a}_p$ shows a better correlation with two variables, intensity and distance. Besides, regression (1) we are using was derived for fixed depths of the hypothetical events, and this assumption may have affected b_0. Therefore, the relation between

macroseismic intensity I and its synthetic counterpart, whenever the latter is available, cannot possibly be an exact one. If the isolines of $\hat{a}_p$ are assumed to be similar for adjacent levels, the expected invariants in the I vs. $\hat{a}_p$ comparison could be the orientation and shape of the isolines. The variation of the inexact parameters M_w and h is a suitable tool for adjusting the theoretical isoseismal area.

3. Isoseismals and the Visualization of Isoseismal Uncertainty

The intensity model does not incorporate site effects due to small–scale geologic and topographic heterogeneities. This difficulty can be overcome to a certain extent by generalizing I–data as isoseismals which act as a smoothing filter. MOLCHAN *et al.* (2002) have developed two methods for tracing isoseismals. The one is a smoothing technique, while the other also visualizes the uncertainty of an isoseismal. Both techniques examine the shape of isoseismal areas, and for this reason play a leading role in solving the problem of comparing spatial distributions of I and $\hat{a}_p$ In order to make this paper self–contained, we recapitulate briefly the two techniques.

The Modified Polynomial Filtering Method (MPF Method)

The method mainly aims at reducing the noise component in the data, including small–scale site effects. A circle $B_R(g)$ of radius R is centered at a point g of a regular grid. The radius is chosen so that at least n_p observations fall into the circle. The data in the circle are fitted with a surface of degree 2, $P_2(.)$, by the method of least-squares. The value of $P_2(.)$ at the center, g, is assumed to be the estimate $\hat{I}(g)$ of I at g. Since I is discrete, the radius R can be increased in the interval $(0, R_0)$ until the number of different intensity values in $B_R(g)$ exceeds a specified amount n_I. The greater the data noise, the higher is n_I. The introduction of the parameter n_I allows the highest degree of smoothing for the data in the annulus between adjacent isolines, where the field ought to be constant by assumption. The typical values of n_I and R_0 for Italy are $n_I = 3$, $R_0 =$ min (70 km, $D/4$), where D is the diameter of the $\{g_k\}$ points. The I value at the periphery is estimated at a point g, when the points that fall into $B_R(g)$ are seen at an angle $\varphi > 200^{\circ}$ looking from the center, thus avoiding unjustified extrapolation of the I observations. For the resulting smoothed $\hat{I}(g)$ field, the area where $\hat{I}(g) > (I - \Delta/2)$ is adopted as the isoseismal area of level I. Here Δ is the step in I.

The Diffuse Boundary Method (DB Method)

The idea of this method is more easily understood, if we consider the one–dimensional case of (g_k, I_k) observations. Suppose for the moment that isoseismals are embedded and that it is required to divide $I_k \geq J$ points (labelled '+' here) and $I_k < J$ points (labelled '–') which lie on a line. In that case there will be (in the

absence of noise) a cluster of pluses enclosed within two clusters of minuses. The empty intervals Δ_1 and Δ_2 that divide the pluses and the minuses cover the true boundary points. They are taken to be the diffuse isoseismal boundary of level J. Only some additional information and not the choice of the method can reduce the objective uncertainty of the boundary $\Delta_1 \cup \Delta_2$.

Let us suppose that the data involve some low noise. The cluster of pluses will then be subdivided, by '–' points, into a series of smaller clusters. Below we show schematically a variant where the plot starts from the barycenter of the pluses taken at zero, and it is required to find an analogue of the interval boundary Δ_2.

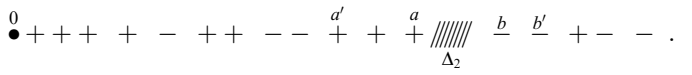

We specify a small parameter ε, to embody our notion of the noise level that is present in the data. It would be natural to suppose that pluses surrounded by minuses, when found at the periphery (on the right in our figure), must be erroneous. Consequently, we will find an interval $\Delta_2 = (a, b)$ that separates the cluster of pluses $[a', a]$ and the cluster of minuses $[b, b']$ and which has the following property: The number of pluses in the interval (a, ∞) is less than $\varepsilon \cdot 100\%$ of the total number of pluses in $(0, \infty)$, while the number of pluses in $[a', \infty)$ is greater than $\varepsilon \cdot 100\%$. In this case Δ_2 is taken to be the right–hand diffuse boundary between pluses and minuses. If the set of pluses is not a connected one, then Δ_2 is the interval estimate of the right–hand boundary itself. A similar definition is valid for Δ_1. In this way the parameter ε specifies the threshold of the possible error in the peripheral pluses.

The two–dimensional case can be reduced to solving a family of one–dimensional problems as follows. Let us assume that the isoseismal area G_I, where the intensity is greater than or equal to I is convex. Let us take in turn all "l" lines (as a matter of fact, this can be done at some discrete interval in the space of their parameters) that intersect the area which contains the intensity points. The $\{g_k\}$ points from the H neighborhood of an l line are projected onto l, the next step being to solve the above one–dimensional problem for l and I. The result will be two intervals Δ_1 and Δ_2 on the l line which characterize the uncertainty of an isoseismal of level I, when the isoseismal is viewed along the l ray. The totality of all intervals forms a jagged diffuse isoseismal boundary of level I (to be called the DB isoseismal from now on). The boundary looks rather unconventional, being as it is a family of line segments of various lengths and all possible directions. The decision about a diffuse boundary with respect to an individual straight line is not stable. However, a population of these decisions yields an additional quantity, namely, the intensity of superposition of the intervals, Δ_i (l), which makes the boundary rather stable.

The algorithm described above is valid for a convex G_I. As a matter of fact, G_I is not convex and it is not always simply connected, even when site effects have been

taken into account. Consequently, a DB isoseismal will lose some of the Δ_i intervals for those boundary points of G_I which are internal to the convex hull of G_I . This is due to the fact that only two (leftmost and rightmost) boundary points of G_I are taken into consideration in any I–data cross section. Nevertheless, this does not impede the identification of large–scale disconnected components of G_I (see KRONROD *et al.*, 2002; MOLCHAN *et al.*, 2002) or of peculiarities of the boundary of G_I . For example, a well–defined cross shape of the I = V isoseismal is seen in Figure. 2b instead of the conventional oval. Some elements of a cross shape can tentatively be discerned in the I = IV isoseismal derived by the MPF method (Fig. 2a).

The DB method involves two basic parameters: the bandwidth H and the noise parameter ε. The former is a smoothing parameter governed by the density of the observations: the higher the density, the smaller is H. The typical ε value for Italy is 5%, while H is 20–40 km.

We conclude by noting that the DB method is well adapted to deal with the comparison of a_p and I distribution in space. The preceding analysis shows that the relation between I_a and I cannot be an exact one, while a diffuse boundary can well estimate the shape of an isoseismal, but it is a rather poor estimate of its area.

4. Comparison of Synthetic and Empirical Intensities

Our joint analysis of I (MCS scale) and I_a is based on sixteen Italian earthquakes of magnitude $M_L \leq 6$ (Fig. 1). These sixteen are those events in the Atlas of KRONROD *et al.* (2002) for which the equivalent point source parameters are available, both MPF and DB techniques yield satisfactory isoseismals, and the number of site intensity observations is ~100 or greater. The isoseismals for each (I, I_a) pair are obtained using all I–data points and identical parameter sets. The comparison involves diffuse boundaries, the MPF method being merely used to identify strong local anomalies in the I–data. We test our conclusions about the relation between I and I_a by adding residuals at anomalous points to I_a When the conclusion remained unchanged, we treated it as robust with respect to the noise component in the I–data. (Part of the noise could also be caused by small–scale site effects among other factors.)

We use the trial–and–error strategy in our comparison between I and I_a fields. The source parameters (depth, magnitude, and FPS) borrowed from the literature are treated as the basic ones. In the case of multivalence of a parameter all its values are basic for us unless more arguments are advanced. In our strategy the relevant standard deviation of a parameter is the guide to fit I–data. The fitting possibilities have been extremely restricted owing to the time factor. A systematic variation of values of two or three parameters was not feasible. For this reason our fitting is far from optimal.

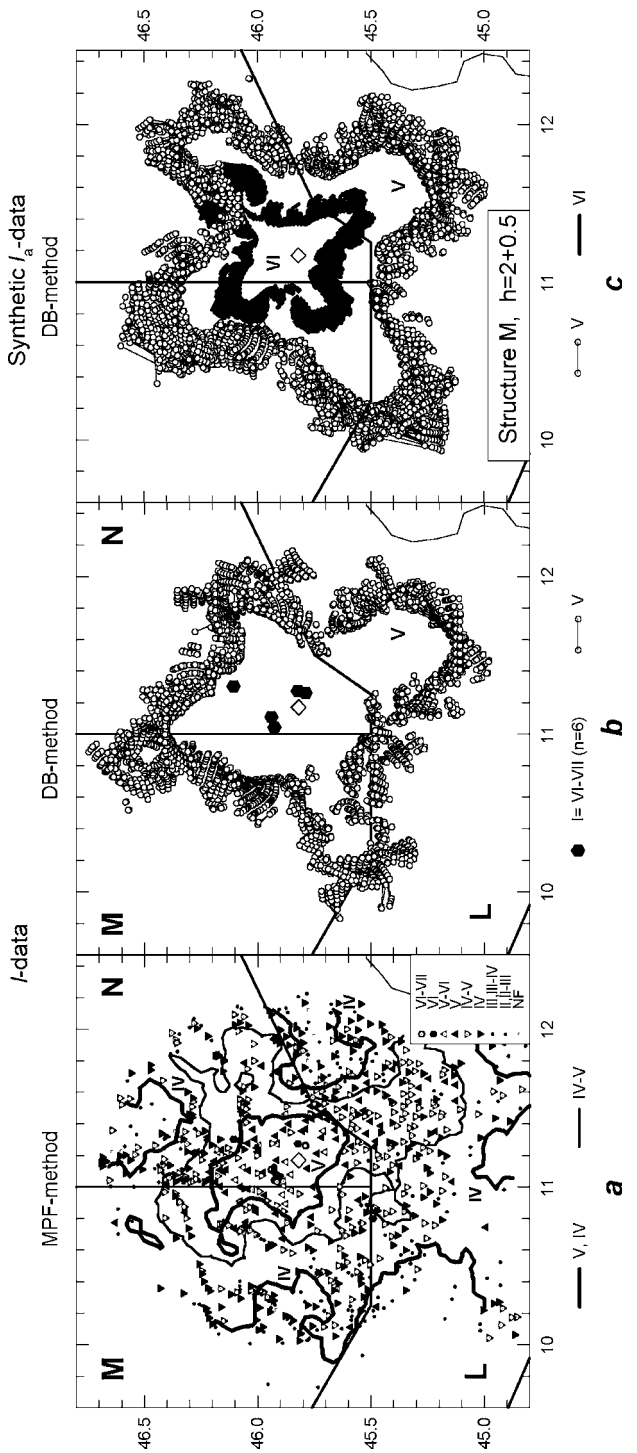

Figure 2

13/09/1989 Pasubio earthquake: Epicenter (45.86, 11.17); $h = 2$ (CS, 2001); FPS = (145°,85°,−180°) by A. Frepoli (class A); $M_L = 5.1$ (ISC), 4.4 (CS, 2001). a) MPF isoseismals and observations (symbols); b) I = VI–VII raw data (symbols) and DB isoseismal of level $I = V$; c) theoretical DB isoseismals of levels I_a = V, VI. Background: Epicenter (rhombus) and structural zones **M**, **N**, **L**.

Below we discuss six events for which the synthetic and empirical DB isoseismals are similar enough. The comparison between I and I_a involves individual isoseismals that are mostly within a single structural zone or within zones with similar parameters (Fig. 1). Our discussion of the six events will be confined to those parameters which have been varied in the analysis. They are specified in the figures either by giving the name of a structure (when the isoseismal intersects more structures than that specified) or as $a + \delta$, where a is the value of a parameter taken from the literature and δ is our correction with the sign.

The earthquake of 13/09/1989, $M_L = 4.4$ (CS), 5.1 (ISC), $I_0 =$ VI–VII, *Pasubio* (foothills of the Dolomite Alps). The I map is from BM (1989), the number of observations is $N_{\text{obs}} = 779$, and the results of the application of the MPF and DB methods are shown in Figure 2.

The DB method when applied to these data identifies the $I =$ V isoseismal pretty clearly. One observation site (Suzzara) has been eliminated from the data in Figure 2b, the reason being that the intensity value there seems to have been overestimated by one intensity unit. From Figure 2b it is seen that the DB isoseismal of level $I =$ V is cross–shaped. This kind of seismic energy radiation is typical of pure strike-slip earthquakes. We asked A. Frepoli to determine the earthquake mechanism for this event, and his results confirm our strike-slip hypothesis: dip $\delta = 85^{\circ}$, rake $\lambda = -180^{\circ}$. A more accurate inference can be drawn by comparing the $I =$ V isoseismal to its theoretical counterpart, the isoline of $I_a =$ V (Fig. 2c). Most of the $I =$ V isoseismal occupies two structural zones, **M** and **N** (see Fig. 2), just a small part falling into zone **L**. The earth models for **M** and **N** are very similar, so the theoretical calculations of $\hat{a}_p$ were based on the parameters of a single structural zone **M**, and the subsequent conclusions are not affected by the choice of **M** or **N**.

The similarity of the DB isoseismals of level V is achieved by using the magnitude $M_w = 5.1$ and the depth $h = 2.5$ km instead of $h = 2$ km (CS, 2001). The choice $M_w = 5.1$ instead of $M_L = 4.4$ (CS, 2001) is in agreement with the values given by the International Seismological Centre, namely, $M_L = 5.1$ and $m_b = 5.1$ (NAO Network). Besides, PERESAN *et al.* (2000) note that the post–1987 M_L magnitudes for Italian earthquakes, as reported in the ING Bulletins, are underestimated by an average of 0.5. For this reason the estimate $M_L = 4.4$ is less preferable.

The empirical I–data for this earthquake are contaminated by a strong "noise." For example, the residual of I is found to be in excess of one unit, after smoothing the data by the MPF method, at 42 sites (of a total of 779). Adding these residuals to the theoretical values of I_a does not affect the shape of the theoretical DB isoseismal at $I_a =$ V. In other words, the conclusion that the I and I_a isoseismals of level V are similar will not be affected by the noise component that may be present in the I–data.

The earthquake of 27/03/1928, $M_L = 5.6$, $I_0 =$ VIII, *Carnia* (Carnian Alps). The I map is from BOSCHI *et al.* (2000), $N_{\text{obs}} = 289$, and the result of the application of the DB method is shown in Figure 3.

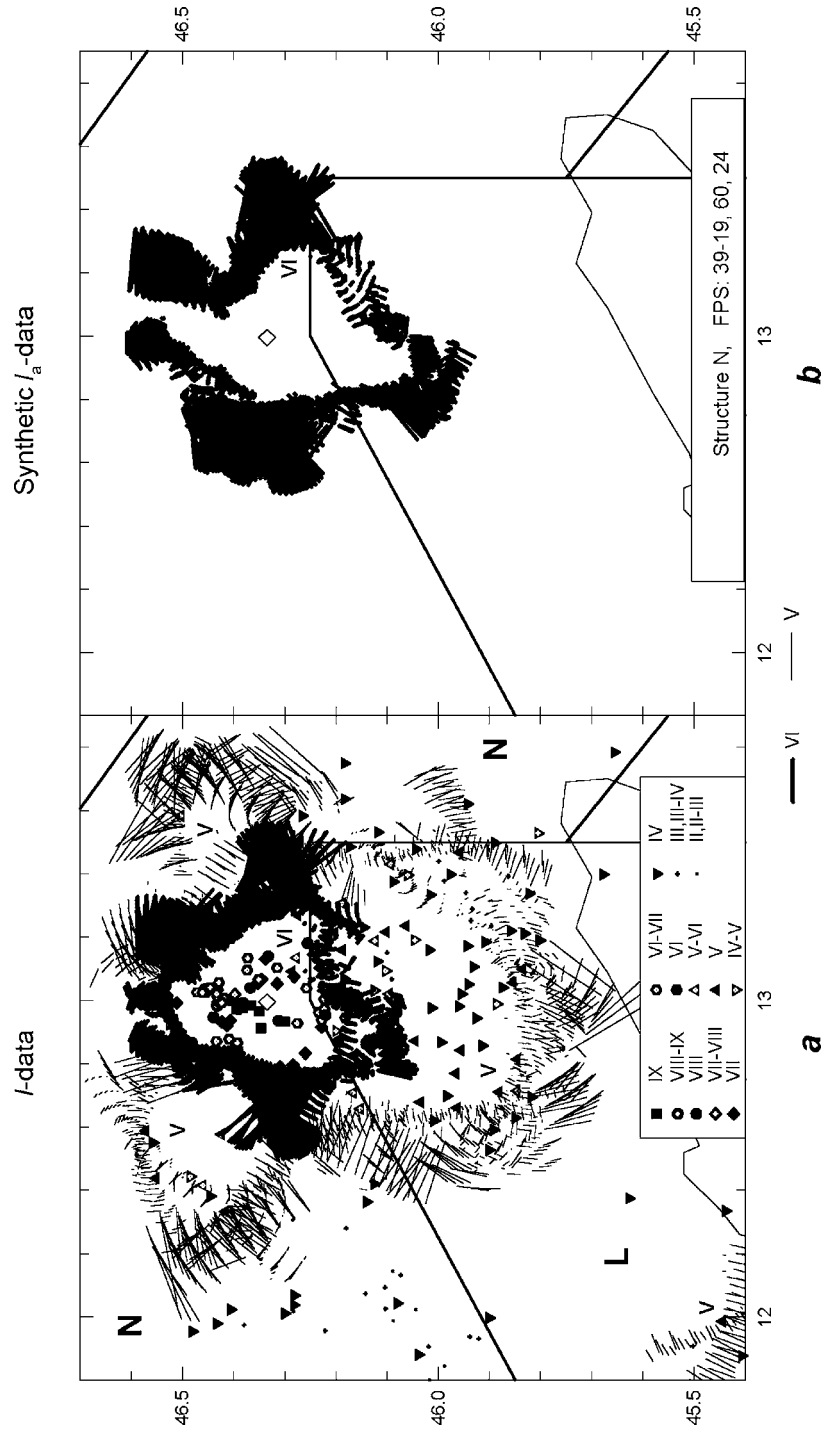
Synthetic I_a-data
I-data
Structure N, FPS: 39-19, 60, 24
IX
VIII-IX
VIII
VII-VIII
VII
VI-VII
VI
V-VI
V
IV-V
IV
III,III-IV
II,II-III
N
L
a
b
VI
V
46.5
46.0
45.5
12
13

Figure 3 compares the DB isoseismals of level VI for I and I_a. The $I > V$ isoseismal area is entirely contained in the structural zone **N** (Fig. 1), while, to the south, it approaches the boundary of zone **L**, representative of the Padan basin, where the structural parameters are significantly different from those of **L**. For this reason it is unlikely that the details in the southern part of the $I = VI$ isoseismal can be identified. In the example we are discussing, we choose the value $h = 4$ among the three available estimates $h = 4.5$ and 20 km and we set $M_w = M_L = 5.6$. Only the azimuth of the fault has been modified by (-19°), i.e., the angles (20°, 60°, 24°) have been used instead of the ones given by the FPS = (39°, 60°, 24°). The FPS solution can hardly belong to class A, since there is a different option in the literature (GI, 1985): FPS = (112°, 90°, 0°) which shows that the strike-slip nodal planes have been determined inaccurately. Nevertheless, our correction to the azimuth does not exceed 20°. Overall, the DB boundaries of level VI for the observed and theoretical intensities are in a qualitative agreement.

The earthquake of 15/05/1951, $M_L = 5.0$, $I_0 = VI$, *Lodigiano* (western Padan basin, Lombardy). The I map is from MONARCHESI and STUCCHI (1997), $N_{obs} = 88$ for the main shock and $N_{obs} = 32$ for the aftershock, and the result of the application of the DB method is shown in Figure 4.

The event is not easy to analyze, because the $I \geq V$ isoseismal zone (rank 1) is in the Padan basin, while its boundary is in the transition zones between **M** and **L** to the north, and between **I** and **L** to the south, the structural parameters for **M** and **I** being very different from those for L. For this reason the $\hat{a}_p$ field for each of the three zones (L, M, N) was calculated from the structural parameters of its own zone. The main shock, $M_L = 5.0$, $h = 6$ km, FPS = (221°, 74°, 209°), was followed by an $M_L = 4.2$–4.6 aftershock. When one deals with a sequence of large events, the counterpart of the theoretical intensity I_a at a site is the largest of the theoretical values of I_a corresponding to these events. In the example under discussion, the value $M = 5.0$ was selected from the three magnitude estimates $M_L = 4.9$, 5.0, 5.5 available for the main shock, while the depth $h = 6$ km was modified to become 4 km. For the aftershock we adopted the value $M_w = 4.5$ (CAGNETTI *et al.* (1976) give $M = 4.5$ without specifying the type of M), while the depth $h_{aft} = 6$ km was modified to become 3 km. This minimal adjustment of the depths leads to a satisfactory agreement between the isoseismals of level V (see Fig. 4). The discrepancies for the southern part of the boundary are quite understandable, since the structural parameters of a transition zone seem to be valid there.

◀

Figure 3

27/03/1928 Carnia earthquake: Epicenter (46.38, 12.98); $h = 4$ (KUNZE, 1982), 5 (NT, 1997), 20 (CAGNETTI *et al.*, 1976); FPS = (39°,60°,24°) (CAGNETTI *et al.*, 1976), (112°,90°,0°) (GI, 1985); $M_L = 5.6$ (NT, 1997), 5.8 (CAGNETTI *et al.*, 1976); a) raw data (symbols) and DB isoseismals of levels $I = VI, V$; b) theoretical DB isoseismal of level $I_a = VI$; Background: epicenter (rhombus) and structural zones N, L.

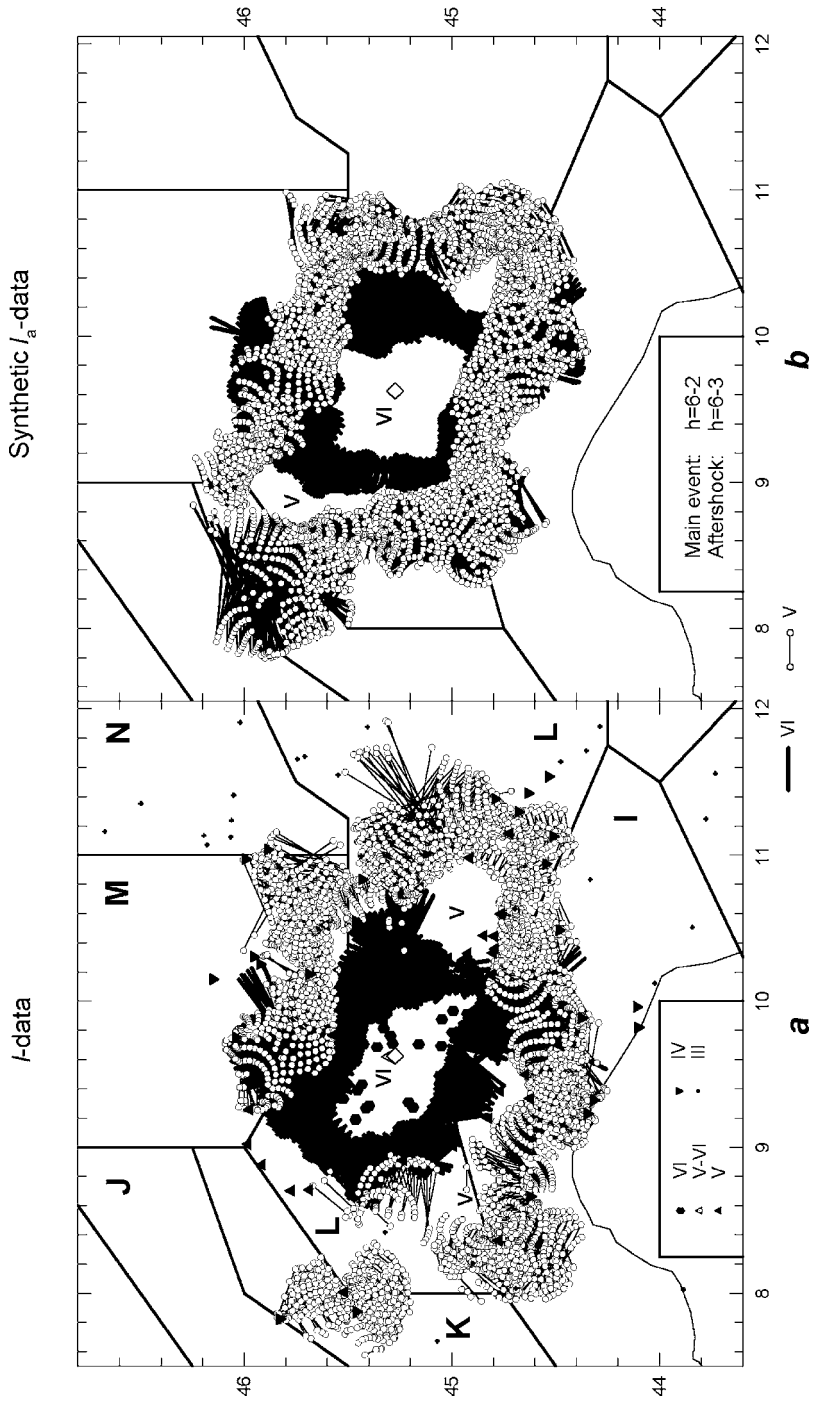
Synthetic I_a-data
I-data
a
b
VI
V-VI
V
IV
III
Main event: h=6-2
Aftershock: h=6-3
J
L
K
M
N
I
L
V
VI
46
45
44
8
9
10
11
12

The earthquake of 10/10/1995, $M_L = 5.1$, $I_0 =$ VI, *Lunigiana* (Ligurian Apennines, Northern Italy). The I map is from BM (1995), $N_{\text{obs}} = 330$, and the result of the application of the DB method is shown in Figure 5.

The event is strike slip as indicated by the FPS parameters, dip = 80°, rake = 170°, and by the DB boundary for $I =$ IV (Fig. 5a). One objection against drawing that inference from the macroseismic data consists in the fact that one lobe of the cross–shaped $I =$ IV isoseismal is at sea, where no observations are available. A very good agreement for the level IV isoseismals of I and I_a is achieved by modifying a single parameter, namely, adding $+30°$ to the fault azimuth. That (possibly overestimated) correction affects the orientation of the isoseismal, but not its shape. The calculation of $\hat{a}_p$ was for $M_w = 5.1$ (NEIC) and $h = 2$ km (FREPOLI and AMATO, 1997) selected from four known depth values in the range (2–10) . The greater southward elongation of the empirical DB isoseismals of levels $I =$ IV and V, compared with theory, can well be accounted for by low attenuation in zone G (Toscana).

The earthquake of 05/09/1950, $M_L = 5.6$, $I_0 =$ VIII, *Gran Sasso* (Abrutian Apennines, Central Italy). The I map is from (MONACHESI and STUCCHI, 1997), $N_{\text{obs}} = 136$, and the result of the application of the DB method is shown in Figure 6.

In our experience, the junction of zones **G**, **H** and **F** in the central Apennines (Fig. 1) is one of the most difficult regions in Italy for isoseismal analysis. The boundaries of the structural zones deserve a special study. The $I =$ VII isoseismal (rank 1) for the Gran Sasso earthquake is mostly in the structural zone F, but its western part covers the boundary of zones G and H. This circumstance, in principle, should require a more sophisticated procedure than the one used here for the analysis and modeling of the $I =$ VII isoseismal. Nevertheless, adding $+0.4$ to $M_L = 5.6$, $-10°$ to the azimuth 207°, $+20°$ to the rake 262°, and -0.5 km to the depth $h = 3$ km, we have achieved a very good agreement for the isoseismal shape at level VII of I and I_a. These variations of the parameters are quite justified for an event occurring in the mid–20th century.

The earthquake of 15/01/1968, $M_L = 6.0$, $I_0 =$ X, *Valle del Belice* (Sicily). The I map is from BOSCHI *et al.* (2000), $N_{\text{obs}} = 168$, and the result of the application of the DB method is shown in Figure 7.

The event includes a main shock with $M_L = 5.9$–6.0, a large foreshock with $M_L = 5.6$ which occurred 30 minutes before the main shock, and two aftershocks with $M_L = 5.5$–5.6 and $M_L = 5.5$–5.7 occurred 1 and 10 days after the main

◀

Figure 4

15/05/1951 Lodigiano earthquake: Epicenter (45.30, 9.62); $h = 6$ (GI, 1985), 12 (NT, 1997); FPS = (236°,74°,192°) (GI, 1985); $M_L = 4.9$ (NT, 1997), 5.0 (GI, 1985), 5.5 (NEIC). Aftershock (epicenter: triangle): $h = 6$ (GI, 1985), FPS = (221°,74°,209°) (GI, 1985), $M = 4.5$ (GI, 1985); a) raw data (symbols) and DB isoseismals of level $I =$ VI, V; b) theoretical DB isoseismals of level $I_a =$ V, VI; Background: epicenter (rhombus) and structural zones I, J, K, L, M, N.

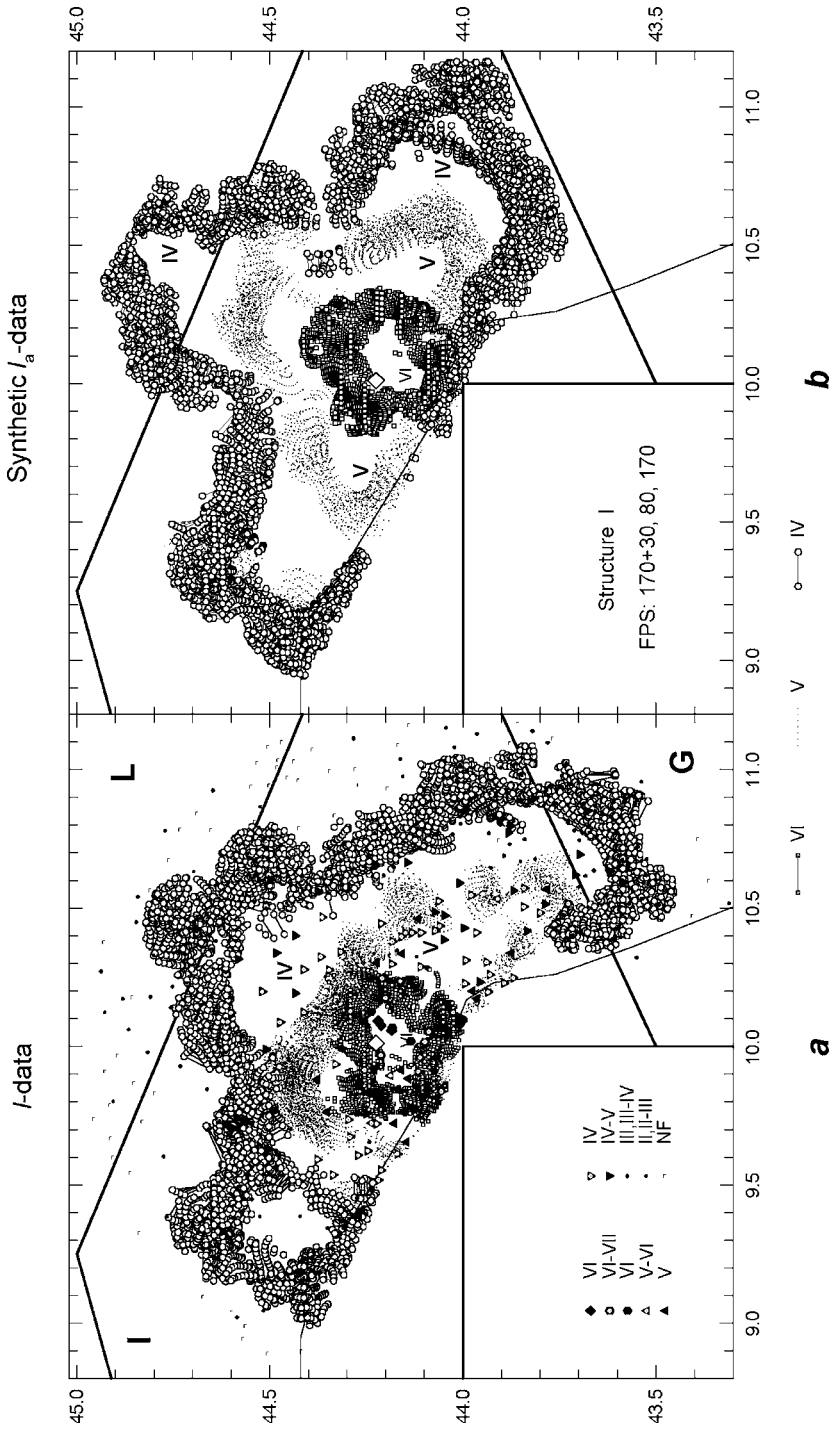
Synthetic I_a-data
I-data
Structure I
FPS: 170+30, 80, 170
L
G
I
VI
VI-VII
VI
V-VI
V
IV
IV-V
III, III-IV
II, II-III
NF
a
b
45.0
44.5
44.0
43.5
9.0
9.5
10.0
10.5
11.0

shock, respectively. For all the events one and the same epicenter is reported, except for the first aftershock. For the main shock two FPS solutions have been determined: (250°, 50°, 35°), (204°, 70°, 15°). It is very difficult to conduct parametric experiments when dealing with a composite event. Therefore we have limited our analysis to the following set of parameters: magnitude of the main shock, $M_w = 6.0$, and magnitudes of the aftershocks, $M_w = 5.5$ and 5.6, depth $h = 7$ km for all events. The literature and catalogs report very discrepant data on the depths, giving values ranging from 3 to 44 km. The comparison of the DB isoseismals at level VII of I and I_a (Fig. 7) shows good agreement between theory and observations. We recall that the value of I_a at a site is the largest of the theoretical values of I_a corresponding to the main shock and its fore– and aftershocks.

5. Conclusion and Discussion

We have presented results (Figs. 2 through 7) of a comparative analysis of empirical and theoretical isoseismal shapes for six Italian $M_L = 5$–6 earthquakes. Our modeling of isoseismals uses a plane–stratified earth model and reduces the number of parameters to a minimum. The statement applies both to our description of the source and to the method used for calibrating the theoretical intensity.

Our comparison of isoseismals is a qualitative one, but it is based in this particular case on a special method of isoseismal visualization that incorporates isoseismal uncertainty (MOLCHAN *et al.*, 2002). This circumstance removes from isoseismals the reputation of being a subjective tool for the I–data analysis. The examples in Figures 2 through 7 display the shape of the lower isoseismals of level I_{MCS} = IV–VII and show that their shape can be well fitted with models. In particular, Figures 2 ,3 and 5 clearly show a radiation pattern (cross shape) related to the source geometry. In five cases of the six, the agreement in shape is achieved by varying a single parameter, namely, depth of focus or azimuth, with respect to values given in the literature. (We have not bothered to choose a suitable parameter value, when this is found in the literature in a few variants.) The computational complexity does not admit a simultaneous successive variation of several parameters. Consequently, our fitting is not the result of a complete systematic variation of parameters.

◀

Figure 5

10/10/1995 Lunigiana earthquake: epicenter (44.23, 10.01); $h = 2$ (FREPOLI and AMATO, 1997), 5 (CS, 2001), 7 ± 4 (TERTULLIANI and MARAMAI, 1998), 10 (NEIC); FPS = (170°,80°, 170°) (FREPOLI and AMATO, 1997, class A); $M_L = 5.1$ (NEIC), 5.3 (ISC); a) raw data (symbols) and DB isoseismals of level I = VI, V, IV; b) theoretical DB isoseismals for I_a = VI, V, IV; Background: epicenter (rhombus) and structural zones I, G, L.

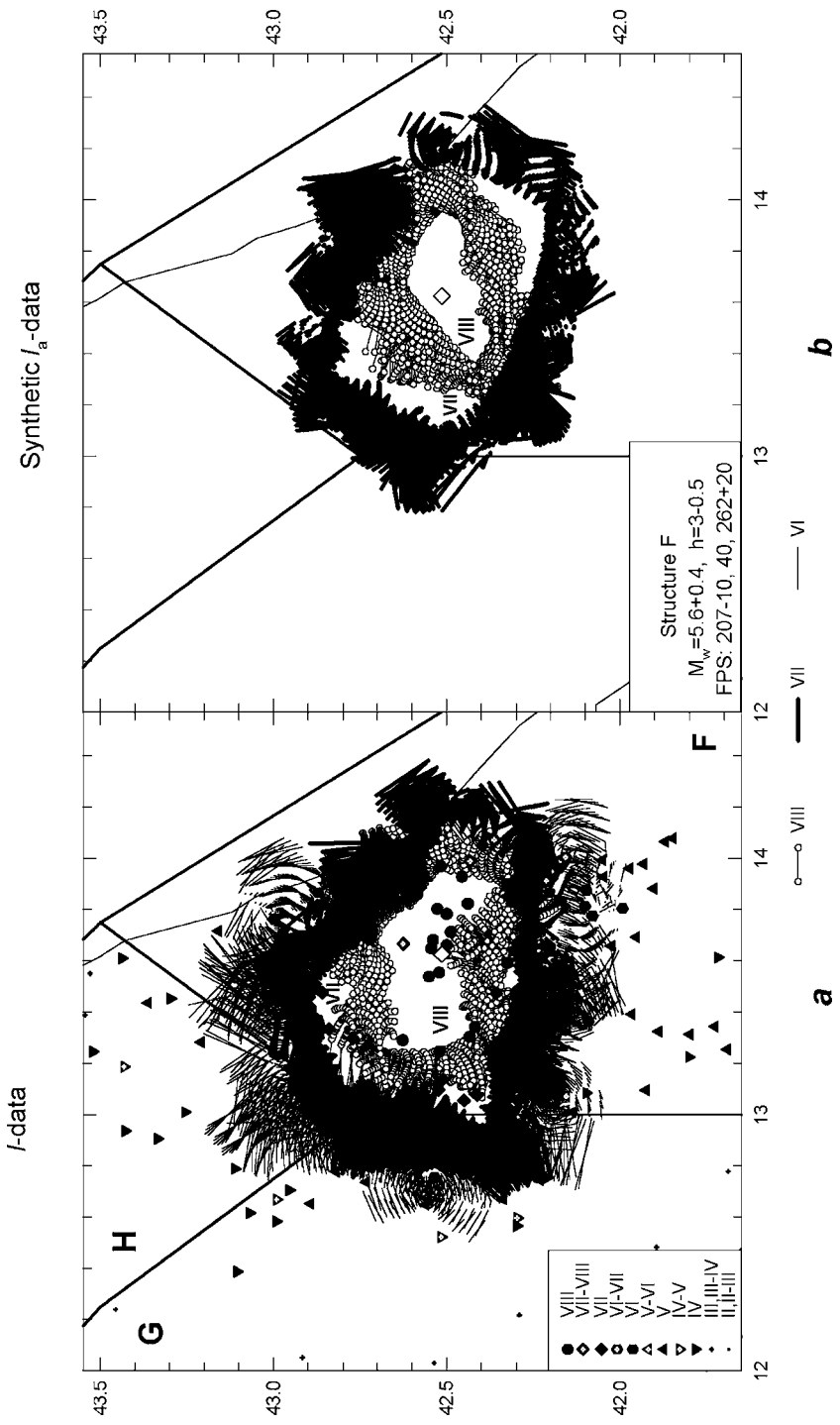
Synthetic I_a-data
I-data
Structure F
M_w=5.6+0.4, h=3-0.5
FPS: 207-10, 40, 262+20
VIII
VII-VIII
VII
VI-VII
VI
V-VI
V
IV-V
IV
III, III-IV
II, II-III
VIII
VII
VI
a
b
F
G
H
43.5
43.0
42.5
42.0
12
13
14

On the other hand, the fact that the fitting of the five events has been easy argues for the informativeness of the diffuse boundaries, I = IV–VII (MCS), for moderate earthquakes.

We have made a point of mentioning other 10 events (Fig. 1) where our theoretical calculations are not sufficient to substantiate the observed isoseismal shapes. During the course of this work we found that the isoseismal shapes are dependent on the earth's velocity parameters. To simplify the calculation of the wavefields we use a lateral averaging of the earth model for Italy in zones **A** through **N** (Fig. 1). Three of these (F, G, H) cover central Italy, which is too crude an approximation judging from the literature (see, e.g., DELLA VEDOVA *et al.*, 1991; CHIMERA *et al.*, 2002). Five of these ten events occurred in this part of Italy (Fig. 1), therefore it is not ruled out that the negative result for these five events is due to the crudeness of the velocity model.

In this connection we wish to draw the attention to those methods of I modeling which disregard the earth structure (BERARDI *et al.*, 1995; SIROVICH, 1996). Such approaches are relevant to larger events and higher intensities. Owing to the simplicity of the calculation involved they allow practically complete successive variation of the parameters whose number is increased by 3 when an extended source is concerned (the Mach number plus source dimensions). BERARDI *et al.* (1995) use three more parameters for the calibration of theoretical intensity, and this may result in overfitting the I–data.

The earthquake source information, as contained in the lower isoseismals of relatively small events ($5 = M_L = 6$) is not obvious. This is borne out by the persistent tendency of drawing isoseismals as ovals. Our examples of a fine relation between I–data and models are derived under at least three crude assumptions: regionalization (Fig. 1), calibration of theoretical intensity (2), and possibly the frequency range ($f \leq 1$ Hz), as far as the analysis of $I \leq$ VI is concerned. This is, to some degree, a certain reserve for further analysis of events from the catalog of KRONROD *et al.* (2002).

Acknowledgements

Dr. G. Leydecker and the other, anonymous, reviewer have made many critical remarks, which have been gratefully accepted and taken into consideration. We are very grateful to A. Gusev for a discussion of our work, as well as to A. Frepoli for the

◀

Figure 6

05/09/1950 Gran Sasso earthquake: epicenter (42.50, 13.60); h = 3 (NT, 1997), 10 (GI, 1985); FPS = (207°, 40°, 262°) (GI, 1985), M_L = 5.6 (NT, 1997); a) raw data (symbols) and DB isoseismals of level I = VIII, VII, VI; b) theoretical DB isoseismals for I_a = VIII, VII; Background: epicenter (rhombus) and structural zones F, G, H.

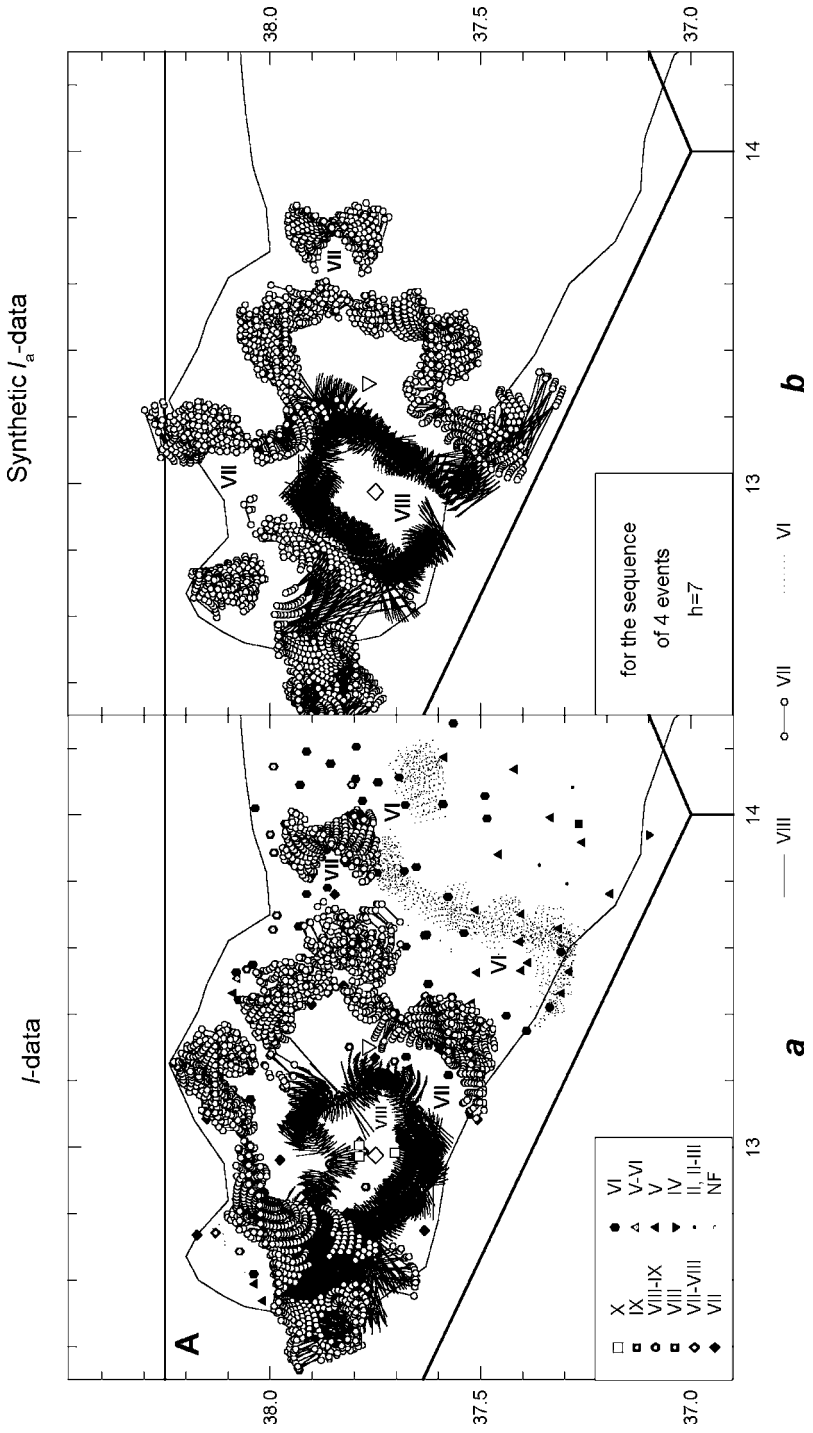
Synthetic I_a-data
I-data
A
a
b
38.0
37.5
37.0
13
14
X
IX
VIII-IX
VIII
VII-VIII
VII
VI
V-VI
V
IV
II, II-III
NF
VIII
VII
VI
for the sequence
of 4 events
h=7

materials he let us to use and for his FPS computations for the Pasubio earthquake. This work was supported by NATO SfP 972266, COFIN2000-2002 (MIUR), and by the James McDonell Foundation.

References

AJ: Anderson, H. and Jackson, J. (1987), *Active Tectonics of the Adriatic Region*, Geophys. J. *91*, 937–983.

Aki, K., *Strong motion seismology*. In (Erdik, M.O. and Toksöz, M.N., eds) *Strong Motion in Seismology* (D. Reidel Publ., 1987) pp. 3–39.

Ambraseys, N. (1974), *Notes on engineering seismology*. In (J. Solnes, ed), *Engineering Seismology and Earthquake Engineering,* Nato Advanced Study, 33–54.

Aptikaev, F.F. (2001), *Strong Ground Motion Due to Earthquakes* (in Russian), Doctoral Thesis, United Institute of Physics of the Earth, Moscow.

Arias, A., *A measure of earthquake intensity*. In (R. Hansen, ed), *Seismic Design for Nuclear Power Plant* (MIT Pres, Cambridge, 1970).

Bakun, W. and Wentworth, C. (1997), *Estimating Earthquake Location and Magnitude from Seismic Intensity Data,* Bull. Seismol. Soc. Am. *87*(6), 1502–1521.

Berardi, R., Merdez, A., Mucciarelli, M., Pactor, F., Longhi, G., and Petrungaro, C. (1995), *On the Modeling of Strong Motion Parameters and Correlation with Historical Macroseismic Data: An Application to 1915 Avezzano Earthquake,* Annali di Geofisica *38*(5-6), 851–866.

Bernard, P. and Madariaga, R. (1984), *A New Asymptotic Method for the Modeling of Near–field Accelerograms,* Bull. Seismol. Soc. Am. *74*(2), 539–557.

BM: *Bolletino Macrosismico*; 1988-1995, Instituto di Geoficica, Unita Operativa Geodinamica, Roma.

Bolt, B. and Abrahamson, N. (1982), *New Attenuation for Peak and Expected Accelerations of Strong Ground Motion,* Bull. Seismol. Soc. Am. *72*(6), 2307–2322.

Boschi, E., Guidoboni, E., Ferrari, G., Valensise, G., and Gasperini, P. (1997), *Catalogo dei Forti Terremoti in Italia dal 461 A.C. al 1990, No. 2,* Instituto Nazionale di Geofisica (ING), Storia Geofisica Abientale (SGA), Roma, Italy. CD and paper version (in Italian).

Boschi, E., Guidoboni, E., Ferrari, G., Margotti, D., Valensise, G., and Gasperini, P. (2000), *Catalogue of Strong Italian Earthquakes from 461 A.C. to 1997,. Introductory Texts and CD-ROM,* Annali di Geofisica *43*(4), 609–868 and CD ROM.

Cagnetti, V., Pasquale, V., and Polinari, S. (1976), *Focal Mechanisms of Earthquakes in Italy and Adjacent Regions*, CNEN RT/AMB, Roma *76*(4), 41 pp.

CCI: Peresan, A., Costa, G., and Vaccari, F. (1997), *The Current Catalogue of Italy,* International Centre for Theoretical Physics, Miramare-Trieste.

◀

Figure 7

15/01/1968 Valle del Belice earthquake: epicenter (37.75, 12.97); h = 3 (GI, 1985), 10 (AJ, 1987), 44 (NT, 1997); FPS = (270°, 50°, 35°) (AJ, 1987), (204°, 70°, 15°) (GI, 1985); M_L = 6.0 (CCI, 1997), 5.9 (NT, 1997). Foreshock: h = 20 (GI, 1985), 48 (CCI, 1997); FPS = (40°, 82°, 46°) (GI, 1985), M_L = 5.6 (Karnik, 1969). 1–day aftershock: h = 14 (GI, 1985), 36 (AJ, 1987), 47 (CCI, 1997); FPS = (250°, 58°, 18°) (AJ, 1987), (327°, 59°, 3°) (GI, 1985); M_L = 5.5 (CCI, 1997), 5.6 (Karnik, 1969). 10–day aftershock: h = 3 (AJ, 1987), 4 (GI, 1985), 30 (CCI, 1997); FPS = (270°, 64°, 31°) (AJ, 1987), (4°, 90°, 125°) (GI, 1985); M_L = 5.7 (CCI, 1997), 5.5 (Karnik, 1969); a) raw data (symbols) and DB isoseismals of levels I = VIII, VII, VI; b) theoretical DB isoseismals for I_a = VIII, VII; Background: epicenter (rhombus), epicenter of 1–day aftershock (triangle) and structural zone A.

CECIĆ, I., MUSSON, R., and STUCCHI, M. (1996), *Do seismologists agree upon epicentre determination from macroseismic data? A survey of ESC Working Group "Macroseimology",* Annali di Geofisica *39*(5), 1013–1040.

CHERNOV, YU. and SOKOLOV, V. (1999), *Correlation of Seismic Intensity with Fourier Acceleration Spectra,* Physics and Chemistry of the Earth, Part A: Solid Earth and Geodesy *24*(6), 522–528.

CHIMERA, G., AOUDIA, A., SARAÒ, A., and PANZA, G. (2002), *Active Tectonics in Central Italy: Constraint from Surface Wave Tomography and Source Moment Tensor Inversion,* Preprint IC/2002/86, The Abdus Salam International Centre for Teoretical Physics, Trieste, Italy.

COSTA, G., PANZA, G.F., SUHADOLC, P., and VACCARI, F. (1993), *Zoning of the Italian Territory in Terms of Expected Peak Ground Acceleration Derived from Complete Synthetic Seismograms,* J. Appl. Geophys. *30*, 149–160.

CS (2001): *Catalogo strumentali dei terremoti 'italiani' dal 1981 al 1996,* Instituto Nazionale di Geofisica, INGV-GNDT, Roma, CD ROM.

DELLA VEDOVA, B., MARSON, I., PANZA, G.F., and SUHADOLC, P. (1991), *Upper Mantle Properties of the Tuscan-Tyrrhenian Area: A Framework for its Recent Tectonic Evolution*, Tectonophysics. *195*, 311–318.

FLORSCH, N., FÄH, D., SUHADOLC, P., and PANZA, G. (1991), *Complete Synthetic Seismograms for High-frequency Multimode Love Waves*, Pure Appl. Geophys. *136*, 529–560.

FREPOLI, A. and AMATO, A. (1997) *Contemporaneous Extension and Compression in the Nothern Apennines from Earthquake Fault-plane Solutions*, Geophys. J. Int. *129*, 368–388.

GASPERINI, P. (2001), *The Attenuation of Seismic Intensity in Italy: A Bilinear Shape Indicates the Dominance of Deep Phases at Epicentral Distances Longer than 45 km,* Bull. Seismol. Soc. Am. *91*(4), 826–841.

GASPERINI, P., BERNARDINI, F., VALENSISE, G., and BOSCHI, E. (1999), *Defining Seismogenic Sources from Historical Earthquake Felt Reports,* Bull. Seismol. Soc. Am. *89*(1), 94–110.

GI: GASPARINI, C., IANNACCONE, G., and SCARPA, R. (1985), *Fault-plane Solutions and Seismicity of the Italian Peninsula*, Tectonophysics *117*, 59–78.

GUSEV, A.A. (1983), *Descriptive Statistical Model of Earthquake Source Radiation and its Application to an Estimation of Short-period Strong Motion*, Geophys. J. R. Astr. Soc. *74*, 787–808.

GUSEV, A.A. and SHUMILINA, L.S. (2000), *Modeling the Intensity-magnitude-distance Relation Based on the Concept of an Incoherent Extended Earthquake Source*, Volc. Seis. *21,* 443–463.

JOHNSTON, A. (1999), *Seismic Moment of Earthquakes in Stable Continental Regions. 2. Historical Seismicity,* Geophys. J. Int. *124*, 381–414.

KARNIK, V., *Seismicity of the European Area, Part 1*. (Reid Publ., Holland, 1969).

KRONROD, T.L., MOLCHAN, G.M., PODGAETSKAYA, V.M., and PANZA, G.F. (2002), *Formalized Representation of Isoseismal Uncertainty for Italian Earthquakes*, Boll. de Geof. Teorica Applicata *41*, 243–313.

KUNZE, T. (1982), *Seismotektonische Bewegungen im Alpenbereich,* Dissertation, Univ. Stuttgart, 167 pp.

MOLCHAN, G., KRONROD, T., and PANZA, D. (2002), *Shape Analysis of Isoseismals Based on Empirical and Synthetic Data*, Pure and Appl. Geophys. *159*(6), 1229-1252.

MONACHESI, G. and STUCCHI, M. (1997), *DOM 4.1, An Intensity Data Base of Damaging Earthquakes in the Italian Area,* GNDT, Web site: emidius.itim.mi.cnr.it/DOM/home.html.

MUSSON, R. (1996), *Determination of Parameters for Historical British Earthquakes,* Annali di Geofisica *38*(5), 1041–1047.

NT: CAMASSI, R. and STUCCHI, M. (1998), *NT4.1, un catalogo parametrico di terremoti di area italiana al di sopra della soglia del danno: a parametric catalogue of damaging earthquakes in the Italian area. NT4.1.1, 1997; NT4.1.1/81-92*, Web site: emidius.itim.mi.cnr.it/NT/home.html.

PANZA, G. F. (1985), *Synthetic Seismograms: The Rayleigh Waves Modal Summation*, J. Geophys. *58*, 125–145.

PANZA, G., GRAGLIETTO, A., and SUHADOLC, P. (1991), *Source Geometry of Historical Events Retrieved by Synthetic Isoseismals,* Techtonophysics *193*, 173–184.

PANZA, G.F., MUELLER, S., CALCAGNILE, G., and KNOPOFF, L. (1982), *Delineation of the North Central Italian Upper Mantle Anomaly*, Nature *296*, 238–239.

PANZA, G.F., VACCARI, F., and CAZZARO, R. (1999), *Deterministic seismic hazard assessment*. In (Wenzel, F. et. al.), *Vrancea Earthquakes: Tectonics, Hazard and Risk Mitigation* (Kluwer Academic Publ., Netherlands) pp. 269–286.

PERESAN, A., PANZA, G.F., and COSTA, G. (2000), *CN Algorithm and Long-lasting Changes in Reported Magnitudes: The Case of Italy*, Geophys. J. Int. *141*, 425–437.

PERUZZA, L. (2000), *Macroseismic Attenuation Relationships of Italian Earthquakes for Seismic Hazard Assesment Purposes,* Boll. di Geof. Teorica Applicata, *41*, 31–48.

PETTENATI, F., SIROVICH, L., and CAVALLINI, F. (1999), *Objective Treatment and Synthesis of Macroseismic Intensity,* Bull. Seismol. Soc. Am. *89*(5), 1203–1213.

SIROVICH, L. (1996), *A Simple Algorithm for Tracing Synthetic Isoseismals,* Bull. Seismol. Soc. Am. *86*(4), 1019–1027.

SIROVICH, L., CAVALLINI, F., PETTENATI, F., and BOBBIO, M. (2002), *Natural–neighbor Isoseismals,* Bull. Seismol. Soc. Am. *92*(5), 1933–1940.

SOKOLOV, V. and CHERNOV, Yu. (1998), *On the Correlation of Seismic Intensity with Fourier Acceleration Spectra,* Earthquake Spectra *14*(4), 679–694.

SPUDICH, P. and FRAZER, L. (1984), *Use of Ray Theory to Calculate High–frequency Radiation from Earthquake Sources Having Spatially Variable Rupture Velocity and Stress Drop,* Bull. Seismol. Soc. Am. *74*, 2061–2082.

TERTULLIANI, A. and MARAMAI, A. (1998), *Macroseismic evidence and Site Effects for the Lunigiana (Italy) 1995 Earthquake*, J. Seismol. *2*, 209–222.

TOSI, P., DE RUBEIS, V. and GASPARINI, C. (1995), *An Analytic Method for Separating Local from Regional Effects on Macroseismic Intensity,* Annali di Geofisica *38*(1), 55–65.

TRIFUNAC, M.D. and BRADY, A.G. (1975), *On the Correlation of Seismic Intensity Scales with the Peaks of Recorded Strong Ground Motion*, Bull. Seismol. Soc. Am. *65*(1), 139–162.

(Received June 6, 2002, accepted June 10, 2003)

References

Boatwright, J., Fletcher, J.B., Fumal, T. (1991). "A general inversion scheme for source, site and propagation characteristics using multiply recorded sets of moderate size earthquakes", *Bull. Seism. Soc. Am.*, 81, 1754-1782.

Borcherdt, R.D. (1970). "Effects of local geology on ground motion near San Francisco Bay", *Bull. Seism. Soc. Am.*, 60, 29-61.

Cancani, A. (1904). Sue l'emploi d'une double echelle seismique des intensites, empirique et absolue, G. Beitr., 2, 281-283.

Castanos, H. and Lomnitz, C., (2002) PSHA: is it science?, Engineering Geology, 66, 315-317.

Chandler, A.M., Lam, N.T.K., Wilson, J.L., Hutchinson, G.L. (2001). "Response spectrum for regions lacking earthquake records", *Electronic Journal of Structural Engineering*, 1, 60-73.

Decanini, L., Mollaioli, F. (1998). "Formulation of Elastic Earthquake Input Energy Spectra", *Earthquake Engineering and Structural Dynamics*, 27, 1503-1522.

Decanini, L., Mollaioli, F., Panza, G.F., Romanelli, F. (1999). "The realistic definition of the seismic input: an application to the Catania area", In: *Earthquake Resistant Engineering Structures II*, G. Oliveto and C.A. Brebbia (Editors.), WIT press, Boston, 425-434.

Field, E.H., the SCEC Phase III Working Group (2000). "Accounting for site effects in probabilistic seismic hazard analyses of Southern California: overview of the SCEC Phase III report", *Bull. Seism. Soc. Am.*, 90, 6B, S1-S31.

Giampiccolo, E., Gresta, S., Mucciarelli, M., De Guidi, G., Gallipoli, M.R. (2001). "Information on subsoil geological structure in the city of Catania (Eastern Sicily) from microtremor measurements", *Annali di Geofisica*, 44, 1, 1-12.

Kronrod, T.L., Molchan, G.M., Podgaetskaya, V.M., Panza G.F. (2002). "Formalized representation of isoseismal uncertainty for italian earthquakes", *Bollettino di Geofisica Teorica ed Applicata*, 41, 243-313.

Langston, C.A. (1979). "Structure under Mount Rainier, Washington, inferred from teleseismic body waves", *J. Geophys. Res.*, 84, 4749-4762.

Molchan, G., Kronrod, T., Panza G.F. (2002). "Shape analysis of isoseismals based on empirical and synthetic data", *PAGEOPH*, 159, 1229-1251.

Molchan, G., Kronrod, T., Panza, G.F. (1997). "Multi-scale seismicity model for seismic risk", *Bull. Seism. Soc. Am.*, 87, 1220-1229.

Molchan, G.M., Kronrod, T.L. and Panza, G.F., (2004). Shape of Empirical and Synthetic Isoseismals:

Comparison for Italian M≤6 Earthquakes, PAGEOPH, 161, 1725-1247.

Nunziata, C., Costa, G., Natale, M. and Panza, G.F., (1999). FTAN and SASW methods to evaluate Vs of

Neapolitan Pyroclastic Soils. Paper 14b, S.I.C.E.G.E., Portogallo 21-25 June, 1999, 15-19. A.A. Balkema, Rotterdam.

Panza, G.F., Romanelli, F., Vaccari, F. (2001). "Seismic wave propagation in laterally heterogeneous anelastic media: theory and applications to the seismic zonation", *Advances in Geophysics*, Academic press, 43, 1-95.

Panza, G.F., Romanelli, F., Vaccari, F. (2000a). "Realistic modelling of waveforms in laterally heterogeneous anelastic media by modal summation", *Geophys. J. Int.*, 143, 1-20.

Panza, G.F., Romanelli, F., Vaccari, F., Decanini, L., Mollaioli, F. (2000b). "Contribution of the deterministic approach to the characterization of seismic input", *OECD-NEA Workshop on Engineering characterization of Seismic Input*, BNL, Upton, New York, 15-17 November, 1999, NEA/CSNI/R(2000)2.

Panza, G.F., Vaccari, F., Cazzaro, R. (1999). "Deterministic seismic hazard assessment", In: *Vrancea Earthquakes: Tectonics, Hazard and Risk Mitigation*, F. Wenzel, D. Lungu and O. Novak (Editors), Kluwer Academy Publishers, 269-286.

Panza, G.F., Vaccari, F., Costa, G., Suhadolc, P., Fäh, D. (1996). "Seismic input modelling for Zoning and microzoning", *Earthquake Spectra*, 12, 529-566.

Romanelli, F., Vaccari, F. (1999). "Site response estimation and ground motion spectral scenario in the Catania Area", *J. of Seism.*, 3, 311-326.

Wang, H., Nisimura, A. (1999). "On the behaviour of near-source strong ground motion from the seismic records in down-hole array at Hyogoken-Nanbu earthquake", In: *Earthquake Resistant Engineering Structures II*, G. Oliveto and C.A. Brebbia (Editors), WIT Press, Southampton, 363-372.